

# FerryBox

## From On-line Oceanographic Observations to Environmental Information



## Report on Non-Standard Sensor Trials

Contract number : EVK2-2002-00144  
Deliverable number : D-2-4  
Revision : 2.0

Co-ordinator:

Professor Dr. Franciscus Colijn

GKSS Research Centre  
Institute for Coastal Research  
Max-Planck-Strasse  
D-21502 Geesthacht

<http://www.ferrybox.org>

## Document Reference Sheet

This document has been elaborated and issued by the European FerryBox Consortium.

P 1		<b>GKSS</b>	<b>GKSS Research Centre Institute for Coastal Research</b>	<b>Coordinator</b>
P 2		<b>NERC.NOC</b>	<b>NERC.NOC – National Oceanography Centre Southampton University and National Environment Res. Council</b> formerly NERC.SOC – Southampton Oceanography Centre	
P 3		<b>NIOZ</b>	<b>Royal Netherlands Institute of Sea Research</b>	
P 4		<b>FIMR</b>	<b>Finnish Institute of Marine Research</b>	
P 5		<b>HCMR</b> (formerly NCMR)	<b>Hellenic Centre for Marine Research</b> (formerly National Centre for Marine Research)	
P 6		<b>NERC.POL</b>	<b>Proudman Oceanographic Laboratory</b>	
P 7		<b>NIVA</b>	<b>Norwegian Institute for Water Research</b>	
P 8		<b>HYDROMOD</b>	<b>HYDROMOD Scientific Consulting</b>	
P 9		<b>CTG</b> (formerly CIL)	<b>Chelsea Technology Group</b> (formerly Chelsea Instruments Ltd.)	
P 10		<b>IEO</b>	<b>Spanish Institute of Oceanography</b>	
P 11		<b>EMI</b>	<b>Estonian Marine Institute</b> (in cooperation with the Estonian Maritime Academy)	

This document is sole property of the European FerryBox Project Consortium.

It must be treated in compliance with its classification.

Any unauthorised distribution and/or copying without written permission by the author(s) and/or the FerryBox Consortium in terms of the *FerryBox Consortium Agreement* and the relevant project contracts is strictly prohibited and shall be treated as a criminal act and as a violation of copyright and whatsoever applicable laws.

The responsibility of the content of this document is fully at the author(s).



The European FerryBox Project was co-funded by the European Commission under the Fifth Framework Programme of the European Commission 1998-2002 – Energy, Environment and Sustainable Development (EESD) Programme under contract no. EVK2-2002-00144.





## Document Control Table

Project acronym:	FerryBox	Contract no.:	EVK2-2002-00144		
Deliverable No.:	D-2-4	Revision:	2.0		
WP number and title:	FerryBox WP-2	Operation and metrology of the FerryBox systems			
Work Package Manager:	Wilhelm Petersen – GKSS				
Work Package Team:	FerryBox WP -2 Team				
Document title:					
Document owner:	European FerryBox Project Consortium				
Document category:	Deliverable				
Document classification:	PU – Public				
Status:	Final				
Purpose of release:	Publication on the FerryBox website and the FerryBox Report CD-ROM				
Contents of deliverable:					
Pages (total):	77	Figures:	47	Tables:	0
Remarks:	Updated revision for publication on the FerryBox report CD and website				
Main author / editor:	Friedhelm Schroeder	FerryBox WP-2	GKSS		
Contributors:	FerryBox WP-2 Team				
Main contacts:	FerryBox project coordinator:		Contact for this report:		
	Professor Dr. Franciscus Colijn GKSS Research Centre Institute for Coastal Research Max-Planck-Strasse D-21502 Geesthacht, Germany Tel.: +49 4152 87 – 1533 Fax.: +49 4152 87 – 2020 E-mail: franciscus.colijn@gkss.de		Dr. Friedhelm Schroeder GKSS Research Centre Institute for Coastal Research Max-Planck-Strasse D-21502 Geesthacht, Germany Tel.: +49 4152 87 – 2371 Fax.: +49 4152 87 – 2366 E-mail: friedhelm.schroeder@gkss.de		
Project website:	<a href="http://www.ferrybox.org">http://www.ferrybox.org</a>				



## Table of Contents

<b>1</b>	<b>Overview</b>	<b>5</b>
<b>2</b>	<b>Scientific Aims</b>	<b>6</b>
2.1	Motivation	6
2.2	Objectives	7
2.2.1	Oxygen Measurements	7
2.2.2	pH Measurements	8
2.2.3	Current Profile Measurements (ADCP)	9
2.2.4	Multi-Wavelength Fluorescence for the Detection of Algal Groups	9
2.2.5	Fast Repetition Rate Fluorometry (FRRF) for the Detection of Algal Activity	10
2.2.6	Sensors and Analysers for the Determination of Nutrients	11
2.2.7	Light Measurements	11
2.2.8	Application of Water Samplers	11
2.2.9	New Emerging Technologies for the Assessment of Biological-Chemical Parameters	12
<b>3</b>	<b>Detailed Description of the Sensors</b>	<b>13</b>
3.1	Oxygen Sensor: Membrane-Covered Sensor	13
3.1.1	Physical Relationships in Sea Water	13
3.1.2	Description of the Sensor	14
3.1.3	Calibration of the Sensor	15
3.1.4	Reliability and Applicability	16
3.1.5	Data Availability	16
3.1.6	Maintenance	16
3.1.7	Quality Assurance	16
3.2	Oxygen Sensor: Fluorescence Quenching ("Optode")	18
3.2.1	Description of the Sensor	18
3.2.2	Reliability and Applicability	20
3.2.3	Data Availability	21
3.2.4	Maintenance	21
3.2.5	Quality Assurance	21
3.3	pH Sensor	24
3.3.1	General Description	24
3.3.2	Description of the Sensor	24
3.3.3	Calibration	25
3.3.4	Reliability and Applicability	25
3.3.5	Data Availability	25
3.3.6	Maintenance	26
3.3.7	Quality Assurance	26
3.4	Acoustic Doppler Current Profiler (ADCP)	27
3.4.1	Description of the Sensor	27
3.4.2	Reliability and Applicability	27
3.4.3	Data Availability	28
3.4.4	Maintenance	29
3.4.5	Quality Assurance	29
3.5	Multi-wavelength Fluorometer for the Detection of Algal Groups	30
3.5.1	Description of the Sensor	30
3.5.2	Reliability and Applicability	32
3.5.3	Data Availability	32
3.5.4	Maintenance	32
3.5.5	Quality Assurance	32
3.6	Fast Repetition Rate Fluorometer (FRRF)	33
3.6.1	Description of the Sensor	33
3.6.2	Reliability and Applicability	34
3.6.3	Data Availability	35
3.6.4	Maintenance	36
3.6.5	Quality Assurance	36

3.7	Chemical Nutrient Analysers (Wet Chemistry)	37
3.7.1	Description of the Analysers	37
3.7.2	Reliability and Applicability	40
3.7.3	Data Availability	40
3.7.4	Maintenance	41
3.7.5	Quality Assurance	41
3.8	Optical Analyser for Nitrate ("In situ Nitrate")	42
3.8.1	Description of the Sensor	42
3.8.2	Reliability and Applicability	44
3.8.3	Data Availability	45
3.8.4	Maintenance	45
3.8.5	Quality Assurance	46
3.9	Light Sensor	48
3.9.1	Description of the Sensor	48
3.9.2	Reliability and Applicability	48
3.9.3	Data Availability	48
3.9.4	Maintenance	48
3.9.5	Quality Assurance	48
3.10	Water Sampler	49
3.10.1	Description of the Sensor	49
3.10.2	Reliability and Applicability	50
3.10.3	Data Availability	50
3.10.4	Maintenance	50
3.11	New Emerging Technologies	51
3.11.1	Flow Cytometer (Cytosense) for a Structural Assessment of Algal Species Composition	51
3.11.2	Measurement of CO <sub>2</sub>	53
<b>4</b>	<b>Scientific Value</b>	<b>54</b>
4.1	Oxygen Measurements	54
4.2	pH Measurements	55
4.3	Current Profile Measurements (ADCP)	56
4.4	Detection of Algae Groups	58
4.5	Measurement of Algal Activity/Productivity (FRRF)	59
4.6	Measurement of Nutrients	61
4.7	Light Measurements	61
4.8	Application of Water Samplers	62
4.9	Applications of New Emerging Technologies	63
4.9.1	Example of Measurements with the Cytosense	63
4.9.2	Examples of CO <sub>2</sub> Measurements	65
<b>5</b>	<b>Recommendations for Ferrybox Applications, Known Problems and Limitations</b>	<b>66</b>
5.1	Membrane-Covered Oxygen Sensor	66
5.2	Optode	66
5.3	pH	66
5.4	Current Profilers (ADCP)	67
5.5	Multi-wavelength Fluorometer for Algal Group Detection	67
5.6	FRRF	68
5.7	Chemical Nutrient Analyser	68
5.8	In situ Nitrate Sensor	68
5.9	Light Sensor (PAR)	69
5.10	Water Sampler	69
<b>6</b>	<b>Conclusions</b>	<b>70</b>
<b>7</b>	<b>References</b>	<b>71</b>

## List of Figures

Figure 3-1:	Endress & Hauser oxygen sensor with electronic unit (Source: E&H) .....	15
Figure 3-2:	Dot plot of the archived data from the GKSS Ferrybox Cuxhaven – Harwich in 2003 and 2003.....	17
Figure 3-3:	Dot plot of the archived data from the GKSS Ferrybox Cuxhaven – Harwich in 2005. ....	17
Figure 3-4:	Photograph of the Aanderaa Optode removed from its housing for cleaning as installed on the NERC.NOC Ferrybox on “Pride of Bilbao”. ....	19
Figure 3-5:	Diagram of the optical design of the Aanderaa oxygen Optode (taken from Tenberg et al., submitted). ....	20
Figure 3-6:	Dot plot of all Aanderaa oxygen Optode data for 2005 for the NERC.NOC Ferrybox, using 5 minute averaged data and showing the calculated oxygen anomaly which is the difference between the measured oxygen concentration and the saturation concentration for water of the same temperature. ....	21
Figure 3-7:	Plot of all lower values of pairs of oxygen water samples against corresponding Optode values (303 samples, from the NERC.NOC Ferrybox on “Pride of Bilbao”). ....	22
Figure 3-8:	Plot of all lower values of pairs of oxygen water samples against corresponding Optode values as in Figure 3-7 but with the data from the 6 individual calibration crossings identified (from the NERC.NOC Ferrybox on “Pride of Bilbao”). ....	22
Figure 3-9:	Plot of the values of the calculated calibration coefficient and r2 values for each set of calibration data shown in Figure 3-7 on the basis of a least squares fit forced through the origin (from the NERC.NOC Ferrybox on “Pride of Bilbao”). ....	22
Figure 3-10:	Comparison of oxygen measurements between membrane-covered electrode (Clark) and an Optode (Aanderaa) on the GKSS Ferrybox Cuxhaven – Harwich, June – September 2005. ....	23
Figure 3-11:	Endress & Hauser pH electrode and electronic unit.....	24
Figure 3-12:	Dot plot of the archived data from the GKSS Ferrybox Cuxhaven – Harwich in 2003 and 2004.....	25
Figure 3-13:	Dot plot of the archived data from the GKSS Ferrybox Cuxhaven – Harwich in 2005. ....	26
Figure 3-14:	Percentage of good ADCP data return, as compared to a 100 % return if the ferry would sail and measure always. The months run from January 2004 (1) to August 2005 (20).....	28
Figure 3-15:	Water volume transport through the Marsdiep tidal inlet as derived from observations with an ADCP installed on the Texel – Den Helder ferry. ....	29
Figure 3-16:	Spectral intensities of used LEDs (intensity is normalised to the maximum of each LED (Source: bbe moldaenke). ....	30
Figure 3-17:	Spectra and Fluorescence intensities of the 5 algal divisions multiplied by the intensity of the LED and normalised to the maximum intensity of each division. ....	31
Figure 3-18:	Photo of the bbe Algal Online Analyser (AOA).....	31
Figure 3-19:	Recovery of a normal research deployment of an FRRF in which it is used in conjunction with net sampling of the associated plankton so the taxa present in the water are known and the FRRF response can be correlated with the taxa. ....	33
Figure 3-20:	Initial test installation of the FRRF in December 2004 as part of the NERC.NOC Ferrybox system on “Pride of Bilbao”. ....	34
Figure 3-21:	Data recorded by the FRRF during the test deployment in December 2004.....	35
Figure 3-22:	Plot of all the Fm data successfully recovered from the CTG FRRF used on the ferry “Pride of Bilbao” in 2005.....	35
Figure 3-23:	Plot of all the fluorescence data available from the NERC.NOC “Pride of Bilbao” Ferrybox system for 2005. ....	36
Figure 3-24:	Nutrient Analyser APP 5003 (left) and Micromac 1000 (right).....	37
Figure 3-25:	Hydraulic Principle of the APP 5003 (Source: ME Grisard GmbH). ....	38
Figure 3-26:	Ribbon filter for nutrient analyses (left) and experimental cross-flow unit (right). ....	39

Figure 3-27: Availability of nutrient data in 2003-2004 on the GKSS Ferrybox Cuxhaven – Harwich as measured with the APP 5003.....	40
Figure 3-28: Availability of nutrient data in 2005 on the GKSS Ferrybox Cuxhaven – Harwich as measured with the APP 5003. ....	41
Figure 3-29: Absorbance spectra (from Kenneth & Coletti 2002). ....	42
Figure 3-30: Optical layout of the In situ Nitrate sensor (Source: Zeiss, Heraeus & TriOS). ....	43
Figure 3-31: Photo of the desktop version of the UV Nitrate analyser (left) and its dual-path length cuvette (right).....	43
Figure 3-32: Photo of the In situ Analyser "ProPS" (left) with adapters that change the optical wavelengths and a cuvette for lab check (right) .....	44
Figure 3-33: The ProPS analyser with customised flow-through unit. ....	44
Figure 3-34: Calibration of the UV Nitrate sensor in the lab at two optical path lengths. ....	45
Figure 3-35: Calibration of the ProPS sensor for lower concentration ranges. ....	46
Figure 3-36: Comparison of Data from the UV Nitrate Sensor with Data from APP 5003 and Lab Analyses. ....	47
Figure 3-37: The Li-Cor light sensor and the sensitivity diagram (from: Li-Cor). ....	48
Figure 3-38: ISCO 3700R ISCO refrigerated sampler. ....	49
Figure 3-39: Portable Sampler Bühler 1029 (Dr. Lange). ....	50
Figure 3-40: Photo of the Cytosense with laptop for data analysis.....	51
Figure 3-41: General functionality of the Cytosense (from <a href="http://www.cytobuoy.com">http://www.cytobuoy.com</a> ). ....	52
Figure 4-1: Ferrybox Route Cuxhaven –Harwich (top) and measurements of chlorophyll-fluorescence (left) and oxygen saturation index (right) from March to June 2005. ....	54
Figure 4-2: Ferrybox Route Cuxhaven – Harwich (top) and measurements of chlorophyll-fluorescence (left) and pH values (right) from March to June 2005. ....	55
Figure 4-3: Current velocity during two ferry cruise. ....	56
Figure 4-4: Average residual currents on the ferry track. ....	57
Figure 4-5: Transect-averaged suspended sediment concentrations as function of the water volume transport. Red: Accelerating tidal phase, green: decelerating tidal phase.....	58
Figure 4-6: Results from Algal Group Measurements on May 15th (left) and May 28th (right) 2005.....	59
Figure 4-7: Plot of all the night time (PAR less than 200) Fm values from FRRF.....	60
Figure 4-8: Plot of all the night time (PAR less than 200) Fv/Fm values from FRRF.....	60
Figure 4-9: Plot of all the Fv/Fm data collected in 2005. ....	60
Figure 4-10: Plot of Fv/Fm against sigmaPSII from the FRRF data collected in 2005.....	60
Figure 4-11: Ferry route Cuxhaven – Harwich and results from nitrate measurements March/April 2005. ....	61
Figure 4-12: Cytosense measurements on board of FS Polarstern.....	63
Figure 4-13: First overview with the analysis program "CytoPlus" which is used to select relevant parameter sets. ....	64
Figure 4-14: Results: Cell numbers (left) and fluorescence values (right) of the different parameter sets selected in Figure 4-13 along the transect Bremerhaven – Vigo.....	64

# 1 Overview

One of the features of Ferryboxes is its applicability for many sensors and sensor systems that would be difficult to use on buoys or platforms. This is mainly due to the protected environment on a ship, the availability of stable electric power and the possibility for biofouling protection.

However, from the many sensor principles that have been developed in the last years only some fulfil the requirements of a pre-operational use for unattended measurements. Some other new techniques are discussed in the corresponding paragraphs of “New Emerging Technologies”.

Within the FerryBox project the following selected “mature” sensor types have been investigated and assessed:

- **Membrane-covered oxygen sensor (Clark-type)**
- **Oxygen sensor utilising fluorescence quenching (“Optode”)**
- **pH sensor (glass electrode with gel electrolyte)**
- **Acoustic Doppler Current Profiler (ADCP)**
- **Multi-wavelength Fluorometer for the detection of algal groups**
- **Fast Repetition Rate Fluorometer (FRRF)**
- **(Wet) Chemical Nutrient Analyser**
- **Optical Analyser for Nitrate (“In situ Nitrate”)**
- **Light Sensor for photosynthetic available radiation (PAR) measurements**
- **Water sampler**



## 2 Scientific Aims

### 2.1 Motivation

The motivation for developing and applying these sensors is:

- **Monitoring of coastal waters for water quality.** This includes an assessment of eutrophication problems (nutrients, plankton), contamination with toxic inorganic and organic trace constituents and movement of sediments, suspended matter and water bodies to aid the interpretation of time series. For these tasks operational sensors for the quantification of phytoplankton (fluorometers), nutrients, pH & oxygen (proxy for primary production) and water sampler (to sample contaminants) are needed. In addition, current measurements for water and sediment transport are important.
- **Estimation of water and sediment/suspended matter budgets.** For this task sensors for salinity and turbidity (standard) and current profilers (ADCP) are needed. The measurements within the project between Texel and Den Helder are a good example for such assessments.
- **Insight into plankton/nutrient processes.** Within the complex interactions between physical parameters, such as temperature, light availability and stratification, chemical parameters such as nutrient availability and biological parameters such as initial phyto- and zooplankton concentrations, phyto- and zooplankton species, growth, respiration, mortality and grazing rates many processes are either not quite well understood or not quantified for a specific sea area. Measurements with sensors mentioned above contribute to a better understanding of these processes –a prerequisite for modelling.
- **Improvement, validation and application of ecosystem models.** A realistic application of existent models with ecosystem parts very often fails because of a) lack of knowledge of some key processes or b) lack of data for kinetic variables (rate constants) in the observed sea area. Even when Ferrybox measurements cannot replace rate measurements suitable time series measured with these sensors may be the basis for a validation and improvement of ecosystem models. As supplementary information, some methods, e.g., the Fast Repetition Rate Fluorimetry, measure algal activity and production.

## 2.2 Objectives

### 2.2.1 Oxygen Measurements

Oxygen is a component that responds to both physical changes (temperature and salinity dependence of oxygen solubility, ventilation) as well as biological changes (e.g., different temperature dependence of photosynthesis and respiration, effect of stratification changes on vertical nutrient supply, and utilization efficiency) and therefore can potentially be used as a sensitive indicator of environmental change in the ocean (Körtzinger et al 2004, Joos et al. 2003).

The waters of the Northwest European shelf have been the subject of investigation for many years (e.g. Pingree et al., 1975; Puillat et al., 2004). Constraining estimates of seasonal primary production has proven difficult. Data sets tend to be sparse and incomplete (Frankignoulle and Borges, 2001) relative to the high temporal and spatial variability in the area (Wollast and Chou, 2001; Joint et al., 2001).

Estimates of seasonal primary production for whole shelf regions are usually extrapolated from sampling programmes of at best a few weeks in each of several years (Joint et al., 2001; Borges and Frankignoulle, 2003). The quest for improved sampling frequency and geographical coverage persists (Borges and Frankignoulle, 2003; Puillat et al., 2004), especially in winter (Hydes et al., 2004). In particular measurements need to be able to assess the relative contributions of physically relatively small areas of high productivity, such as fronts, (Holligan, 1981 and 1989; Richardson & Pedersen, 1998) but which may make disproportionately large contributions to total production. No such published comprehensive carbon budget exists for even a relatively well studied region such as the English Channel (Borges and Frankignoulle, 2003).

To improve the quantification of the carbon cycle of ocean margins requires access to more regular data, which represent both temporal changes and the proportionately samples different production regimes and biogeochemical zones. The use of ships of opportunity (SOO) may offer the required spatio-temporal resolution (Hydes et al., 2003) but this platform requires a complimentary method for measuring and assessing productivity and respiration. Oxygen cycle studies have been also been used and offer the potential of using a basic chemical measurement which is well understood and now using newly developed sensors to make autonomous measurements (Tenberg et al., submitted). The flow of oxygen across the air-sea surface is driven by differences in oxygen concentration in the atmosphere and ocean, with equilibration occurring in a few days to weeks following perturbations (Broecker and Peng, 1982). The physical processes controlling concentrations at the sea surface include air-sea gas exchange through surface turbulence and bubble breaking, solubility changes due to temperature and also mixing of surface and deeper waters. Biochemical processes include production, respiration and remineralisation of organic matter where photosynthesis produces oxygen and respiration consumes oxygen. The biological component of the outgassing can be calculated and used to estimate productivity, especially during the spring and summer blooms.

Recent estimations of global new production have been made in the North Atlantic using oxygen fluxes to calculate biological Seasonal Net Outgassing (SNO) and this showed good agreement with site-specific new production and remineralisation estimates (Najjar and Keeling). The measurements are, however, too sparse to provide the kind of regional analysis that would distinguish the importance of features such as fronts.

SNO is a measure of air-sea oxygen exchange and is defined as the spatially and temporally integrated oxygen flux over the annual periods (seasons) when the flux is positive i.e. sea to air in spring and summer. It is composed of biological and thermal components (Keeling and Shertz, 1992). The biological contribution, Biological Seasonal Net Outgassing ( $SNO_B$ ), can be separated from the thermal contribution ( $SNO_T$ ).

A key assumption of the method is that biological seasonal net outgassing, determined as the sum of positive oxygen fluxes, is approximately equivalent to net community production, NCP, the excess of gross primary production over total community respiration. NCP is considered almost equivalent to new production (Minas and Minas, 1992), the maximum exportable biomass that will preserve the long-term integrity of the system (Eppley and Peterson, 1979).

In 2005 (Barger et al., in preparation) the NERC.NOC Portsmouth – Bilbao Ferrybox was used to test the hypothesis that calculations of oxygen flux based on regular measurements of oxygen concentrations along the regular route of a SOO coupled with available wind speed data could be used to effectively estimate new production, and that the resolution of the method would be sufficient to be able to distinguish the relative magnitude of the contribution to the carbon cycle of hydrodynamically and biogeochemically different region along the route.

In addition the estimates of seasonal new production based on oxygen measurements were compared with estimates based on seasonal depth integrated carbon production implied by changes in concentrations of nitrate chlorophyll-*a*. This initial study was based the collection of water samples during the monthly calibration crossing undertaken by NERC.NOC between February and July 2005. The results were successful. The calculations of productivity based oxygen fluxes gave results, which fitted with expected levels of productivity and regional differences. In particular the oxygen method was able to detect the relatively high productivity associated with the Ushant frontal area. This was not the case with estimates based on nutrients or chlorophyll-*a* standing stock.

In earlier times only membrane-covered type of oxygen electrodes (“Clark-type”) were used. In the last years another technology that uses fluorescence quenching emerged. It was therefore decided to use as well the membrane-covered oxygen sensor as the newly developed oxygen Optode available from the Norwegian Company Aanderaa to make continuous measurements of oxygen as a routine part of the Ferrybox systems of GKSS and NERC.NOC. The functioning of the systems was checked against each other and –in the case of the NERC.NOC system against oxygen concentrations measured by Winkler titrations during the calibration crossing done in 2005.

### 2.2.2 pH Measurements

Seawater pH is an important parameter in quantitative descriptions of ocean chemistry. It is very important for oceanic processes and properties that are strongly pH-dependent. This includes chemical speciation and adsorption, bioavailability, and redox equilibria. Since buffering of seawater pH is dominated by the marine  $CO_2/HCO_3^-/CO_3^{2-}$  system, a very precise measurement of pH (accuracy of better than 0.05) is important for an assessment of the  $CO_2$  budget of oceans. Another important application, mainly for coastal processes, is the detection of primary production by phytoplankton: Since during the production process  $CO_2$  is consumed this shifts the  $CO_2/HCO_3^-$ -equilibrium to  $HCO_3^-$  and  $CO_3^{2-}$  and the pH increases. On the other hand, mineralization of organic matter (microbial respiration) and algal respiration produces  $CO_2$  and diminishes the pH. Together with oxygen measurements these parameters can be used as “proxy” for the detection of these processes.

pH measurements are predominantly conducted with pH-sensitive glass electrodes. Another, more precise also but more expensive method uses the spectrometric measurement of a continuously added pH-sensitive dye. Within the FerryBox project only glass electrodes have been tested.

### 2.2.3 Current Profile Measurements (ADCP)

Current measurements are important not only for the interpretation of oceanographic phenomena but also for the study of fluxes of water constituents and particulate matter. The interaction of tidal flow with coastal bathymetry plays a fundamental role in horizontal mass and momentum transport subsequently affecting the dispersal of pollutants and nutrients. Another application is the validation of hydrodynamic models in near coast environment. Especially for this purpose not only surface current but also the whole three-dimensional field has to be measured. For this an “Acoustic Doppler Current Profilers (ADCP)” is used.

Another important application is the measurement of sediment flux in coastal estuarine and river engineering and scientific applications. For example, at the largest scale sediment flux controls the morphological evolution of whole channels whilst at smaller scales it impacts on the design of ports and harbours and other engineering structures through its impact on sedimentation rates and hence the requirement for maintenance dredging.

Today ADCPs are widely used to measure the variation of flow field and although these instruments were primarily developed for the measurement of current profiles in the last years different scientists have attempted to derive sediment flux estimates from inversion of the backscattered pressure field recorded by these instruments. Within the project ADCP observations were used to study long-term variability in

- Currents
- Sediment transport and
- Bed forms.

The investigation area was in the Marsdiep tidal inlet that forms the connection between the largest tidal basin of the Dutch Wadden Sea and the adjacent North Sea.

### 2.2.4 Multi-Wavelength Fluorescence for the Detection of Algal Groups

Many fluorimetric methods for the semi-quantitative measurement of chlorophyll-a exist. However, for the assessment of marine waters not only the total amount of chlorophyll is important but as well the composition/abundance of algae species. For example, for monitoring it is of paramount interest to know whether there exist harmful algae blooms (HABs), e.g. blue-green algae, in a sea area. The main methods for the detection of algae species are manual microscopic counts. New emerging technologies either by structural characterisation or by biochemical detection are not yet operational for unmanned use. One is discussed shortly in the paragraph for “New Emerging technologies”.

Since some years fluorimetric methods are available which use wavelength-specific excitation of algal pigments and consecutive measurement of the resulting chlorophyll fluorescence. With such sensors algal groups such as green algae, diatoms/flagellates and blue-green algae can be differentiated. This helps in the interpretation of results, which cannot be explained by pure chlorophyll measurements (e.g., the fluorescence yield is dependent on the species).

## 2.2.5 Fast Repetition Rate Fluorometry (FRRF) for the Detection of Algal Activity

Phytoplankton activity is continually in flux, discrete sampling can give a distorted view of short and long-term changes in phytoplankton characteristics. In addition, the current practice of measuring chlorophyll alone, as a marker of phytoplankton biomass gives insufficient information to determine biomass (Qurban et al. 2004). For this reason, new research tools, such as the Fast Repetition Rate Fluorometer (FRRF), have been developed and are being evaluated to test the extent to which they can provide improved spatial coverage and estimates of plankton biomass and primary production. The claimed benefits of FRRF are that it can be used to estimate the relative photosynthetic state and so differentiate marine plankton populations and so provide information about the stage of the bloom (i.e. growing or dying off) and how active it is. However it has to be born in mind that this is a challenging aspiration as the method was developed originally to look at the photosynthetic properties of well characterised leaves of terrestrial plants in the laboratory rather than the poorly known and variable mixes of microscopic plankton found as one moves through sea water.

Estimating the primary productivity of phytoplankton as they are mixed through the surface layer is often hampered by methodological or conceptual constraints. Fast Repetition Rate Fluorimetry (FRRF) allows some of these constraints to be overcome by providing measurements of the instantaneous, depth-dependent rates of primary productivity of phytoplankton in situ. Data acquired by FRRF can be used (e.g. Smyth et al., 2004) to determine the parameters of the photosynthesis–irradiance curve and the instantaneous photosynthetic rates for phytoplankton from the mixed layer. The FRRF determined values of light saturated photosynthesis rate have been shown to be consistent with those measured using radiocarbon techniques (e.g., Smyth et al., 2004).

Two outputs from the FRRF in addition to the measurement of fluorescence ( $F_m$ ) are  $F_v/F_m$  and  $\sigma_{PSII}$  ( $\sigma_{PSII}$ ) both of which are functions of photo-system II (PSII) which is one of two reaction centres (PSI and PSII) in phytoplankton chloroplasts. These reaction centres absorb light energy that is used in hydrolysis as one of the first steps in photosynthesis. The wavelengths used by the reaction centres differ; type I absorbs most strongly at 700 nm and type II at 680 nm (Kirk 1994). At ambient marine temperatures the majority of fluorescence is emitted by PSII (Kolber and Falkowski 1993).  $F_v/F_m$  is the photochemical quantum efficiency. It represents the probability that de-excitation of the photo-system occurs via photochemistry relative to other pathways such as fluorescence or dissipation of energy through heat loss.  $\sigma_{PSII}$  is the functional cross section of PSII and measures the photochemical target size. It represents the probability that an excitation within an antennae pigment will cause a photochemical reaction (Kolber et al 1998). Limiting concentrations of nutrients prevent assembly of functional photosynthetic reaction centres and result in reduced values of  $F_v/F_m$  and increased values of  $\sigma_{PSII}$  (Falkowski et al 1992). Factors other than nutrient stress such as photo-inhibition, such as diel variability photo-protection and community composition can cause changes in FRRF parameters (Geider et al 1993).

A major potential difficulty in the interpretation of FRRF data is its taxon specific variability as well as nutrient stress that can result in similar specific values of  $F_v/F_m$  and  $\sigma_{PSII}$  (Moore et al 2005). This can be valuable scientifically where information is available on the taxa present in the sampled water. This is currently easier to achieve on research cruises (see Figure 1) than during operational activities with Ferrybox type systems.



## 2.2.6 Sensors and Analysers for the Determination of Nutrients

Nutrient concentrations in coastal waters are the most important parameters for an assessment of eutrophication since they are –together with the light conditions and hydrography (e.g., stratification) – the driving forces for algal growth. In general, the determination of the nutrients ammonium, nitrite, nitrate, ortho-phosphate and silicate is carried out by sampling and consecutive lab analysis. However, due to complex hydrographic and biological processes the temporal variability and spatial heterogeneity is high. This is even enhanced by local processes such as remobilisation from sediments, patchy algae blooms and atmospheric deposition. Therefore, automated quasi-continuous nutrient measurements, e.g., from Ferryboxes, are required.

In the last years two technologies have emerged and are already in a more or less “mature” status:

- 1) Chemical analysers that apply “wet” chemistry, i.e., the standard procedures normally applied in marine chemistry lab work, in an automated way and
- 2) “Chemical-free” direct spectroscopic measurements in seawater (in situ UV spectrum) for nitrate exclusively.

Both techniques have been tested within the project.

## 2.2.7 Light Measurements

Light sensors are used for the determination of the total down welling irradiance (PAR). This is required together with the chlorophyll-a fluorescence for an estimation of primary production. However, much more important is it for a check on the correctness of fluorescence measurements for the determination of chlorophyll-a: Since the chlorophyll fluorescence very much depends on the “light history”, i.e., the illumination of the algae prior and during the measurement by ambient light (fluorescence yield), accompanying light measurements are needed.

## 2.2.8 Application of Water Samplers

Water samplers are an important addition to the sensor systems of a Ferrybox. They are mainly used for two purposes:

- 1) Quality assurance (retrieval of reference samples for check of sensor calibration) and
  - 2) Supplemental analyses of parameters or substances, which -at the time being - cannot yet be determined automatically.
- 1) The application of a sampler for quality assurance is important in order to have control data in between calibration cycles of sensors. Since the calibration mostly is carried out in the lab the reference samples provide means to compare the sensor by other, independent methods. On the other hand, care should be taken not to make a thorough lab calibration worse by an analysis of a sample which either
    - does not exactly correspond to a sensor reading due to different time constants or averaging times or
    - which had changed during storage (e.g., evaporation of salinity samples or deterioration of nutrient samples).

- 2) Sampling for the assessment of parameters or substances, which cannot yet determined otherwise is an important addition to the automated Ferrybox concept. However, the same caution as was mentioned in the preceding section should be observed: A careful preservation of the samples and only short storage periods should be followed.

### 2.2.9 New Emerging Technologies for the Assessment of Biological-Chemical Parameters

For ocean observations which do not only cover physical parameters but have to solve as well biological-chemical questions sensors for parameters such as pH, oxygen, chlorophyll are not sufficient for a satisfactory description of ecological systems. Investigations during field cruises with research ships often provide the possibility of special investigations by applying sophisticated lab analyses on samples. However, most of these methods cannot yet be applied to unattended automated measurements, e.g., from ferries or ships-of-opportunity.

Within the FerryBox project only sensors and analysers have been evaluated the technology of which was already proven for operational observations (“mature sensors”). However, since in the next years new sensors will play an important role in this field, an overview of some of these techniques which are on the “brim of operational use” are given.

From these “emerging technologies” the following sensors will be shortly described:

- Experiences of an inline flow cytometer (“Cytosense®”) during a research cruise)
- A short literature review of CO<sub>2</sub>- analysers and their applications

## 3 Detailed Description of the Sensors

### 3.1 Oxygen Sensor: Membrane-Covered Sensor

#### 3.1.1 Physical Relationships in Sea Water

Oxygen exists in a dissolved state in seawater. A state of equilibrium is reached when the partial pressure of oxygen, i.e. the part of the total pressure that is due to oxygen, is equal in air and in seawater. The seawater is then saturated with oxygen. In dry, atmospheric air, the oxygen partial pressure (20.95% of the air pressure) is reduced over a water surface because water vapour has its own vapour pressure and a corresponding partial pressure.

When air is saturated the partial pressure of oxygen  $p_{O_2}$  is

$$P_{O_2} = 0.2095 (P_{air} - P_{vapour}) \quad \text{Equ. 1}$$

with  $P_{air}$  = air pressure and  $P_{vapour}$  = water vapour pressure

$P_{O_2}$  and  $P_{vapour}$  are temperature-dependent

The vapour pressure of water calculated from an empirical equation derived from the Handbook of Chemistry and Physics (Chemical Rubber Company, (Cleveland, Ohio, 1964) is

$$\log P_{vapour} = 8.10765 (1750.286/235+t) \quad (3)$$

where  $t$  is temperature in degrees C.

The oxygen concentration  $c_{O_2}$  in water is

$$c_{O_2} = (a_{O_2} P_{O_2} M_{O_2}) / V_M$$

with  $a_{O_2}$  = Bunsen coefficient,  $M_{O_2}$  = molar mass of oxygen and  $V_M$  = molar volume.  
 $c_{O_2}$ ,  $P_{O_2}$  and  $a_{O_2}$  are temperature-dependent

(Remark: The Bunsen coefficient ( $a_{O_2}$ ) is defined as the volume of oxygen, reduced to 0°C and 1 atm (101.325 kPa), which is absorbed by the unit volume of seawater at the temperature of measurement when the partial pressure of oxygen is equal to one standard atmosphere).

Due to the different temperature-dependences an exact knowledge of the temperature is important. Since water vapour pressure increases as temperature rises, the partial pressure of oxygen decreases. The salt content of seawater decreases the solubility of oxygen in comparison to fresh water. Therefore, the oxygen concentration depends on salinity.

For the assessment of biological processes under varying salinity (estuary, coastal waters) and temperature very often the saturation index is used: The oxygen saturation is calculated as the percent of dissolved oxygen relative to a theoretical maximum concentration given the temperature, pressure, and salinity of the water. The oxygen saturation index shows the over- or under-saturation of a water body due to biological processes -independent of salinity or temperature.



For a calculation of the oxygen saturation at a specific temperature and salinity corrections from the US Geological Survey are given at <http://water.usgs.gov/admin/memo/QW/qw81.11.html>.

The calculations are based on an equation by Weiss (1970, Deep-Sea Res. 17: 721-735) which fits the data by Carpenter (1966, Limnol. Oceanogr. 11: 264-277) with a maximum difference of 0.04 mg/L. Carpenter's values are, at the present time, widely accepted as the most accurate determinations of saturation DO available.<sup>1</sup>

### 3.1.2 Description of the Sensor

The basic principle underlying the electrochemical determination of oxygen concentration is the use of membrane-covered polarographic sensors. The main components of the sensors are the oxygen-permeable membrane (mainly Teflon), the working electrode, the counter electrode, the electrolyte solution and a reference electrode.

A voltage is applied between the gold cathode and the silver anode and causes the oxygen to react electrochemically. The higher the oxygen concentration, the higher the resulting electric current will be. The current in the sensor is measured and, after calibration, converted into the concentration of dissolved oxygen.

During this process the cathode provides electrons and the oxygen that diffuses through the membrane reacts with water to form hydroxide ions. The metal of the electrode is oxidized at the anode, a process that releases the electrons required for the cathode reaction. The components of the electrolyte solution bind the metal ions generated by the anode reaction.

With the addition of another silver/silver bromide electrode, the polarographic sensors can be connected to form a three-electrode cell. They no longer have an anode in the classical sense. One of the silver/silver bromide electrodes acts as a counter electrode (to provide the current) and the other one acts as an independent reference electrode. Current does not flow through this electrode and, thus, it can maintain a much more constant potential than a conventional electrode could.

In the preceding chapter the significance of the sample temperature for oxygen measurements was already outlined (dependency of the various variables on temperature).

Furthermore, the oxygen permeability of the membrane is temperature-dependents. Therefore, in addition to the external temperature probe (sample temperature!), another probe is required and is built into the sensor head. With these two temperature values, the instrument can compensate for the influence of temperature on the oxygen permeability of the membrane.

Another important factor for in situ oxygen probes is the flow of water across the membrane that has to be ensured during measurement in order to prevent an oxygen-depletion near the membrane. However, this is uncritical in Ferrybox measurements due to their inherent flow system. The membrane properties mainly determine the stability of the sensor: Since inside the sensor chamber oxygen is consumed by the polarographic process there is a steep gradient of the oxygen concentration over the membrane. This gradient is dependent on the thickness and permeability of the membrane. Any change, e.g. an increased permeability due to a biofilm formation on the membrane (biofouling), directly changes the reading of the sensor.

---

<sup>1</sup> Tables for salinity correction can be found e.g. at <http://water.usgs.gov/owq/FieldManual/Chapter6/6.2.4.pdf>.

Another critical factor for these sensors is the mechanical behaviour of the membrane: If the tension changes due to handling or stress there is a direct influence on the measured value.

In the GKSS Ferrybox Cuxhaven – Harwich an Endress & Hauser oxygen sensor COS 4 with electronic unit LiquiSis COM 223 was used. In Figure 3-1 a photo of the sensor and electronic unit is shown.

The measuring range of the sensor is 0.05- 20 mg/L; the time constant is 3 min (90%).



Figure 3-1: Endress & Hauser oxygen sensor with electronic unit (Source: E&H).

### 3.1.3 Calibration of the Sensor

Because the measuring process consumes the electrolyte solution in the sensor head calibration must also be carried out for dissolved oxygen measurements at regular intervals. The ions of the electrolyte solution bind the released metal ions, thereby changing the composition of the solution. The recommended calibration interval depends on the oxygen sensor used and ranges from two weeks to one month.

In principle, each linear calibration function is defined by two points: Zero and near 100% saturation. However, with modern sensors such as the Endress & Hauser sensor, the sensor signal obtained in the absence of oxygen (“zero point”) lies below the resolution of the sensor. Therefore, only a one-point calibration has to be carried out.

There are three possibilities for calibration of oxygen sensors:

- 1) Comparison with water samples and measurement by Winkler titration.

This is the most exact method, however, the whole process is complex and requires experienced personal.

- 2) Calibration in air-saturated water.

This method is prone to errors concerning over-saturation of the water under certain circumstances. Care has to be taken to provide enough water movement (stirring, bubbling of air) during the calibration.

- 3) Calibration in water-saturated air.

When using this method care has to be taken to avoid temperature fluctuations by evaporation etc. in the closed calibration chamber.

Within the FerryBox project method 1) was used on the NERC.NOC ferry “Pride of Bilbao” and method 3) was used on the GKSS ferry Cuxhaven – Harwich.

The calibration is carried out by placing the sensor into a small semi-closed container with a wet sponge at the bottom (free pressure exchange with the atmosphere is necessary). It is important to ensure that there are no water droplets on the membrane. Otherwise, the calibration would partially take place in water! It is particularly important to take precautions after the sensor has been stored in the calibration vessel for an extended period of time and condensation droplets may have formed on the membrane.

Modern instruments such as the one used within the FerryBox project (Endress & Hauser Sensor COS 4 with electronic unit COM 223) totally automate the calibration process: After having the sensor equilibrated in the enclosed container just the appropriate method (“water in air”) is chosen. All necessary constants are stored in the instrument and the slope is determined automatically.

### 3.1.4 Reliability and Applicability

The Endress & Hauser oxygen electrode is a robust sensor. It is very stable due to its large membrane-covered area and relatively thick membrane (which increases the time constant to about 3 min).

Under normal conditions, i.e., no additional stress on the membrane due to the constant water flow of the Ferrybox system, a membrane lasts for more than a year before it has to be replaced (together with a replacement of the internal electrolyte). At this occasion a cleaning/regeneration of the silver anode should be carried out.

In the GKSS Ferrybox system with automated cleaning (acidified water) a calibration only had to be carried out in intervals of 1-2 months. However, this not necessarily can be applied on other systems with different cleaning procedures.

### 3.1.5 Data Availability

In Figure 3-2 and Figure 3-3 the archived data from measurements on the German Ferrybox Cuxhaven – Harwich are shown.

As can be seen from the graphs in each spring high over saturation values of up to 130% occur due to plankton blooms. The blooms start near 5°E, afterwards spread to more eastern and western regions and finally decline in summer, mainly due to nutrient deficiencies.

### 3.1.6 Maintenance

Apart from the 1-2 monthly calibrations and yearly membrane/electrolyte replacements no other maintenance is required. However, as with all other Ferrybox data a daily check on the data with following plausibility check is necessary.

### 3.1.7 Quality Assurance

For quality assurance a thorough calibration of the sensor is required. When the reading of the sensor is in concentration units (mg/l or mmol/m<sup>3</sup>) the dependence of oxygen solubility on salinity has to be taken into account.

In order to avoid measuring errors due to outgassing of oxygen or input of air into the measuring system initial checks should be carried out when installing a new system on a ferry. Even if the sensor measures the oxygen content inside the Ferrybox system accurately the question is whether this exactly corresponds to the oxygen content in the outside water. Depending on the construction of the Ferrybox system (type of water inlet, pumps etc.) there could be an input of oxygen in under-saturated waters or an outgassing of over-saturated water. This should be checked during the initial tests or by reference samples from a separate ship.

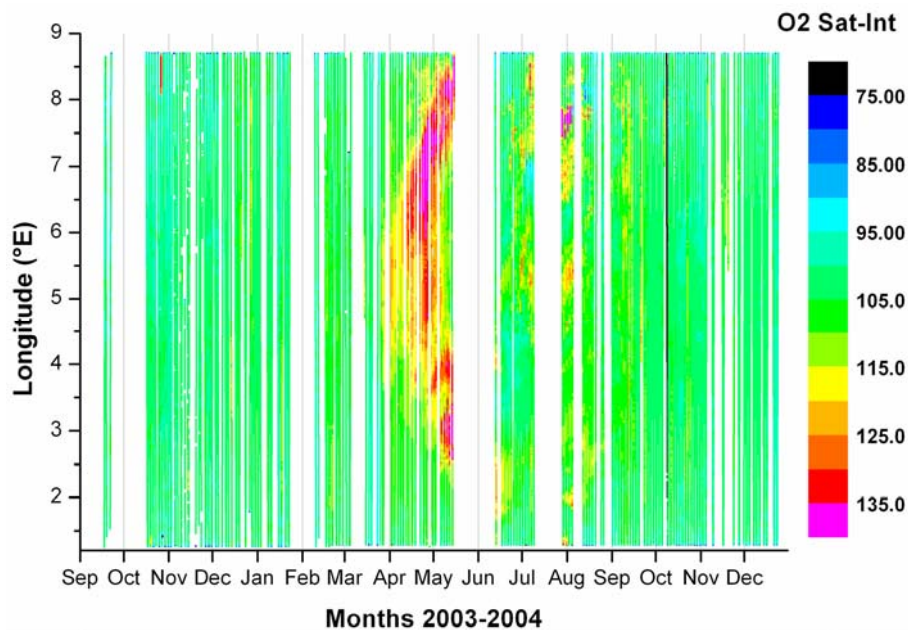


Figure 3-2: Dot plot of the archived data from the GKSS Ferrybox Cuxhaven – Harwich in 2003 and 2004.

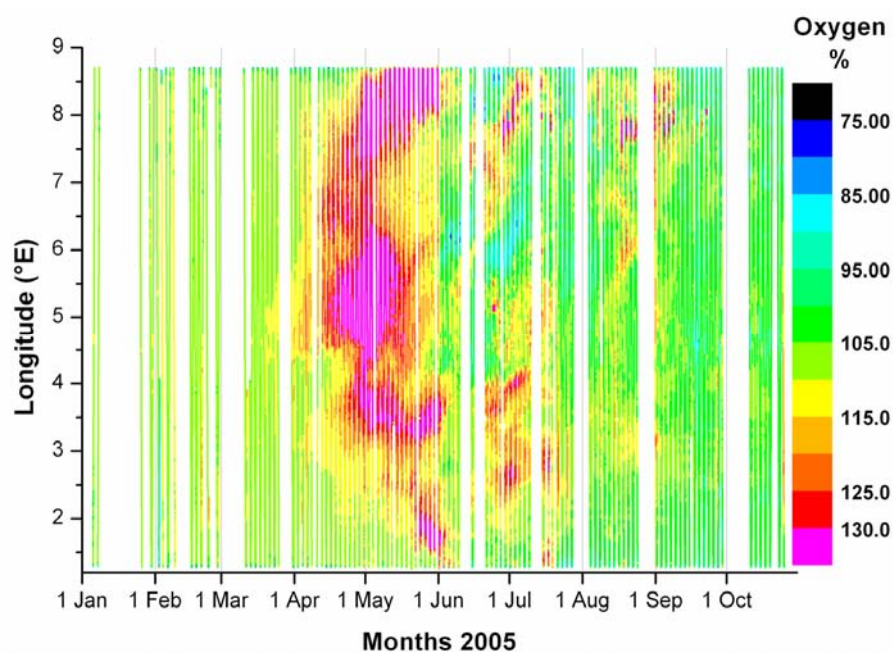


Figure 3-3: Dot plot of the archived data from the GKSS Ferrybox Cuxhaven – Harwich in 2005.

## 3.2 Oxygen Sensor: Fluorescence Quenching ("Optode")

### 3.2.1 Description of the Sensor

Tenberg et al (submitted) have produced a paper, which describes in detail the development of the idea of the oxygen Optode and its application in a number of environments including long-term deployments on mooring. The reference point for all oxygen measurements is the "Winkler Method". The standard method to determine concentrations of oxygen in water is a two-step wet chemistry precipitation of the dissolved oxygen followed by a titration. The method was first described by Winkler (1888) and has since become the standard method. Winkler titration is always performed on collected water samples. The collection and handling of water samples can induce errors and the analytical work is time consuming and demands meticulous care. It is therefore not a suitable method to obtain in-situ data with high spatial and temporal resolution.

Tenberg et al (submitted) have shown that the oxygen Optode provides a more suitable method than electrochemical sensors for direct measurement of dissolved oxygen. Optode technology has been known for years but it is relatively new to the aquatic research. The fundamental principle is based on the ability of selected substances to act as dynamic fluorescence quenchers. In the case of oxygen, if a ruthenium complex is illuminated with a blue light it will be excited and emits a red luminescence with an intensity and lifetime that depends on the ambient oxygen concentration. It is important to distinguish between three different principles in detecting the red luminescence: Intensity (how strong the return is), life-time (how quickly the return dies out) and phase shift (in principle also a life time based measurement, see below Measurement Principle). Intensity based measurements are technically easier to do, but they can drift over time. The different signal detection techniques are summarized by Wolfbeis (1991), Demas et al. (1999) and Glud et al. (2000) along with a wide range of applications. The function and use of lifetime-based Optodes was described by Holst et al. (1995) and Klimant et al. (1996).

### Measurement Principle

The "Oxygen Optode" from Aanderaa Instruments is based on oxygen luminescence quenching of a platinum porphyrins complex. The lifetime and hence the oxygen measurement is made by a so-called phase shift detection of the returning, oxygen quenched red luminescence. The relationship between oxygen concentration and the luminescent decay time can be described by the *Stern- Volmer* equation:

$$[O_2] = \frac{1}{K_{SV}} \left\{ \frac{\tau_0}{\tau} - 1 \right\}$$

Where:  $\tau$  = decay time,  $\tau_0$  = decay time in the absence of oxygen and  $K_{SV}$  = Stern-Volmer constant (the quenching efficiency).

The foil is excited with a blue-green light modulated at 5 kHz. The decay time is a direct function of the phase of the received red light, which is used, directly for oxygen detection, without calculating the decay time. The basic working principles of dynamic fluorescence quenching, lifetime-based Optodes and phase shift detection can be found in e.g. Klimant et al. (1996); Demas et al. (1999); Glud et al. (2000). The sensor housing is made of Titanium, rated to 6000 dbar pressure, with a diameter of 36 mm and a total length of 86 mm.



This housing includes an optical part (Figure 3-4), a temperature sensor and the necessary electronics (a microprocessor with digital signal processing capacity) to process signals and output absolute temperature compensated oxygen readings (in  $\mu\text{M}$  or % saturation). The sensing foil is composed of the oxygen sensitive fluorescent substance (luminophore) that is embedded in a polymer layer, which is coated onto a thin film of polyester support. The most commonly used oxygen luminophores have been ruthenium complexes (e.g. Klimant et al.) but for this sensor an oxygen sensitive luminophore based on a platinum porphyrine complex, commercial available from PreSens GmbH (Regensburg, Germany) was used due to its higher dynamics.



Figure 3-4: Photograph of the Aanderaa Optode removed from its housing for cleaning as installed on the NERC.NOC Ferrybox on “Pride of Bilbao”.

Two types of foils, with and without, a gas permeable protective black silicon layer are available (Figure 3-5). Figure 3-5: Diagram of the optical design of the Aanderaa oxygen Optode (taken from Tenberg et al., submitted).

). The silicon layer also acts as an optical isolation layer to avoid potential influence from fluorescent material in the surrounding water and/or direct incoming sunlight, when measuring in the photic zone. The disadvantage of this layer is that the sensor response time becomes

longer. On the NERC.NOC Ferrybox the silicon coated type is used as it was considered it might be more durable for long-term deployments such as on the Ferrybox.

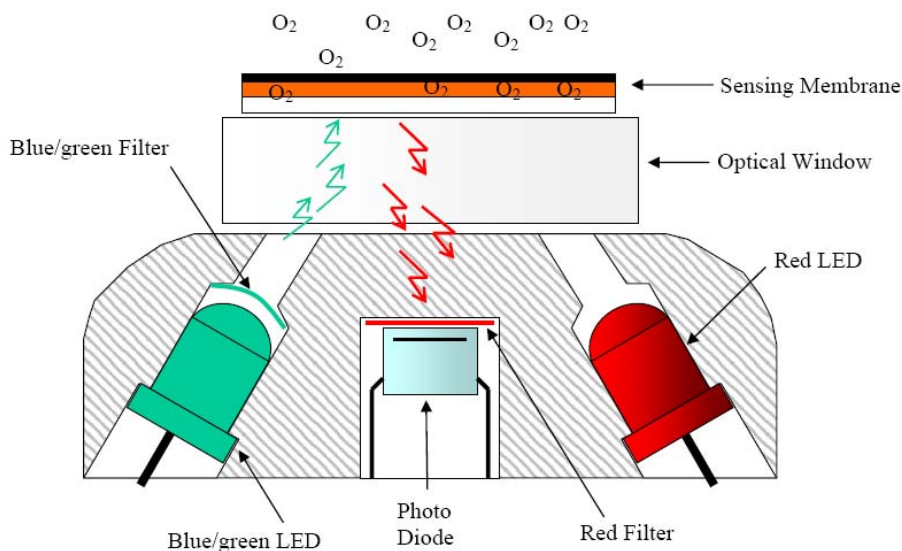


Figure 3-5: Diagram of the optical design of the Aanderaa oxygen Optode (taken from Tenberg et al., submitted).

### 3.2.2 Reliability and Applicability

The Aanderaa Optode is easy to fit in a Ferrybox system as it is compact unit with single lead to take power to the sensor and return RS 232 based data output to what ever logging system is used. The data output string is the Optode temperature and the temperature compensated oxygen readings in  $\mu\text{M}/\text{litre}$  and % saturation. This data is based on the assumption that the water sampled is zero salinity. It has to be post processed to calculate the true oxygen concentration at the temperature and salinity measured at the time of sampling and to calculate the % saturation in-situ. This latter calculation is made using the best available measurement of the in-situ temperature.

#### Experiences from the NERC.NOC Ferrybox

The Aanderaa Optode proved to be a highly reliable piece of equipment. The unit was first fitted to test its use in December 2004. While the ship was in refit in January 2005 the unit was returned to Aanderaa for recalibration, and it was refitted to ferry on the 16 February. Since then the same unit has run continuously without need for intervention other than cleaning of the membrane which as been done approximately every nine days during 2005, after the first three months of operation when the sensor was not cleaned. No jumps in sensor output have been detectable in conjunction with servicing events.

The unit had to be returned to Aanderaa for recalibration as we were wrongly advised by Aanderaa's UK agents to calibrate the units ourselves. This proved difficult to do because calibration has to be done using water, which is 100%, saturated. We discovered that such water is difficult to achieve without using equipment, which is not normally available in a laboratory. User recalibration of the units would be relatively simple if a measured oxygen value could be entered into the unit through its software rather than telling it is in saturated water.

### 3.2.3 Data Availability

There have been no problems with data availability from the unit itself. However, a minor problem exists with the data at the moment due to faults with other parts of the system. The success of the system in this respect is shown in Figure 3-6. This is dot plot of all the data archived for 2005 between 19 February and 5 November. The missing data around day 260 is due to a power supply failure to the whole Ferrybox system.

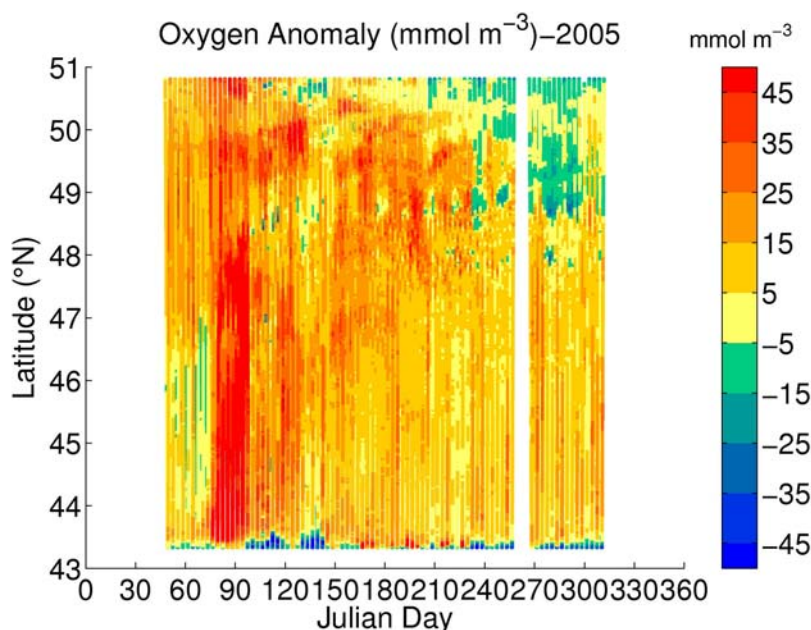


Figure 3-6: Dot plot of all Aanderaa oxygen Optode data for 2005 for the NERC.NOC Ferrybox, using 5 minute averaged data and showing the calculated oxygen anomaly which is the difference between the measured oxygen concentration and the saturation concentration for water of the same temperature.

### 3.2.4 Maintenance

This sensor requires no significant level of extra maintenance.

### 3.2.5 Quality Assurance

On the 6 calibrations crossing carried out from February to July 2005 a total of 608 Winkler titrations were performed on pairs of samples. The average absolute difference between Winkler samples was  $1.8\mu\text{M/l}$ . The mean difference between Optode and Winkler values was  $0.9\mu\text{M}$  with mean absolute difference of  $6.8\mu\text{M/l}$ .

Taking the lower value of each pair to be the more reliable value, and regressing these values against the Optode values, the calibration coefficient calculated by a least squares fit forced through the origin is 1.007 with an  $r^2$  value of 0.95, see Figure 3-7. The variation of the calibration from month to month is shown in Figure 3-8 and Figure 3-9.

There is no sign in these plots of any significant drift in the data produced by the Optode. This level of accuracy is better than the value advertised by Aanderaa of " $8\mu\text{M}$  or 5%".



However, because of the problem we have experienced with calibration of the CTG MiniPack in 2005, as the data has to be recalculated on the basis of the salinity of the samples, a final oxygen data set has not been produced at the time of this report. We are still trying to find a rigorous method for removing jumps in the conductivity determined by the MiniPack associated with cleaning events in 2005. At present we consider that the salinity data measured in 2005 is not reliable to levels better than 0.5. This gives a potential error in the calculated oxygen value of  $1\mu\text{M/l}$ , which is probably not significant compared to the level to which the data can be calibrated on the basis of Winkler titration determinations of oxygen concentration of water samples to the nearest corresponding recorded Optode value.

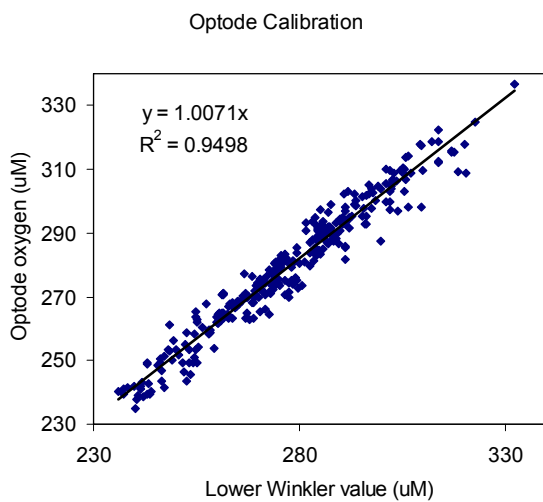


Figure 3-7: Plot of all lower values of pairs of oxygen water samples against corresponding Optode values (303 samples, from the NERC.NOC Ferrybox on "Pride of Bilbao").

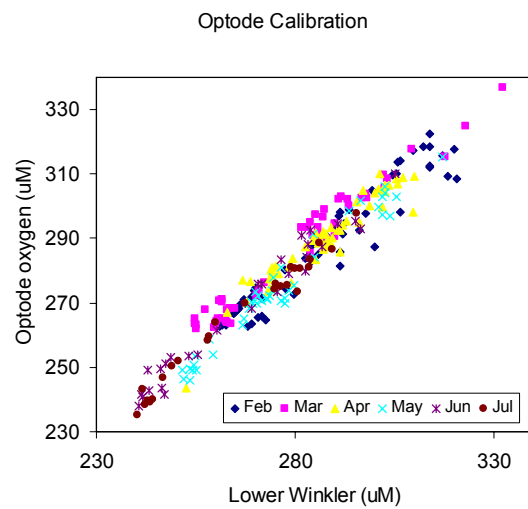


Figure 3-8: Plot of all lower values of pairs of oxygen water samples against corresponding Optode values as in Figure 3-7 but with the data from the 6 individual calibration crossings identified (from the NERC.NOC Ferrybox on "Pride of Bilbao").

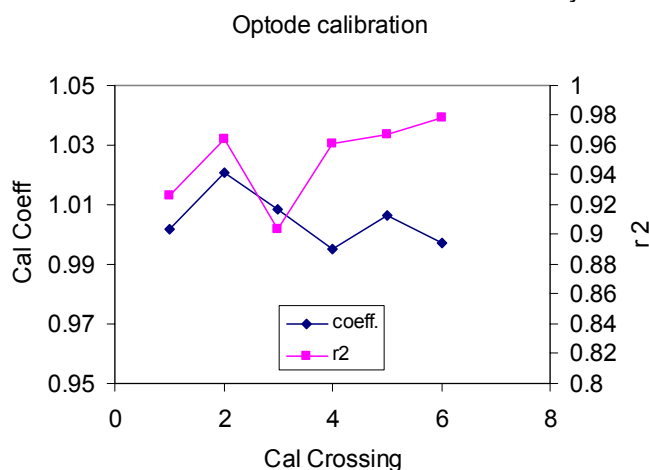


Figure 3-9: Plot of the values of the calculated calibration coefficient and  $r^2$  values for each set of calibration data shown in Figure 3-7 on the basis of a least squares fit forced through the origin (from the NERC.NOC Ferrybox on "Pride of Bilbao").

## Results from the GKSS Ferrybox

A comparison between oxygen concentrations (saturation index) of measurements with the Endress & Hauser membrane-covered sensor and an Aanderaa Optode on the GKSS Ferrybox Cuxhaven – Harwich is depicted in Figure 3-10. As can be seen the correlation is good. However, there are small deviations of maximal  $\pm 4\%$  O<sub>2</sub> saturation. The reasons are not quite clear. It may be attributed to deviations in the calibrations of the membrane-covered electrode or to different time constants of the two sensors.

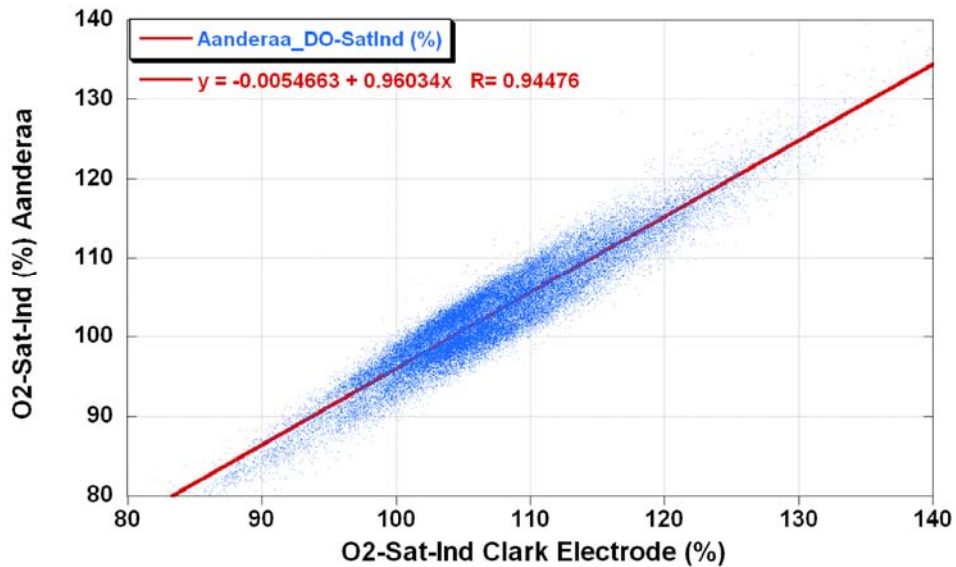


Figure 3-10: Comparison of oxygen measurements between membrane-covered electrode (Clark) and an Optode (Aanderaa) on the GKSS Ferrybox Cuxhaven – Harwich, June – September 2005.

## 3.3 pH Sensor

### 3.3.1 General Description

pH measurements are predominantly conducted with pH-sensitive glass electrodes, which have, in general, proven satisfactory in measurements of pH. However, the behaviour of pH-sensitive glass electrodes often falls short of what precision is required.

Even with the most careful treatment, the potential of cells containing glass electrodes often drifts slowly with time after such cells were placed in a new solution. Drift of cell potentials is an especially severe problem in investigations dependent on precise observation of small pH differences.

Measurements involving cells with liquid junctions are subject to further uncertainties due to the dependence of liquid junction potentials upon medium concentration and composition and due to pressure changes in the Ferrybox system.

Ideally, the change in liquid junction potential (residual liquid junction potential) between test solution and standardizing buffer should be small or at least highly reproducible. In practice, systematic errors between many measurements suggest that the reproducibility of the residual liquid junction potential is often poor and that residual liquid junction potentials are dependent on the construction and/or history of the liquid junctions used in various investigations.

Since pH fluctuations in marine waters are very small an absolute accuracy of less than 0.1 pH units and a resolution of at least 0.01 pH units is required. For an assessment of the CO<sub>2</sub>/CO<sub>3</sub> systems even a higher accuracy is necessary.

### 3.3.2 Description of the Sensor

Within the FerryBox project GKSS used a standard pH Glass Electrode, Endress & Hauser Orbisint CPS 11 together with an electronic unit Liquisys M CPM 223. The electrode is fitted with a PTFE diaphragm, is filled with gel and contains an integrated Pt100 temperature sensor for temperature compensation. It is relatively stable against pressure fluctuations within the Ferrybox system. A photo of the system is shown in Figure 3-11.



Figure 3-11: Endress & Hauser pH electrode and electronic unit.

### 3.3.3 Calibration

For calibration the standard procedure is applied, using two buffer solutions with  $\text{pH}=7\pm 0.02$  and  $\text{pH}=9\pm 0.02$  (Titrisol from Merck) which can be traced to SRM (NIST) and PTB (Germany). Temperature corrections of the buffer solution as given by the manufacturer were applied.

### 3.3.4 Reliability and Applicability

When installing a pH electrode in a Ferrybox system, e.g., in a T-connection of the flow system, care has to be taken to include the temperature sensor near the glass electrode, immersed in the flow system. This is made easier with the Endress & Hauser electrode in which a Pt100 sensor is integrated. The glass membrane should be installed directly in the water stream in order to keep it clean. On the other hand, too high pressures on the diaphragm could reduce the lifetime and produce noise on the reading.

During the frequent calibrations care has to be taken in the handling of the fragile glass electrode.

If a “closed” Ferrybox system with higher internal pressures is used, the applicability of the gel junction has to be checked. (In critical cases pressure compensation has to be applied).

### 3.3.5 Data Availability

Figure 3-12 shows a dot plot of the data archived for 2003 – 2004 and Figure 3-13 depicts the archived data for 2005. The primary production period that has already been discussed in the section for oxygen can clearly be seen, starting in late April and ending in June. In principle the diagram shows a similar picture like the chlorophyll-fluorescence. However, here not only the plankton concentration but also the productivity is reflected.

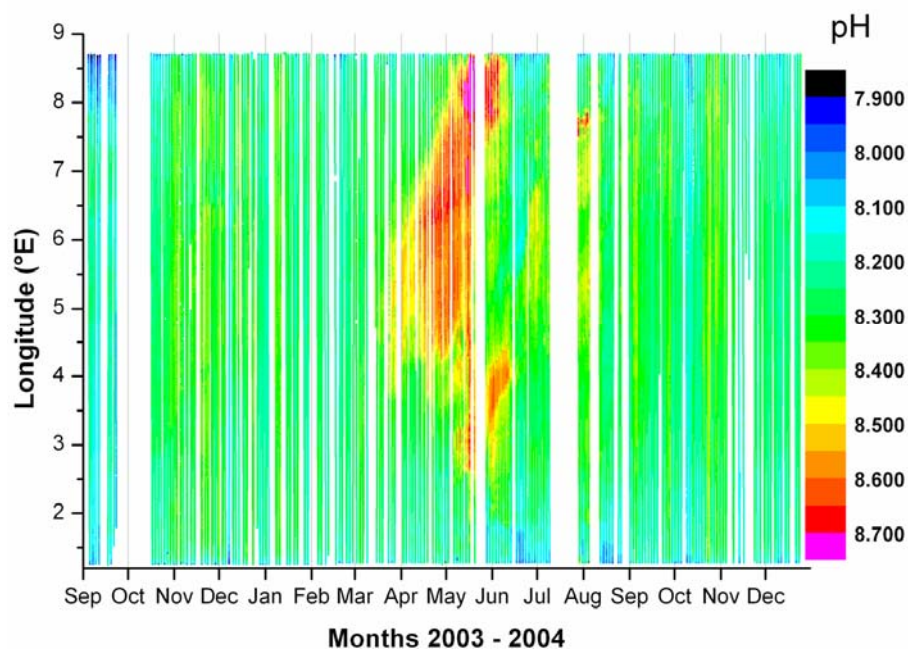


Figure 3-12: Dot plot of the archived data from the GKSS Ferrybox Cuxhaven – Harwich in 2003 and 2004.

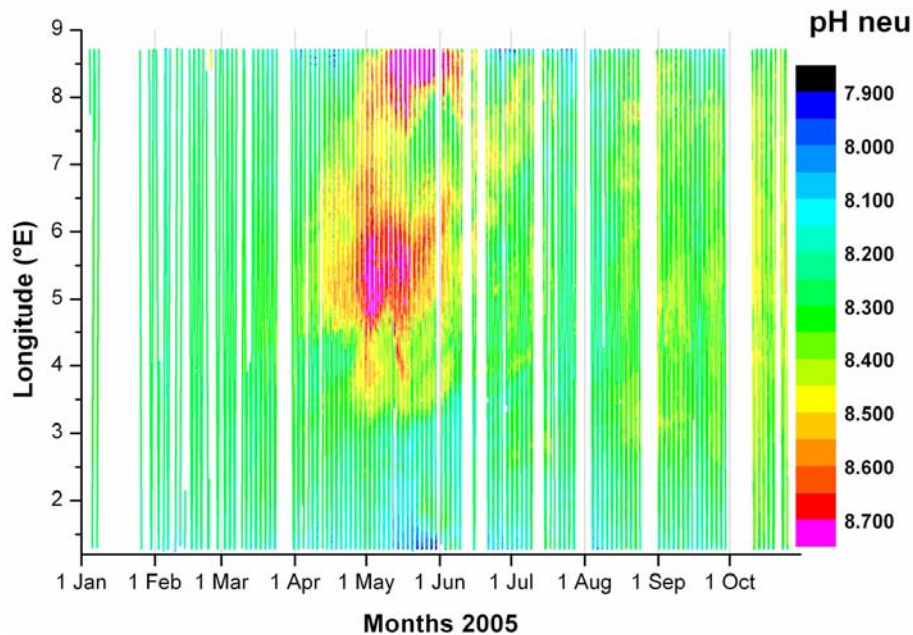


Figure 3-13: Dot plot of the archived data from the GKSS Ferrybox Cuxhaven – Harwich in 2005.

### 3.3.6 Maintenance

For quality assurance a weekly calibration is necessary in order to reach an accuracy of 0.05 pH units. With the antifouling strategies of the Ferrybox (automated pressure cleaning with acidified water) a lifetime of the electrode of about one year is reached.

### 3.3.7 Quality Assurance

Due to the required high accuracy a check on the calibration each week is necessary. This requires the removal of the electrode and calibration with the two buffer solutions. Under these conditions –together with the antifouling strategies of the Ferrybox – an absolute accuracy of about 0.05 pH units can be maintained between the calibration intervals.

## 3.4 Acoustic Doppler Current Profiler (ADCP)

### 3.4.1 Description of the Sensor

#### General

The most popular ADCP uses a scheme of four ceramic transducers, which are aimed in such a way that the mono-frequency, sound pulse they produce travels through the water in four different directions. As scatterers in the water return the echo of the sound, it is shifted in frequency due to the Doppler effect.

The device used in the project is manufactured by NORTEK, Norway (Type: Vessel Mounted Current Profiler (VMCP), bronze housing). It emits sound waves at a frequency of 1 MHz. The sound waves are partly reflected by particles in the water at different depths. The reflected waves are registered by the ADCP. The deeper the signal reaches, the later it returns. Thus, by measuring both the strength of the returned signal and the time interval between the emission and reflection of the signal, information is gathered on the amount of particles at a certain depth. The main objective of the ADCP, however, is to measure current velocities. For this it uses the Doppler shift. If a particle reflecting the sound wave is being transported at a velocity relative to the ADCP, then the frequency of the reflected signal is different from the frequency of the emitted signal. If a particle does not move with respect to the ADCP or moves perpendicular to the emitted wave, no Doppler shift occurs, so no velocity can be determined. For all three directions from which the ADCP detects reflected waves, the velocity components are determined. Combining the individual results of three arms yields a three dimensional picture of the velocity field. For current profile measurements from a moving system, e.g., a ship, the velocity of the ship has to be determined since the absolute current velocities and not the velocities relative to the ship movement are required. In shallow waters this is carried out by using the "bottom signal" of the ADCP, which gives the ship velocity in two directions.

On the ferry between Den Helder and Texel the instrument is attached to the haul of the ferry at some 30 cm below the haul itself to prevent problems with air bubbles. The entire system is protected from debris etc. by an iron cage. A dedicated pipe (diameter some 10 cm) was welded inside the ferry from above the water level to near the instrument (through the haul). All cables for power supply and data transfer run through this pipe. First installation had to be done during a dry dock period.

### 3.4.2 Reliability and Applicability

Once the system is operating, the reliability is large and the instruments need only minor servicing. In principle such a system can be installed under any vessel. Whether or not such a device will give reliable results depends on:

- The speed of the ferry
- The magnitude of the currents
- The concentration of suspended material (number of scatterers)

The quality of the observations in the Marsdiep tidal inlet is relatively good. The speed of the ferry is on average 10-12 knots. This combined with the relative high magnitude of both the tidal currents in this area (up to 2 m/s) and the amount of suspended sediments (typical 10-50 mg/l), makes this area very suitable for such ferry observations.



However, before applying such an ADCP on another ferry and on another route, it is recommended first to test the quality of the data return on that specific route, e.g. by having a test cruise with a research vessel equipped with a similar ADCP.

Another practical difficulty may be to obtain permission and support from the ferry company.

### 3.4.3 Data Availability

The quality of the data is very good. Almost all failures in the complete system of data gathering and data storage are due to problems in the data storage phase, both by hardware (PC) and software problems. Such problems result in a total return of good data of some 90 % (Figure 3-14).

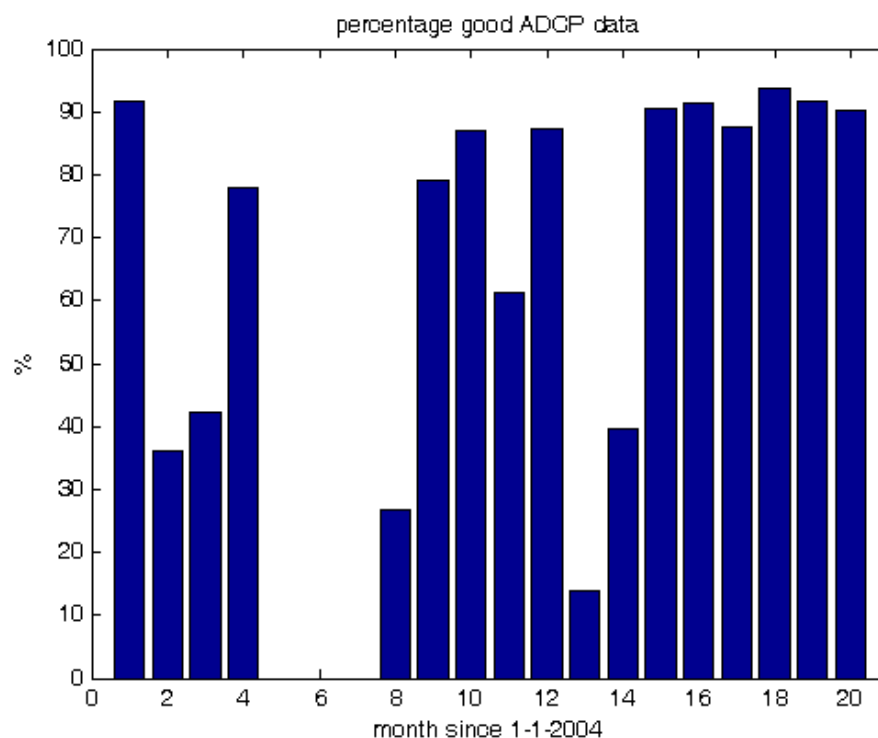


Figure 3-14: Percentage of good ADCP data return, as compared to a 100 % return if the ferry would sail and measure always. The months run from January 2004 (1) to August 2005 (20).

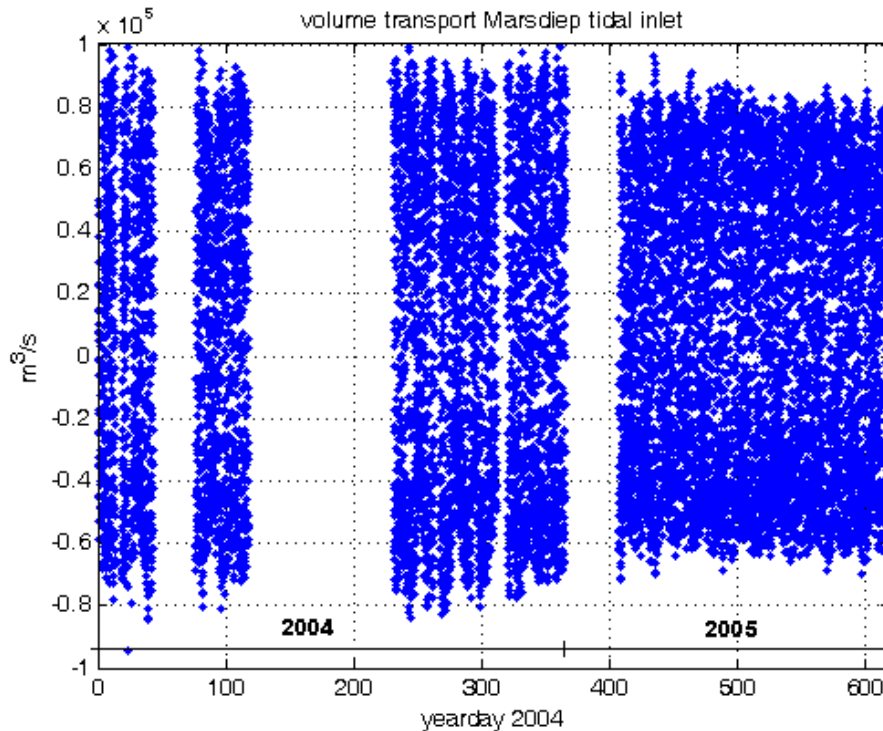


Figure 3-15: Water volume transport through the Marsdiep tidal inlet as derived from observations with an ADCP installed on the Texel – Den Helder ferry.

Other periods with a low data return are simply because the ferry was partly out of service (in the beginning of each year) for maintenance. In the summer of 2004 there is a longer period with no data (3 months). This is because the ferry hit a sandbank and damaged the ADCP seriously in early May 2004. The instrument was sent to the manufacturer and a repaired version was installed again in August 2004.

#### 3.4.4 Maintenance

A big advantage compared to other (especially optical) sensors is that biofouling can easily be prevented and/or does not influence the observations. Thus, maintenance of the sensor itself is minimal and normally done only when the ferry is in dry dock. Strong vibrations in the connecting cables may give problems. In our device maintenance can be done only when divers take the instrument off the ferry. Other maintenance issues have to do with the software that is used to run the ADCP and to store the data. However, due to the high amount of data the evaluation, especially concerning suspended matter concentrations is a full of hard work. In a new ferry a moon-pool is installed which allows an easier maintenance of the ADCP since it can be removed without divers.

#### 3.4.5 Quality Assurance

Part of the quality check of the data is handled by the manufacturer's software. This relates to the calculated velocity profiles. If there is interest in relating the backscatter intensity to the amount of suspended material, intensive calibrations need to be performed



## 3.5 Multi-wavelength Fluorometer for the Detection of Algal Groups

Tested on the GKSS Ferrybox Cuxhaven – Harwich

### 3.5.1 Description of the Sensor

Algae contain a certain quantity of photosynthetic pigments (“antenna pigments”), which enhance the usable part of the light spectrum. The different spectral groups of algae (green group, *Chlorophyta*; blue-green, blue-green algae; brown, *Heterokontophyta*, *Haptophyta*, *Dinophyta*; mixed, *Cryptophyta*) are each characterised by a specific composition of photosynthetic antenna pigments. After excitation of these antenna pigments by a specific wavelength a fluorescence signal at 680 nm (chlorophyll-fluorescence) is emitted. Therefore, it is possible to distinguish between different divisions of algae by their fluorescence excitation spectrum. The “FluoroProbe” (company bbe moldaenke, Germany) for algae differentiation uses 5 LEDs for fluorescence excitation. The LEDs emit successively pulsed light at selected wavelengths (450 nm, 525 nm, 570 nm, 590 nm and 610 nm). Their spectra are shown in Figure 3-16. Fluorimetric emission is measured at 680 nm by a photomultiplier at an angle of 90 degrees to the exciting light source.

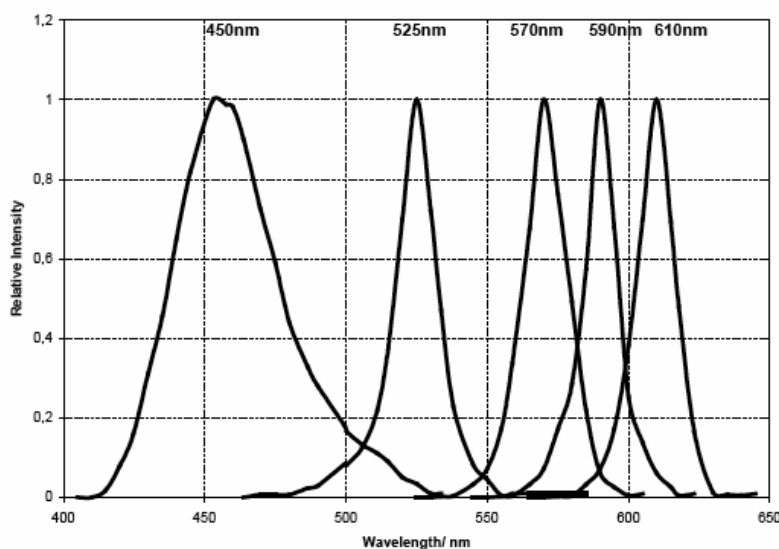


Figure 3-16: Spectral intensities of used LEDs (intensity is normalised to the maximum of each LED (Source: bbe moldaenke).

In Figure 3-17 the spectra of different algae are shown. As can be seen the division of *chlorophyceae* (green algae) shows a broad maximum of fluorescence at the 450 nm LED that corresponds to chlorophyll-a and chlorophyll-b excitation. The *cyanophyceae* (blue green algae) pigments are characterized by a maximal excitation at 610 nm caused by the photosynthetic antenna pigment phycocyanin. Although *cyanophyceae* contain chlorophyll-a too, the spectrum shows only a low intensity at 450 nm. This is due to the masking effect of the phycocyanin.

Furthermore, the high peak at the 525 nm region for the *bacillariophyceae* originates from the xanthophyll fucoxanthin and from peridinin (*dinophyceae*).

The maxima at 450 nm are caused by chlorophyll-a and -c. In the last group, *cryptophyceae*, a significant maximum at 570 nm that originates from phycoerythrin can be found.

It is obvious from Figure 3-17 that it is not possible to differentiate *bacillariophyceae* and *dinophyceae* by their „fluorescent fingerprint“ at this level of discrimination. However, it can be clearly seen that it is possible to distinguish four groups of algae: *chlorophyceae*, *cyanophyceae*, *dinophyceae* plus *bacillariophyceae* (the brown group) and *cryptophyceae*.

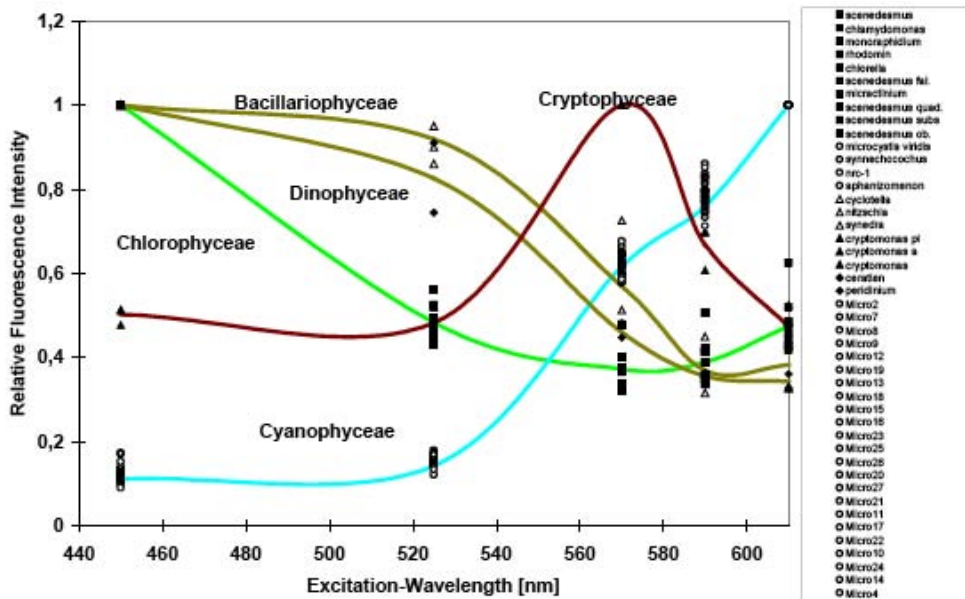


Figure 3-17: Spectra and Fluorescence intensities of the 5 algal divisions multiplied by the intensity of the LED and normalised to the maximum intensity of each division..

For installation into the GKSS Ferrybox Cuxhaven – Harwich a flow-through instrument was chosen (see Figure 3-18 below) which contains a motor-driven cleaning plunger that removes regularly any films or dirt from the wall of the flow cell (in addition to the automated cleaning cycle of the Ferrybox).



Figure 3-18: Photo of the bbe Algal Online Analyser (AOA).

### 3.5.2 Reliability and Applicability

The problem with this sensor is the necessity to be set-up with the “right” types of algae, i.e., for freshwater species other parameters in the algorithms have to be used than in marine waters. The same may apply to tropical waters. Due to the similarities in the pigment distribution of different algae groups, it is possible that some algae are sorted into the “wrong group”. For example, since it is not possible to distinguish accurately between diatoms and flagellates (which in the North Sea are quite common), a part of the signal appears wrongly in the “green channel”. For other waters with other algae the application of the instrument may be more valuable.

The quantification in terms of  $\text{mg/m}^3$  should be taken with caution. However, the instrument is quite useful as indicator for a shift in the algae communities (“finger print”) along a transect or over a seasonal cycle. For example, the output of the sensor can be used to trigger a water sample, which later can be analysed under the microscope (preservation necessary).

### 3.5.3 Data Availability

Due to the high effort needed for laboratory HPLC analyses there were no frequent comparisons with HPLC pigment analyses or microscopic counts of algae species. Therefore, no dot plots of “accurate” algae groups can be presented.

### 3.5.4 Maintenance

There is no additional maintenance necessary when the standard automated cleaning cycles of the Ferrybox are active. In near-shore waters with high load of suspended matter (and occasionally fine sand) after 2 years of operation the walls of the flow tube showed fine scratches from the cleaning plunger, which reduced its sensitivity. The tube had to be replaced by the manufacturer.

### 3.5.5 Quality Assurance

Comparisons of the sensor reading with microscopic counts of algae species were carried out. However, since the instrument measures rather pigments than structural pattern a direct comparison is difficult. Occasional comparison with HPCL pigment analyses also showed a high scatter. It must be concluded that the sensor gives good “hints” which simplifies the interpretation of results, but its quantitative capabilities have to be investigated further. This does not apply to the readings of “total chlorophyll-a”. Mostly, these values correlate much better to chemical analyses than the standard chlorophyll-fluorescence data.

## 3.6 Fast Repetition Rate Fluorometer (FRRF)

### Tested on the NERC.NOC Ferrybox “Pride of Bilbao”

#### 3.6.1 Description of the Sensor

The CTG FAST<sup>tracka</sup> FRRF offers rapid, real-time, *in situ* measurements of photosynthetic characteristics of phytoplankton. It exposes phytoplankton to a series of microsecond flashes of blue light at 200 kHz a repetition rate, a saturation profile of PSII variable fluorescence is observed and recorded. Analysis of the observed fluorescence signal and knowledge of the excitation protocol allows calculations of the absorption cross-section of PSII, the efficiency of photochemical conversion, and the rates of electron transport from PSII to PSI. The FRRF is designed to measure these parameters on dark adapted and ambient irradiated samples *in situ*. In the set up on this Ferrybox only the dark-adapted channel was used.

Analysing the saturation profile of variable fluorescence induced by a sequence of fast repetition flashes allows evaluation of the following parameters:

- F<sub>o</sub> Background fluorescence yield when all reaction centres open
- F<sub>v</sub> Background fluorescence yield under ambient light
- F<sub>m</sub> Maximum fluorescence yield when all reaction centres closed  $\tau$
- $\tau$  Time constants of electron transport from PSII to PSI (s)



Figure 3-19: Recovery of a normal research deployment of an FRRF in which it is used in conjunction with net sampling of the associated plankton so the taxa present in the water are known and the FRRF response can be correlated with the taxa.

Including the measured photosynthetic parameters in appropriate models relating fluorescence and photosynthesis allows calculation of photochemical and non-photochemical quenching, photochemical conversion efficiency, and primary production. Other incidental parameters are recorded by the instrument for monitoring performance and calibration, and include internal temperature, battery status, and error codes.

The electronic system of the FAST<sup>tracka</sup> is built around a Motorola MC68332 microcontroller operating at variable clock speeds up to 16 MHz, a flexible FPGA digital logic system. The FAST<sup>tracka</sup> optical system uses a high-speed fast repetition rate blue LED light source and a sensitive photomultiplier emission detector designed for the excitation and observation of chlorophyll fluorescence. Data may be stored internally on a PCMCIA flash disk, or transmitted serially over a host cable to a computer or terminal device. A separate “deck unit” has to be used to supply power and communicate with the flash disc.

### 3.6.2 Reliability and Applicability

For use on the FerryBox project the planned programme of investigation was that CTG would have made available a Mk 11 version of the FRRF (designed as low cost single (dark) channel instrument) for testing by a number of Ferrybox operating partners. Due to delays in the development of the Mk II only a single MK I instrument was available for testing by NERC.NOC for a limited amount of time.

To install the instrument in the NERC.NOC Ferrybox a water circuit in parallel to the supply to the main sensors was used. This included a valve to control the flow rate past the sensor head to between 0.5 and 1 litre per minute. This was so that plankton would remain in the view of the sensor light source and detector long enough for photo-saturation to be produced by the FRRF flashes. Figure 3-20 shows the initial test installation on the “Pride of Bilbao” during the calibration crossing in December 2004. The data is shown in Figure 3-21.



Figure 3-20: Initial test installation of the FRRF in December 2004 as part of the NERC.NOC Ferrybox system on “Pride of Bilbao”.

No problems were encountered with the reliability of the system.

The weight of the unit was a factor, which had to be taken into account. As shown in Figure 3-20 it could only be mounted in position where its weight could be supported. This was not a problem on the “Pride of Bilbao” where space and access to the installation is easy. However this may be problem on other ships where space and access are limited. Manual handling of the instrument in its transport case was a concern as the combined weight was about 40 kg making it hazard in the restricted space and steep stairways on any ship.



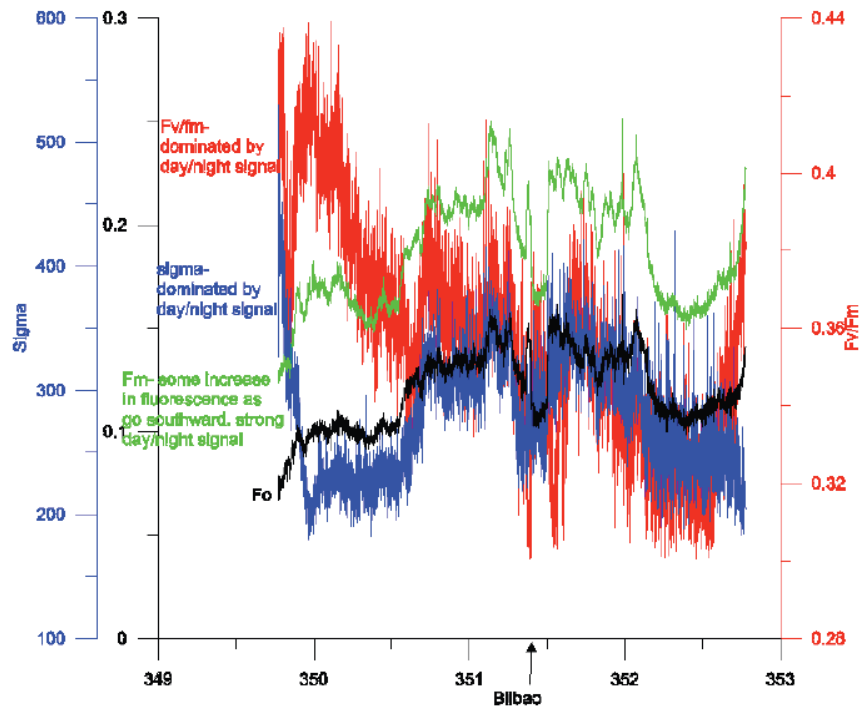


Figure 3-21: Data recorded by the FRRF during the test deployment in December 2004.

Down loading the data through the deck unit and “Windows hyper terminal” is relatively complex when under taken in the heat noise and humidity of the pump room on the “Pride of Bilbao” this lead to number of mistakes with down loading data in May and June.

### 3.6.3 Data Availability

The FRRF was used between March and June 2005. Figure 3-22 shows that between days 85 and 142 little data was lost. A number of errors with down loading the data resulted in substantial loss of data in May and June. Comparison with the fluorescence record from CTG Minipack shows that the FRRF was deployed through the most productive period in 2005.

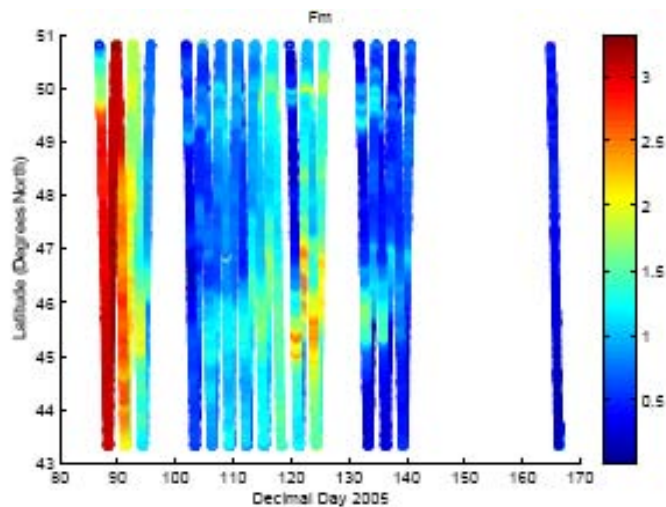


Figure 3-22: Plot of all the Fm data successfully recovered from the CTG FRRF used on the ferry “Pride of Bilbao” in 2005.

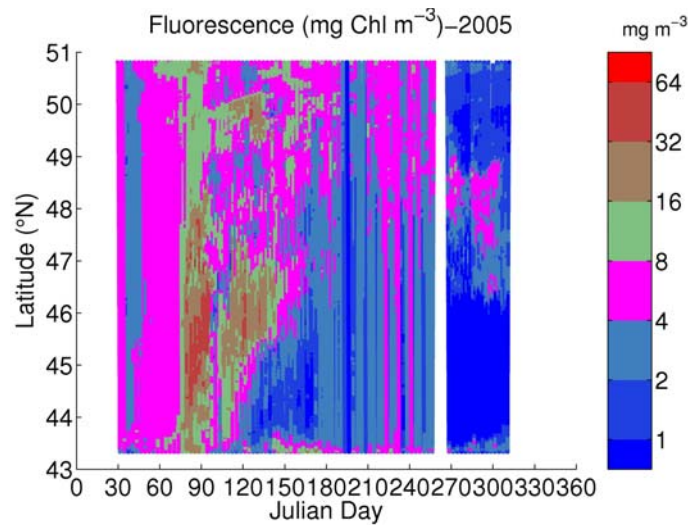


Figure 3-23: Plot of all the fluorescence data available from the NERC.NOC “Pride of Bilbao” Ferrybox system for 2005.

### 3.6.4 Maintenance

No significant level of extra maintenance is required by this sensor other than regular cleaning of the lens windows. CTG currently supplies a wholly inadequate flow cell for use with the Mk 1 instrument. They have not taken into account that the lens surfaces need to be cleaned on a regular basis in any flow through system. The lens could only be cleaned by poking a bottlebrush and cotton buds through the ½ inch diameter hose fittings. Thus getting in contact with the windows is problematic and it not possible to check how successful cleaning has been. After trials of the system in December 2004 CTG failed to meet the request for a redesigned head that would allow proper access to the lens windows.

### 3.6.5 Quality Assurance

The FRRF was only tested by NERC.NOC for a limited period and no quality assurance procedures have been developed.

## 3.7 Chemical Nutrient Analysers (Wet Chemistry)

### 3.7.1 Description of the Analysers

Automated nutrient analysers apply the same chemical methods that are used in laboratory analyses, mainly by applying two principles:

- 1) **Continuous flow analysers:** They either use a segmented flow or flow injection (Flow injection analyses=FIA and Sequential Injection Analysis=SIA) principles. Flow injection analysers are relatively fast since often the reaction (production of a colour which is spectrometrically detected) does not reach its end point (A new development from GKSS even has measurement times of 20 sec). However, due to this principle it is not easy to obtain stable readings and long maintenance-free times.
- 2) **Batch analysers:** They analyse discrete samples after mixing with appropriate reagents. The spectrometric detection is done after the reaction has reached its end point. Therefore, these analysers are slower, but often more reliable than flow analysers.

Within the project only batch analysers have been tested (APP 5003 from ME Grisard GmbH (Germany) and the Micromac 1000 from Systea (Italy)). The latter is based on a technology developed by Systea, named "Loop Flow Analysis", which applies special mixing techniques in a very small hydraulic loop. In Figure 3-24 a photo of these analysers is shown.



Figure 3-24: Nutrient Analyser APP 5003 (left) and Micromac 1000 (right).

Since the majority of the tests have been carried out with the APP 5003 mainly the results from these tests will be presented here.

#### Principle of the APP 5003

The scheme in Figure 3-25 shows the hydraulic principle. For each parameter ( $\text{NH}_4^+$ ,  $\text{NO}_2^-/\text{NO}_3^-$ ,  $\text{o-PO}_4^{3-}$  and  $\text{SiO}_4^{3-}$ ) a separate analyser is necessary.

The heart of APP is a patented pump-photometer carrying out the tasks of dosing the chemicals, adjusting the cuvette length, measurement of light extinction and (if applicable) dilution of the water sample to be examined. A motor-driven multipath valve connects this module with the reaction and compensation vessel. For control of the analytical process a microprocessor is integrated.



The routine communication between instrument and Ferrybox computer is via RS 232 interface. The measurements are carried out after the DIN EN norm. Determination of a concentration value lasts 15 to 25 minutes, depending on the process.

The function is as follows:

A water sample is taken by a syringe pump via the multipath valve. Afterwards it is mixed inside the reaction vessel with the appropriate reagents (specific for each parameter).

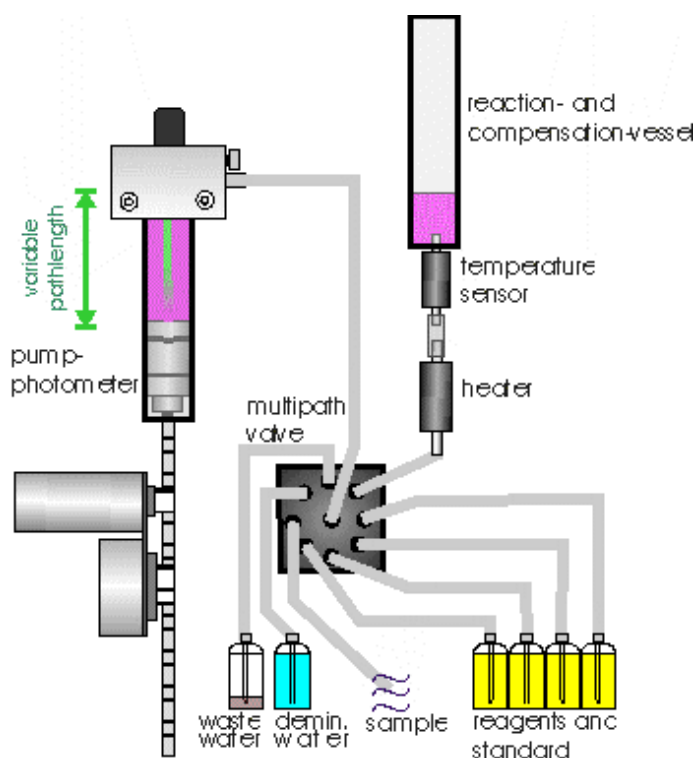


Figure 3-25: Hydraulic Principle of the APP 5003 (Source: ME Grisard GmbH).

Inside the syringe pump a photometer is integrated (“Pump-Photometer”) with a specific LED for each parameter and a sensitive photodiode. After the specific colour is formed the optical extinction is measured by the photometer. One of the great advantages of the APP 5003 in comparison to other instruments is the variable optical path length of the pump photometer. If, for example, the measured concentration is too large for the range (i.e. the resulting extinction is too high for the instrument), a second measurement with a shorter path length can be carried out immediately without any time-consuming dilution steps. On the GKSS Ferrybox Cuxhaven – Harwich two consecutive measurements at two path lengths (1 cm and 5 cm) were carried out and the results from the appropriate length were automatically selected (derived from their extinction values). Prior to the analysis the extinction of the sample is measured (“blank”). This value is subtracted from the measured extinction of the colour reaction for the calculation of the concentration. The advantage is that any colouration of the sample or residues of colloidal suspended matter do not interfere with the measurement. For quality assurance it is important not only to record and store the measured concentrations but as well the “raw data”, i.e., the extinctions of the blank and the sample. Only this ensures that inconsistencies in the data can be interpreted and errors detected.

For nitrite/nitrate determinations the standard method from Grasshoff 1983 is used. Phosphate and silicate are determined by the methods of Strickland & Parson 1968.

For the detection of ammonium the standard colorimetric method of Koroleff that uses phenol-hypochlorite (building of indophenol blue) is too insensitive for many regions in summer. Therefore, alternatively the OPA/sulfit method (ortho-Phthaldialdehyde) described by Kerouel & Aminot 1997 and Aminot et al. 2001 was used. The method is very sensitive and fast. It has a detection limit of about 0,02 - 0,03  $\mu\text{mol/L}$  and a linearity up to 50  $\mu\text{mol/L}$ . The only disadvantage is that the reaction has to be carried out at 85 °C which shortens the lifetime of components.

### Filtration Unit

Since “dissolved nutrients” shall be measured, a filtration, prior to the measurement is required. This is especially important for ammonium and phosphate, which are partly adsorbed or bound on particulate matter. Particles reaching the analyser could release nutrients, which would lead to errors. Another problem in connection with a filter unit is the potential accumulation of organic material, e.g., from algae, on the filter. Microbial remineralisation processes on the filter can release ammonium and phosphate and nitrifying bacteria on the filter can oxidise ammonia to nitrate. In order to avoid such problems two solutions are possible: 1) Frequent renewal of the filter surface by using ribbon filters and 2) Avoidance of accumulation of material on the filter by cross-flow filtration with large flow rates. In the project the first option was intensively tested. However, near the end of the project, some successful tests with cross-flow filters were carried out (see Chapter 5 “Recommendations”).

In the GKSS Ferrybox Cuxhaven – Harwich a ribbon filter (METROHM) was used. In Figure 3-26 photos of the ribbon filter (left) and the cross-flow hollow fibre unit (right) are shown.



Figure 3-26: Ribbon filter for nutrient analyses (left) and experimental cross-flow unit (right).

The filter consists of a ribbon of about 5 cm width, wound on a reel. It passes a small container, which is continuously flushed by the sample water from the Ferrybox. After each nutrient analysis (or continuously) the ribbon moves a small distance so that the next sample is filtered through a “fresh” filter part. This prevents the accumulation of bacteria in the sampling path. The filter loops is included in the antifouling concept of the Ferrybox, i.e., acidified water cleans all hoses and walls of the filter unit.

One problem with ribbon filters is that only filter material with pore sizes of about 15-25  $\mu\text{m}$  pore size can be found on the market. The “effective pore size” is much smaller due to blocking during the filtration process. However, experiments that compared samples of the ribbon filter with manual filtration (0.45 $\mu\text{m}$  filter) there were never any significant deviations of nutrient concentrations found. Nevertheless, this is an annoying fact, which always leads to discussions about the comparability with those that are filtered through 0.45  $\mu\text{m}$  filters. This was the reason that in the last half year of the project a cross-flow filtration with hollow-fibre filters has been successfully tested (Figure 3-26 to the right; also see Chapter 5 “Recommendations”).

### 3.7.2 Reliability and Applicability

In contrast to most sensors nutrient analysers are complex devices, which contain moving parts and show some wear after some time. Concerning the APP 5003, for example, O-rings of the syringe pump have to be greased and replaced and the multi-path valve has to be checked regularly. Due to the mechanics, the system is much more prone to failure than (motionless) sensors (see next paragraph). The Micromac 1000 from Systea has sometimes problems with the tiny magnetic valves, which can stick if salt residues are accumulated. This is especially the case when the instrument was not carefully rinsed with distilled water after it came back from the ship.

Another characteristic of all chemical analysers that differs from conventional sensors is the calibration and handling procedures. Prior to each deployment the instrument has to be calibrated by the measurement of reference substances in the lab.

### 3.7.3 Data Availability

The availability of nutrient data in the years 2003-2005 is shown in Figure 3-27 and Figure 3-28. As can be seen due to the complexity and mechanical sensitivity of the instruments the data availability is much lower than with the other sensors. Nitrate seems to be the most robust and ammonia the least robust method, presumably due to the high reaction temperatures.

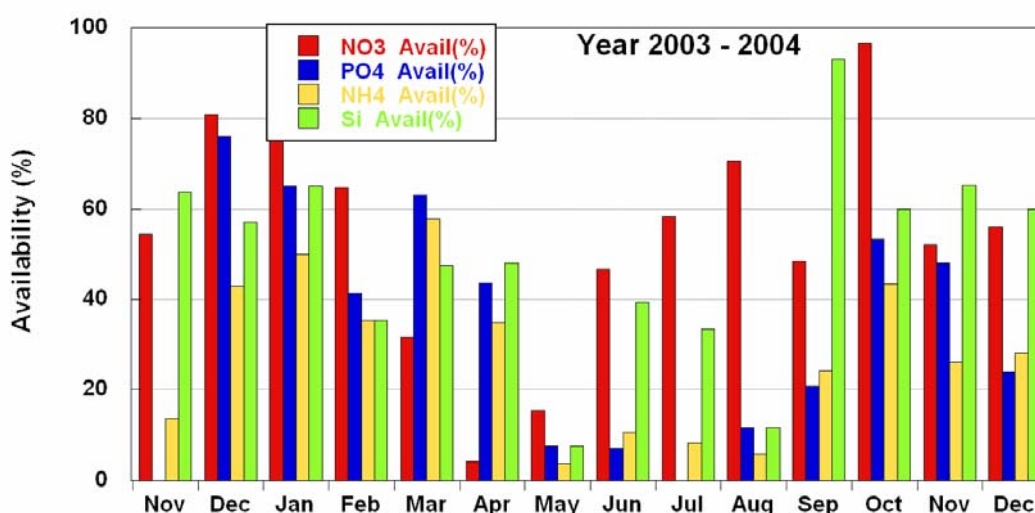


Figure 3-27: Availability of nutrient data in 2003-2004 on the GKSS Ferrybox Cuxhaven – Harwich as measured with the APP 5003.

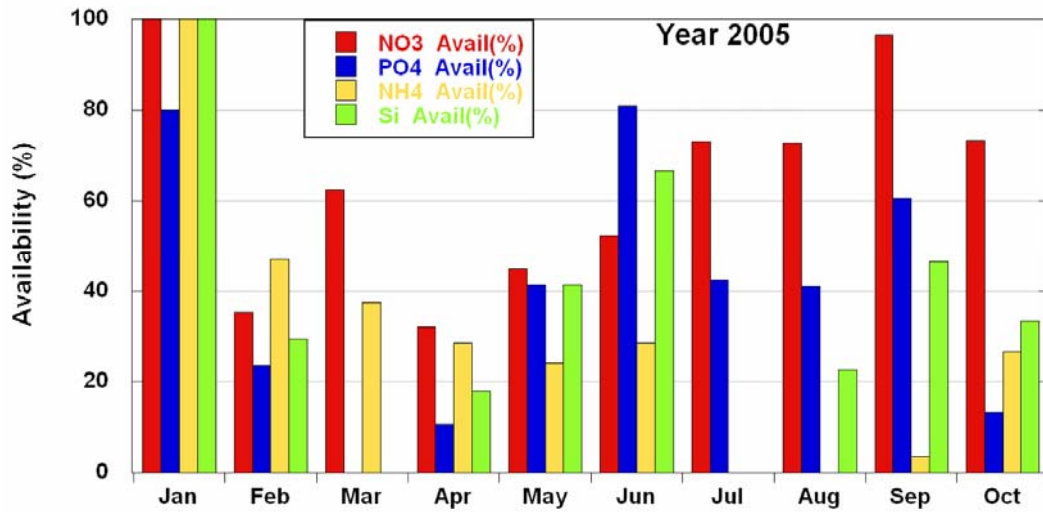


Figure 3-28: Availability of nutrient data in 2005 on the GKSS Ferrybox Cuxhaven – Harwich as measured with the APP 5003.

### 3.7.4 Maintenance

As can be derived from the data availability in the last section maintenance is a major issue with chemical nutrient analysers. As already discussed the mechanical wear on the moving parts and occasional problems due to blocking of valves or sticking of the syringe pump require a frequent check/maintenance every 2-3 weeks. During these checks prophylactic measures such as greasing etc. are carried out. First tests indicate that the Micromac 1000 analysers from Systea require less maintenance.

### 3.7.5 Quality Assurance

Quality assurance for nutrient measurements was carried out by two measures 1) by regular calibration of the nutrient analyser in the lab prior and after each deployment and 2) by reference samples taken with the automated sampler. Figure 3-36 gives an example in which nutrient data were compared with reference samples.

## 3.8 Optical Analyser for Nitrate ("In situ Nitrate")

### 3.8.1 Description of the Sensor

Unlike the chemical analysers, described in the preceding paragraph, there are in situ sensors for the measurement of nitrate, which directly measure the UV spectrum of seawater without additional chemicals. This determination of nitrate using ultra violet spectroscopy is well known (Ogura et al. 1966 & 1967). Several investigations have been carried out (Armstrong & Boalch 1961, Foster & Morris 1971, Thomas & Gallot 1990) to assess the absorption of UV light by natural waters. A number of problems have been found with this method of analysis (Thomas & Gallot 1990), but it has also been suggested that there were grounds for a reappraisal.

Nitrate absorbs significantly at wavelengths between 190 nm and 230 nm. The main ionic species found in seawater exhibiting similar characteristics include  $\text{Cl}^-$  and  $\text{Br}^-$  plus low concentrations of  $\text{SO}_4^{2-}$ ,  $\text{HCO}_3^-$ ,  $\text{HPO}_4^{2-}$ ,  $\text{H}_2\text{PO}_4^-$ ,  $\text{NO}_3^-$ , and  $\text{NO}_2^-$ . Except for  $\text{NO}_2^-$  and  $\text{NO}_3^-$  these anions have their main absorption band well below 210 nm. All other ions, except chloride and bromide, are present in such low concentrations in seawater that the interference they produce is negligible (Ogura et al. 1966). Extinction coefficients for halides are about 106 times less than nitrate, but their concentration in seawater is typically  $5 \times 10^4$  times higher resulting in relative absorbance  $5 \times 10^{-2}$  times that of nitrate.

Figure 3-29 illustrates the UV absorption spectra of nitrate, chloride, bromide, iodide and sulphide solutions in distilled water. In seawater, chloride and bromide are present in a nearly constant ratio, both to one another and to the total salt content (salinity). The critical component is bromide due to its absorption near 210 nm. It prevents the application of long optical path lengths in seawater applications since all light is already absorbed by bromide and the resulting light intensities are too low to detect nitrate. This means that a compromise between path length and resulting intensity has to be made: With longer path lengths the relationship between the disturbing bromide signal and the wanted nitrate signal becomes more unfavourable. This is reason the for a higher detection limit in comparison to the (wet) chemical methods.

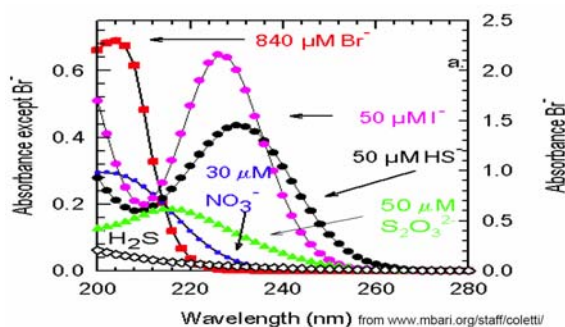


Figure 3-29: Absorbance spectra (from Kenneth & Coletti 2002).

Laboratory and in situ methods for nitrate determination in seawater by direct measurement have not become widely used for in the past, in part, because most of the analytical methods were based on measurements at one or a few wavelengths. Measurements at a small number of wavelengths do not allow robust techniques to be used for separation of overlapping spectra. By measuring the spectrum at some hundred wavelengths and applying spectral deconvolution techniques (Thomas et al. 1990) it is feasible to determine these compounds directly in complex media, such as seawater, without significant interferences, and with no chemical manipulations.



The optical layout of the sensor, manufactured by TriOS GmbH, Germany, („Substance Analyser“) is shown in Figure 3-30. It consists mainly of a Heraeus FiberLight deuterium lamp (200-1100 nm) as light source and a Zeiss miniature spectrometer MMS (190 – 720 nm) as detector.

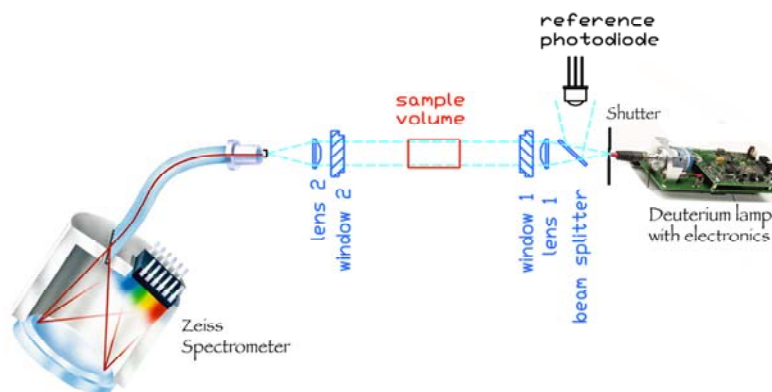


Figure 3-30: Optical layout of the In situ Nitrate sensor (Source: Zeiss, Heraeus & TriOS).

The wavelength at each pixel on the detector array is determined from a calibration polynomial supplied by Zeiss with each spectrometer. The absorbance at each pixel was calculated from the formula:

$$A_{\lambda} = -\log \left( (I_{\lambda} - I_D) / (I_{\lambda,0} - I_D) \right);$$

where  $I_{\lambda}$  is the detector intensity (counts) at wavelength  $\lambda$  for light passing through a sample,  $I_{\lambda,0}$  is the detector intensity (counts) at wavelength  $\lambda$  for light passing through de-ionized water and  $I_D$  is the detector dark current.

The dark current is constant, within detector noise, across the photodiode array. The dark current is determined while the shutter of the FiberLight is closed.

The dark current does increase significantly with temperature and with detector integration time, however. Each scan may, therefore, require a different estimate of dark current.

In Figure 3-31 the desktop version of the sensor („Substance Analyser“) is shown. The instrument contains a flow-through cuvette made of titanium.



Figure 3-31: Photo of the desktop version of the UV Nitrate analyser (left) and its dual-path length cuvette (right).

For different concentration ranges a two-path length cuvette with one sample flow is used. A motor moves the cuvette in such a way that either the short cuvette (27 mm path length) or the



long cuvette (55 mm) is within the beam of the spectrometer. The position is automatically changed according to the measured extinction. Between several measurements a third position can be chosen which moves the cuvette totally out of the spectrometer beam. In this position the (spectral) intensity of the lamp-spectrometer combination can be checked (measurement in air).

In the last year of the project a submersible version of the UV analyser from TriOS GmbH ("ProPS=Hyperspectral Process Photometer") was tested. It contains the same optical components but is assembled in a pressure housing.

In Figure 3-32 a photo of the ProPS sensor is shown.



Figure 3-32: Photo of the In situ Analyser "ProPS" (left) with adapters that change the optical wavelengths and a cuvette for lab check (right).

The sensor is intended for In situ applications. For lab test standard cuvettes of 1-6 cm length can be inserted. For integration in a Ferrybox a customised flow-through unit was build (Figure 3-33).



Figure 3-33: The ProPS analyser with customised flow-through unit.

### 3.8.2 Reliability and Applicability

The sensitivity of the method depends on the optical path lengths used. Figure 3-34 shows the calibration at 10 and 60 mm cuvette length in artificial seawater. Under these conditions (in the laboratory, pure water without yellow substance, no particulate matter and no air bubbles) the lowest detection level is below 1  $\mu\text{mol/L}$  nitrate.

However, under realistic conditions on the ferry, nitrate concentrations below 2-3  $\mu\text{mol}$  or 30-40  $\mu\text{g/l}$  cannot be measured. This is due to the influence of other substances, which have to be compensated by the convolution algorithm (changing salinity, varying concentrations of yellow substance (humic acids) in coastal waters and smallest air bubbles which may be persistent).

Due to the strong absorption of bromide path lengths larger than 6-8 cm cannot be used in seawater (with the Zeiss spectrometer used, maximal extinction values of 1.3 can be measured).

In principle, unfiltered seawater can be measured. However, at particulate matter concentrations  $> 10 \text{ mg/L}$  the sensitivity of the sensors decreases due to the additional light absorption. Therefore, in turbid waters a filtration is necessary in order to reach a high sensitivity.

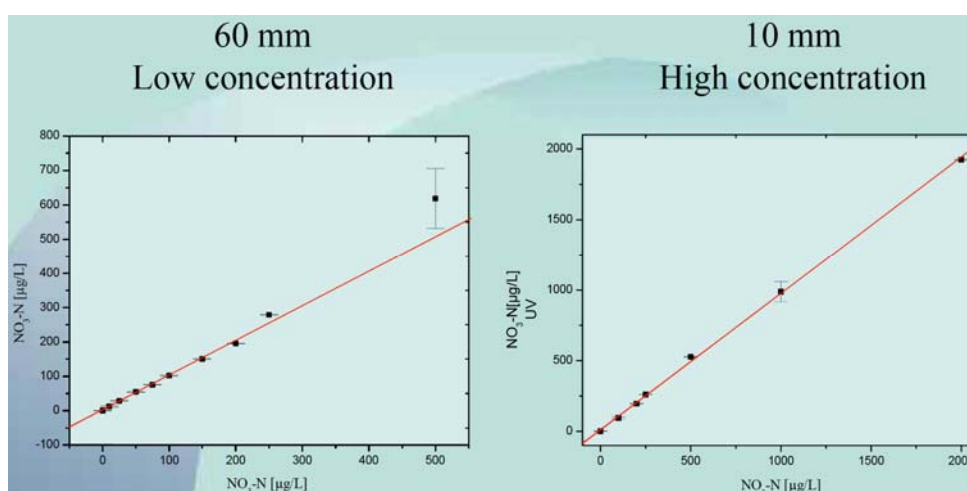


Figure 3-34: Calibration of the UV Nitrate sensor in the lab at two optical path lengths.

### 3.8.3 Data Availability

The two described instruments for the UV nitrate analysis were tested with different configurations. In addition, the performances of systems with and without filtration were assessed. Due to these frequent changes no long-time availability schemes for this parameter can be shown.

### 3.8.4 Maintenance

The sensor does not require any additional maintenance. Care must be taken to avoid the formation of any biofilms on the optical windows (biofouling) since in the UV even small biofilms reduce the sensitivity. However, by applying the regular automated standard cleaning procedures of the GKSS Ferrybox (acidified water) the system runs for several months. As mentioned above, care has to be taken to avoid small air bubbles entering the systems since this causes a high noise, which enhances the error and decreases the sensitivity. Under certain conditions, on some ships precipitation of iron oxides occurs (originating from the ships piping). Such iron oxide films prevent accurate measurements and have to be removed. On the GKSS Ferrybox this is automatically carried out by adding oxalic acid to the cleaning solution.

### 3.8.5 Quality Assurance

#### Calibration and Check

The standard calibration of the sensor for a larger concentration range has already been shown in Figure 3-34. In Figure 3-35 a calibration for smaller concentrations is depicted. As can be seen, the curve is linear.

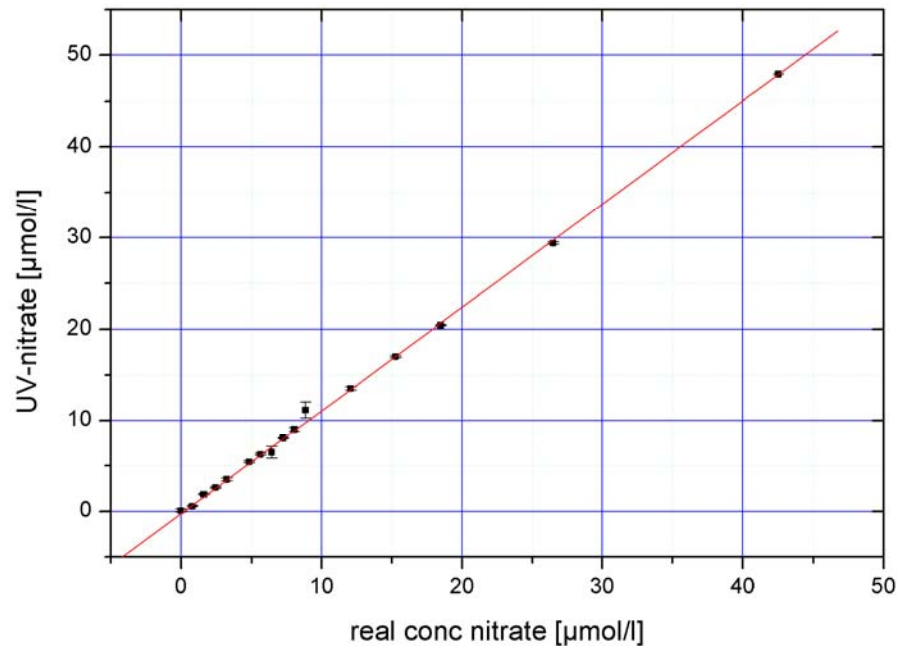


Figure 3-35: Calibration of the ProPS sensor for lower concentration ranges.

#### Comparison with Chemical Analysers and Lab Analyses

In order to check the instrument reading under realistic conditions, comparison measurements were carried out during several Ferrybox cruises on the GKSS route Cuxhaven – Harwich. As a typical example, in Figure 3-36 results from one cruise are shown together with the recorded salinity. In addition to the UV nitrate measurements automated chemical analyses with the APP 5003 and analyses from samples with consecutive lab analyses were carried out. From the graph the following conclusions can be derived:

- 1) The data between the different methods compare well, In general, the lab analyses seem to be systematically a little higher than the other data. However, this deviation is within the analytical error of the methods.
- 2) The higher temporal resolution of the UV nitrate sensors enables the detection of structures, which cannot be observed with the slower (wet) chemical analysers.
- 3) The course of the nitrate concentrations follows – down to small pattern - the course of the salinity measurements. This indicates that nitrogen sources in this region are related to freshwater inputs (river discharge, wet precipitation).

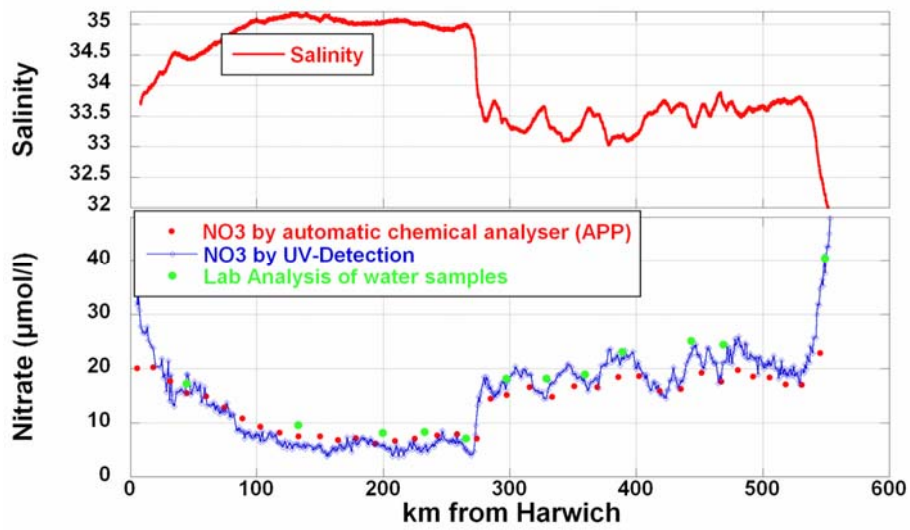


Figure 3-36: Comparison of Data from the UV Nitrate Sensor with Data from APP 5003 and Lab Analyses.

## 3.9 Light Sensor

### 3.9.1 Description of the Sensor

The sensor is a LiCOR cosinus Photosynthetic Available Radiation (PAR) sensor, measuring the light quanta between 350-700 nm. In Figure 3-37 a photo of the sensor and its spectral characteristics are shown.

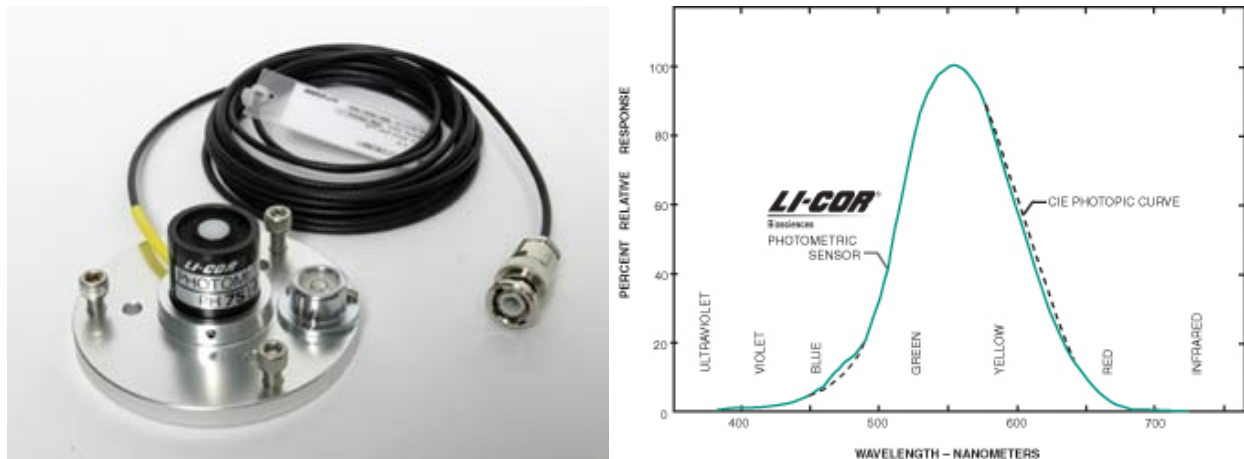


Figure 3-37: The Li-Cor light sensor and the sensitivity diagram (from: Li-Cor).

### 3.9.2 Reliability and Applicability

The sensor itself is a well-used sensor with good performance, but the mounting of the sensor on the top deck and the long connection to the computer in the lower deck of the ferry without any special interface made problems with the signal.

### 3.9.3 Data Availability

Data availability is nearly 100% (no failure). Problems occurred as stated above: The mounting of the sensors caused both signal noise, error on the offset values as well as scaling of the signal was periodically significant and the absolute values can not be used quantitatively.

### 3.9.4 Maintenance

Periodically cleaning of the sensor optic is needed. The sensor should work for many years.

### 3.9.5 Quality Assurance

Control was done with similar LiCOR sensors, but then logged locally at the sensor on deck. Monthly maintenance of the sensor optics seems to be sufficient.

## 3.10 Water Sampler

### 3.10.1 Description of the Sensor

#### NIVA & FIMR

The water sampler used by the partner NIVA and by the Finnish Institute of Marine Research is an ISCO 3700R ISCO refrigerated sampler with 24 one-litre samples (Figure 3-38). The one-litre bottles can be replaced with larger bottles. The sampler has a separate pump that on signal from the PC withdraws a sample from the pipe after the Ferrybox sensors. One advantage of this sampler is the high pumping speed for delivery of samples (< 1 min). Cross contamination between samples is very small.

The sampler is connected to the logging computer with GPS connection. The sampling can be controlled with computer by geographical position, or according to the values measured or directly using the programming unit of the sampler according to the date and time.



Figure 3-38: ISCO 3700R ISCO refrigerated sampler.

In practice, FIMR takes water samples approximately every 30<sup>th</sup> nautical mile along the route Helsinki –Travemünde according to the computer program with GPS control. The sampler is equipped with up to 24 polyethylene bottles with the volume of one litre. The samples are taken only on the way from Travemünde-Helsinki and stored at +4 °C. Samples are collected directly after the arrival of the ferry and immediately transported to the laboratory for the analysis.

#### GKSS

The automated sampler used by GKSS on the Route Cuxhaven – Harwich is a “Refrigerated Portable Sampler Bühler 1029 (Dr. Lange)”. It is much smaller than the ISCO and can be used also under restricted space conditions. It contains 12 one-litre PE bottles. Since one filling cycle allows only a volume of 350 ml three consecutive cycles are necessary to obtain 1 L of water. This leads to disadvantageous filling times of about 3 min. The sampler requires a pressure-free inlet, which is not possible on all Ferrybox systems. The cross contamination between samples seems to be larger than with the ISCO.



The external control by the Ferrybox computer is similar to the ISCO and the operation procedures are as described above.



Figure 3-39: Portable Sampler Bühler 1029 (Dr. Lange).

### 3.10.2 Reliability and Applicability

The water sampler on the Norwegian ferry “Color Festival” has been working without any problems in 5 years.

### 3.10.3 Data Availability

Not applicable.

### 3.10.4 Maintenance

Cleaning of bottles when used (weekly or monthly). Only the tubing of the ISCO needs to be replaced twice per year with a use approximately on weekly basis.

## 3.11 New Emerging Technologies

### 3.11.1 Flow Cytometer (Cytosense) for a Structural Assessment of Algal Species Composition

Flow cytometry is used in the laboratory to rapidly and precisely estimate cell numbers of phytoplankton, i.e. algal cells of less than 200  $\mu\text{m}$  in size, within the frame of microbial food web studies in various marine systems.

The principle is as follows: A stream of the water sample is pumped through a fine capillary which is in the path of a perpendicular laser beam. Detectors measure the light intensity of the forward and at 90° scattered particles at same wavelength as the initial laser beam and fluorescence signals originating from algal pigments are measured at several other wavelengths. Since during analysis only one particle/algae must be in the laser beam filtered seawater (“sheath fluid”) is surrounding the sample stream in the capillary (“hydrodynamic focussing”) to obtain a very narrow flow of the sample stream.

Flow cytometry complements epifluorescence microscopy in studies on the distribution and composition phytoplankton populations.

In addition to abundance estimates, flow cytometry allows to quantify changes in cellular pigmentation (chlorophyll and phycoerythrin concentrations) of different distinguished phytoplankton sub-populations in response to the light or nutrient regime, either along a depth profile or in incubation experiments. Thus, information on the physiological status or response upon different treatments (changes in light conditions, nutrient additions) can be assessed as well by flow cytometry (<http://www.jochemnet.de/cyto1.html>).

In the past flow cytometers were large and not suitable for operational unattended observations. This changed a decade ago with the development of the “Cytosense” by the Dutch company CytoBuoy b.v. Other versions of the instrument include a buoy system (“CytoBuoy”) and a submersible instrument (“Cytosub”).



Figure 3-40: Photo of the Cytosense with laptop for data analysis.

The “Cytosense” is the bench top analyzer version of a basic flow cytometer instrument. The small footprint of Ø 37 cm allows convenient use even when the space on board the ferry or research ship is limited.

The operation is completely computer controlled, interactive or autonomous and no alignment is needed. Various laser wavelengths are available to measure up to 7 fluorescence bands. Use on ferries is easy owing to the vibration- and movement-tolerant design and due to its splash proof housing. A photo of the unit is shown in Figure 3-40.

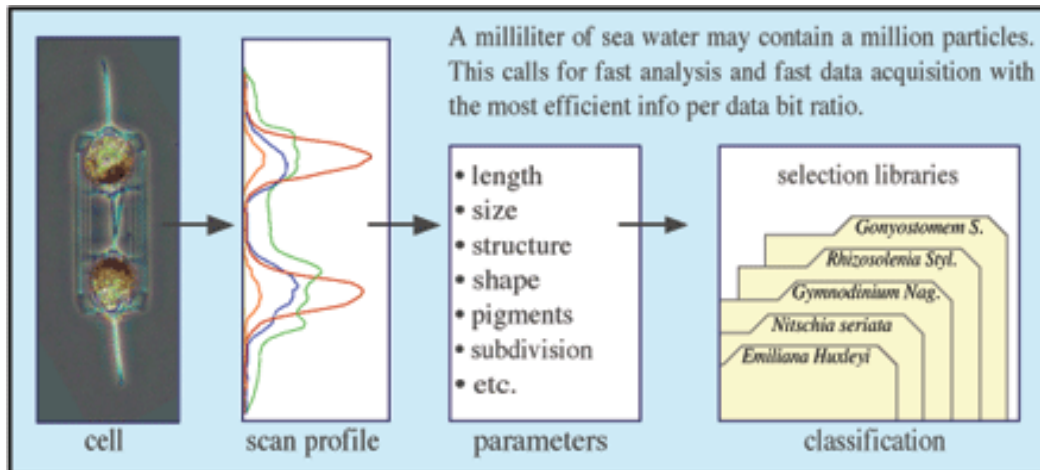


Figure 3-41: General functionality of the Cytosense (from <http://www.cytobuoy.com>).

The principle of the flow cytometer is depicted in Figure 3-41. The outputs of the scatter signal (~size) and different fluorescence signals (~algal pigments) are clustered in different “parameter sets”. With the build-in data analysis information on size, shape, structure, pigments etc. can be obtained. If the system is running continuously a huge amount of data has to be stored, analysed and interpreted.

### 3.11.2 Measurement of CO<sub>2</sub>

#### Overview from Literature

The main principle of pCO<sub>2</sub> measurement is based on the equilibration of a carrier gas phase with a seawater sample and subsequent determination of the CO<sub>2</sub> in the carrier gas by an infrared analyser. As the pCO<sub>2</sub> in seawater strongly varies with temperature a correction is necessary to compensate for the difference between equilibration temperature and the in-situ seawater temperature. The equilibrated surface water values should be accurate within 2 µatm. This will necessitate pressure measurements within 0.2 mBar and water temperature measurements with an accuracy of 0.01 C.

Different underway-measuring systems have been developed and applied for regional and global studies (e.g., in Feely et al. 1998, Cooper et al. 1998, Wanninkhof & Thoning 1993. Another overview on different systems was given at the “Underway pCO<sub>2</sub> System Workshop” October 2-3 2002 at NOAA/AOML in Miami, FL, (<http://www.aoml.noaa.gov/ocd/pco2/descriptions.html>).

A great variety of pCO<sub>2</sub> systems and equilibrators have been described in the literature. Essentially three different design principles can be distinguished (from Körtzinger et al 1996):

- The “shower type” equilibrator (e.g., Keeling et al. 1965; Kelley 1970; Weiss 1981; Inoue et al. 1987; Robertson et al, 1993; Goyet and Peltzer, 1994,
- The “bubble type” equilibrator (e.g., Takahashi 1961; Goyet et al. 1991; Schneider et al. 1992; Kimoto and Harashima 1993; Ohtaki et al. 1993), and
- The “laminary flow type” equilibrator (Poisson et al., 1993).

A design described by Copin-Montegut (1985) combines aspects of the shower and bubble type.

A typical example for two underway pCO<sub>2</sub> systems of the “bubble type”, that were developed independently at the Institute for Marine Sciences, Kiel (IFM-GEOMAR) and at the Baltic Sea Research Institute, Warnemünde (IOW) are described in Körtzinger et al. (1996):

A continuous flow of seawater passes through an open system equilibration cell, which is vented to the atmosphere. This allows the equilibrium process to take place at ambient pressure at any time. A fixed volume of air is re-circulated continuously through the system so as to be in almost continuous equilibrium with the constantly renewed seawater phase. In a “bubble type” equilibrator this airflow is bubbled through the water phase. After passage through the equilibration cell the air stream is pumped to a non-dispersive infrared gas analyzer, where the mole fraction of CO<sub>2</sub> is measured relative to a dry and CO<sub>2</sub>-free reference gas (absolute mode). Both systems feature a LI-COR® LI-6262 CO<sub>2</sub>/H<sub>2</sub>O gas analyser, which is a dual-channel instrument that simultaneously, measures the CO<sub>2</sub>, and H<sub>2</sub>O mole fractions. The gas stream needs no drying prior to infrared gas detection as the biasing effect of water vapour on the measurement of CO<sub>2</sub> is eliminated based on the H<sub>2</sub>O measurement.

These systems were successfully applied in the assessment of regional and global carbon budgets and for the detection of biological processes (see Section 4.9 “Applications of new emerging technologies”).

## 4 Scientific Value

### 4.1 Oxygen Measurements

The scientific value of oxygen measurements is based on the fact that oxygen has through the Redfield ratio (Redfield, 1934; Redfield et al., 1963) a stoichiometric relationship with the amount of organic carbon that is formed during photosynthesis or decay during respiration (close to 1.3:1). This is not the case for the more commonly used use of fluorescence measurements to estimates changes in biomass. Fluorescence is taken as a measure of chlorophyll but due to change in plankton type and photo-physiology of the plankton the ratio can vary widely in time and space. Mean ratios measured on calibration crossing varied by an order of magnitude between Portsmouth and Bilbao in 2003 and 2004 (see Qurban et al., 2004). Order of magnitude variations in the ratio of chlorophyll to carbon content of plankton have also been reported (Steele, 1964).

The potential draw back of oxygen measurements is that concentrations can be changed by physical processes, particularly by gas exchange with the atmosphere. However if wind speed data is available this can be accounted for and oxygen data used to give reliable estimates of biological production as has been shown by Bargeron et al (In preparation) following on from the work of Najjar and Keeling (2000)

As described in Section 3.2 oxygen concentrations, i.e., mainly the saturation index provides information on occurring chemical-biological processes. These are mainly respiration, mineralization and production processes. Most other processes, e.g., nitrification normally are too weak to detect due to the low nutrient concentrations.

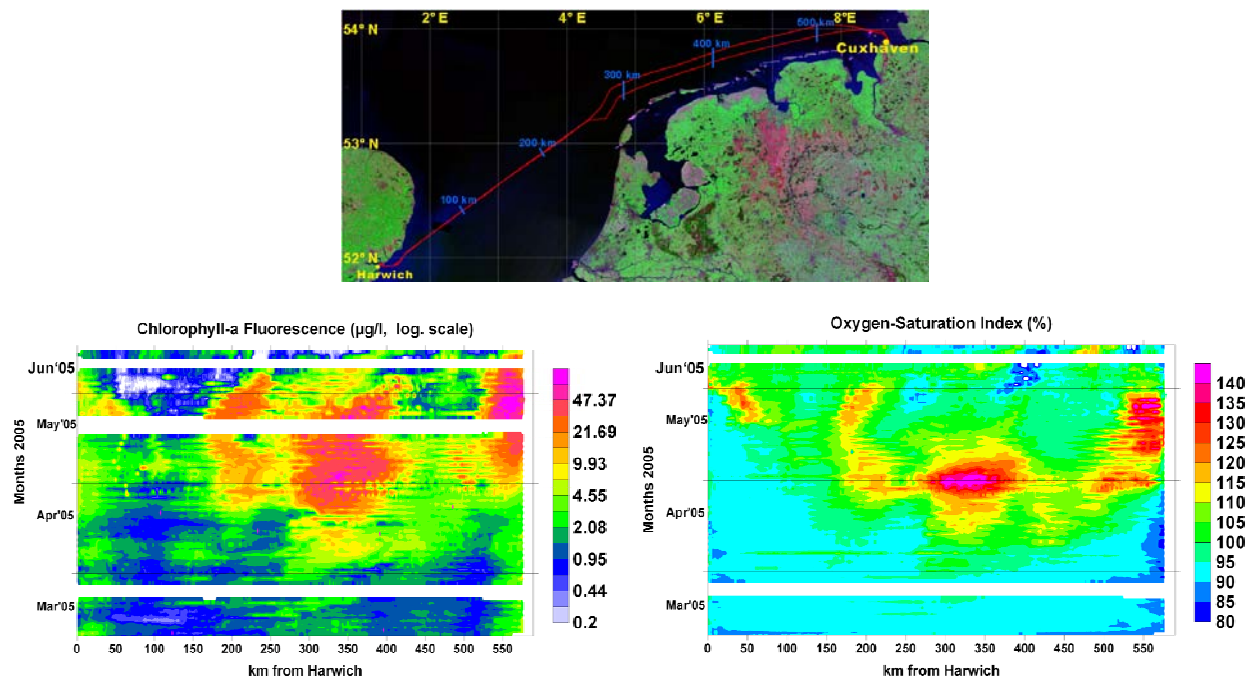


Figure 4-1: Ferrybox Route Cuxhaven –Harwich (top) and measurements of chlorophyll-fluorescence (left) and oxygen saturation index (right) from March to June 2005.

One example is depicted in Figure 4-1, which shows results from the GKSS Ferrybox Cuxhaven – Harwich during March and June 2005. As can be seen on the left graph the persistent algae bloom at km 300 – 400 in late April is reflected in the oxygen diagram on the right with an oversaturation of up to 140%. On the other hand, the break down of the algal bloom at km 400 in late May/early June leads to a short oxygen depletion (saturation index of only 80%) due to the oxygen consumption by carbon mineralization (small blue area in June at km 400). Together with continuous nutrient measurements a better insight into eutrophication processes can be obtained.

## 4.2 pH Measurements

As has been described before, one application of continuous pH measurements on a Ferrybox route is the assessment of eutrophication. In contrast to chlorophyll measurements, which give a measure of the potential of possible primary productivity under good light and nutrient conditions, the pH values indicate the CO<sub>2</sub>-consumption as result of primary production. However, due to the immediate transport of atmospheric CO<sub>2</sub> into the (CO<sub>2</sub>-depleted) surface waters a quantification of primary production is difficult (as with oxygen, see above).

Figure 4-2 depicts measurements of chlorophyll-fluorescence and pH values on the Ferrybox route Cuxhaven – Harwich in spring 2005. As can be clearly seen, in late April a stable plankton bloom occurs between km 300 and 400 over several weeks. Due to favourable light conditions this lead to a high productivity, which can be seen in the pH values in the same region, which reach a value of 8.7. Comparable conditions can be found outside the Elbe estuary near Cuxhaven in early May. In principle, the relationships are similar to oxygen (Figure 4-1).

Due to different air-water exchange coefficients of oxygen and CO<sub>2</sub> a combination of simultaneous pH and oxygen measurements will provide more quantitative information on the algal productivity.

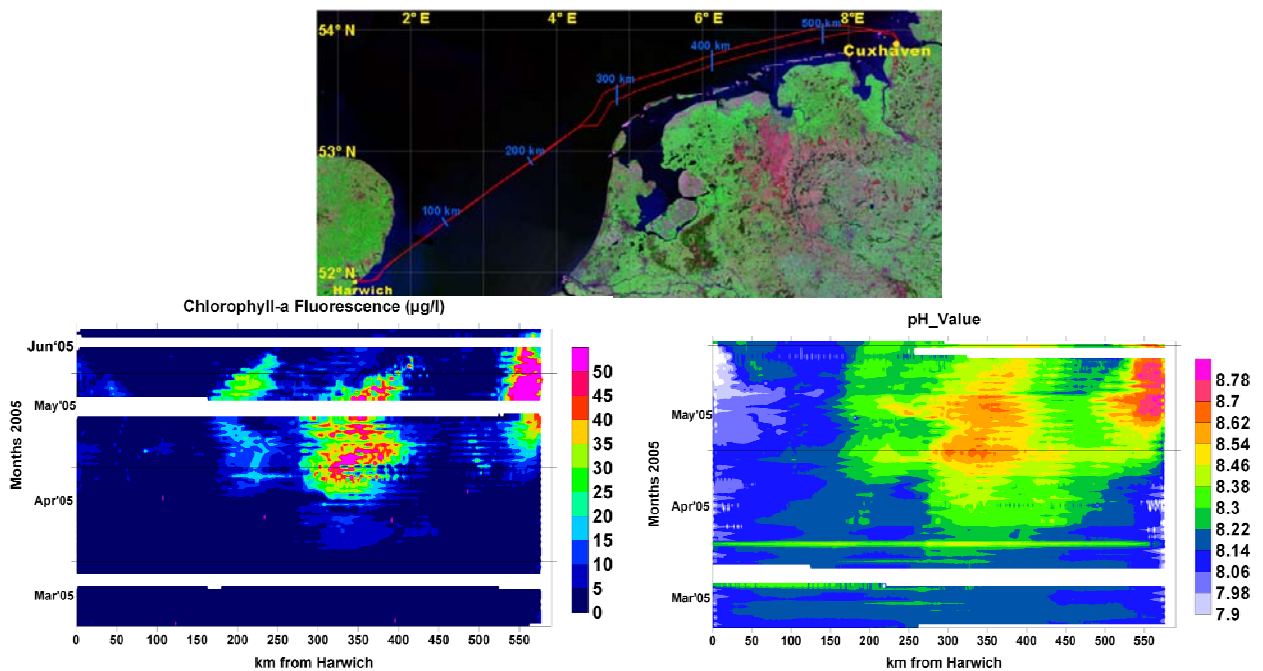


Figure 4-2: Ferrybox Route Cuxhaven – Harwich (top) and measurements of chlorophyll-fluorescence (left) and pH values (right) from March to June 2005.



### 4.3 Current Profile Measurements (ADCP)

Long-term high-frequent ADCP can have an enormous scientific value. Long-term observations ensure that very detailed analysis can be done of the different tidal components that contribute to the observed signal. Moreover, a wide range of meteorological conditions is covered. Besides, the ferry observations have a very strong advantage above observations from single point moorings because, even on such a short route of only 4 km, the spatial variability in the current field is large.

Therefore, the scientific value of these observations is large.

The ferry that crosses the Marsdiep tidal inlet between Den Helder and Texel is an excellent platform to obtain long-term, cost-effective, observations on oceanographic parameters in a tidal inlet. Especially the high frequency of the ferry trips, each 30 minutes during daytime, ensures that a data set is obtained which allows detailed studies on (temporal variability in) the transport and exchange of materials between the Wadden Sea and adjacent North Sea.

First analysis of the data from the through flow system shows a strong spatial and temporal variability. The spatial variability in the tidal inlet is due to the presence of water masses with a different origin. Temporal variations on different time scales varying from intra-tidal to seasonal can be recognized.

First analyses of the ADP data show that the results with respect to the integrated tidal water volume transport through the inlet is in agreement with previous observations and numerical model studies. The analyses suggests also that the noise in the ADP current data can be further reduced by optimizing the calibration procedure. The temporal variability in the strength of the back-scattered signal strongly suggests that it can be used as a measure for the concentration of fine-grained suspended sediments.

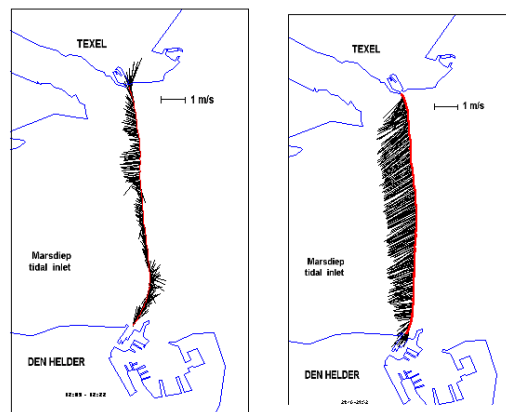


Figure 4-3: Current velocity during two ferry cruise.

*Current speed and direction at about 7.3 m below sea surface, as obtained by averaging the ADP signal from 6.3 to 8.3 m below sea surface (bin 6 to bin 10). On the left side a typical current pattern near the turn of the tide at low water slack is shown. The right side shows the current pattern during maximum ebb.*

Figure 4-3 gives a typical example of the currents measured directly below the ferry. In the central, deeper parts of the channel inertia causes the current to turn later than in the more shallow parts.

During ebb the currents are strongest along the northern part of the inlet. Maximum tidal currents vary between 1.0 and 1.5 m/s, depending on the location in the inlet.

The more or less synoptic observations on the current speed in the tidal inlet allow the calculation of the water volume transport through the inlet during each ferry trip. This integrated measure is used also as a first check on the quality of the observations. It is determined by summing up the east-ward component of the transport rate in each bin over the entire cross-section, using the recorded position of the ferry to determine the north-ward displacement of the ferry between successive ADP observations (on average about 10 m). In this procedure it is assumed that the current speed between the surface and the first reliable observation (at a water depth of 6.3 m) is equal to the average value of the current from bins 6 - 10 (in order to smooth the applied vertical extrapolation).

Other methods, e.g. using less vertical bins for the extrapolation, appeared to give similar results with respect to the calculated total volume transport but more noisy single vertical current profiles. Similarly, the cross-section averaged back-scattered echo-intensity is determined by averaging all reliable observations over each cross-section. Before averaging, the back-scattered signal is first corrected for geometrical spreading and (salinity and temperature dependent) adsorption using standard formulations (Urlick, 1975). This procedure results in 32 values per day for both integrated measures, with an interval of 30 minutes between successive values. Subsequently a harmonic analysis on this data set is performed, using 10 tidal components.

In Figure 4-4 the residual currents averaged over different tides on the ferry transect are shown. As can be seen, the values at the surface are mainly directed from Texel to Den Helder, whereas in greater depths an reverse secondary flow can be observed,

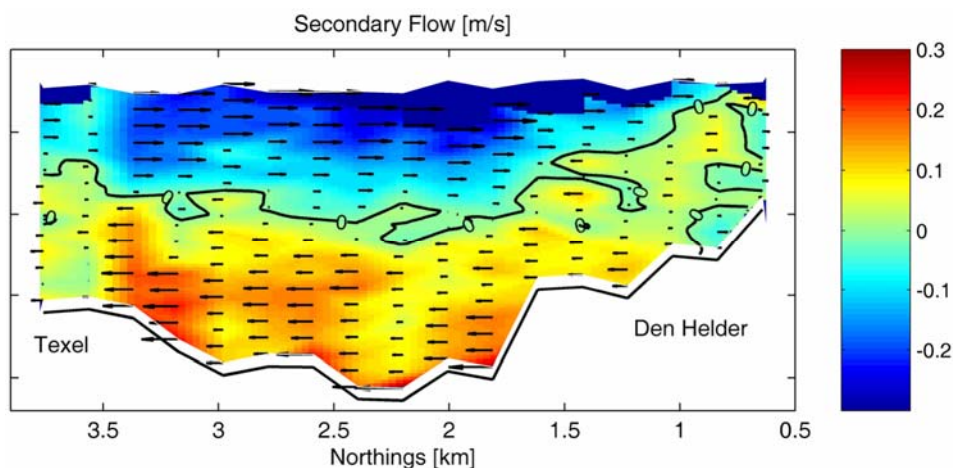


Figure 4-4: Average residual currents on the ferry track.

From many velocity measurements the averaged volume flow through the Marsdiep channel can be calculated. In combination with measured suspended sediment concentrations the dependency of suspended matter from the volume flow can be derived. Figure 4-5 shows the transect-averaged suspended sediment concentration (SSC) (vertical axis) as a function of the water volume transport for measurements during a period of one year. Red lines show the mean SSC during the accelerating phase of the tide, green lines during the decelerating phase. A characteristic phase lag in the response SSC to an increase in the current speed can be recognized. Moreover it is clear that the SSC is larger during flood tide (positive volume transport) than during ebb tide. This causes a net flux of suspended sediments into the Wadden Sea.

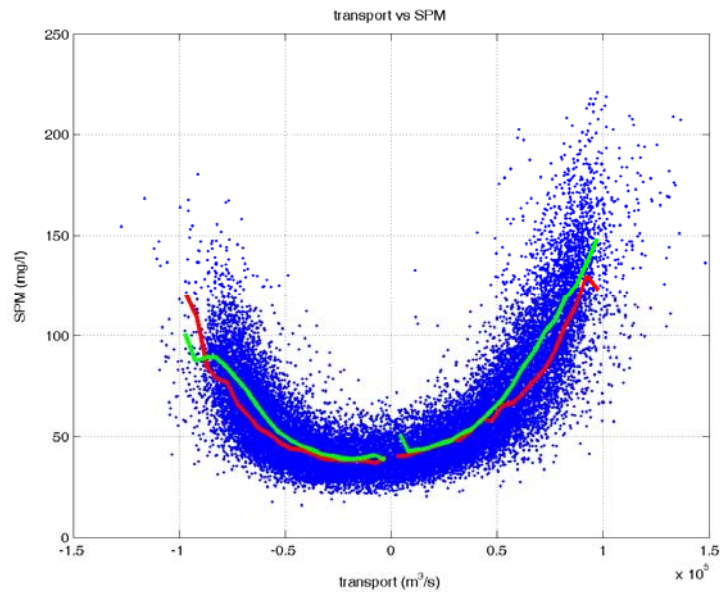


Figure 4-5: Transect-averaged suspended sediment concentrations as function of the water volume transport. Red: Accelerating tidal phase, green: decelerating tidal phase.

#### 4.4 Detection of Algae Groups

In Figure 4-6 the results of algal groups together with pH and oxygen saturation measurements from two cruises Cuxhaven – Harwich are shown (for geographical reference see chart in Figure 4-2).

The relatively large chlorophyll concentrations at 5°-6° longitude indicate the spring bloom in this region (chlorophyll-a total). However, the algal composition is different. In the early stages of the bloom on May 15<sup>th</sup> the dominant algal division seems to consist mainly of diatoms. Later on May 28<sup>th</sup> the reading from the channel, which presumably indicates the occurrence of Dinoflagellates and other diatoms, seems to increase in the westward locations.

The recorded pH and oxygen values show that the productivity of the algae depends on several factors. The small chlorophyll concentrations of about 18 mg/L near the English coast (1°), for example, show similar oxygen concentrations as the extremely high chlorophyll concentrations of 70 mg/L near Cuxhaven (9°). However, the signal of the pH value at near the English coast (1°) is much smaller than the signal at 9°.

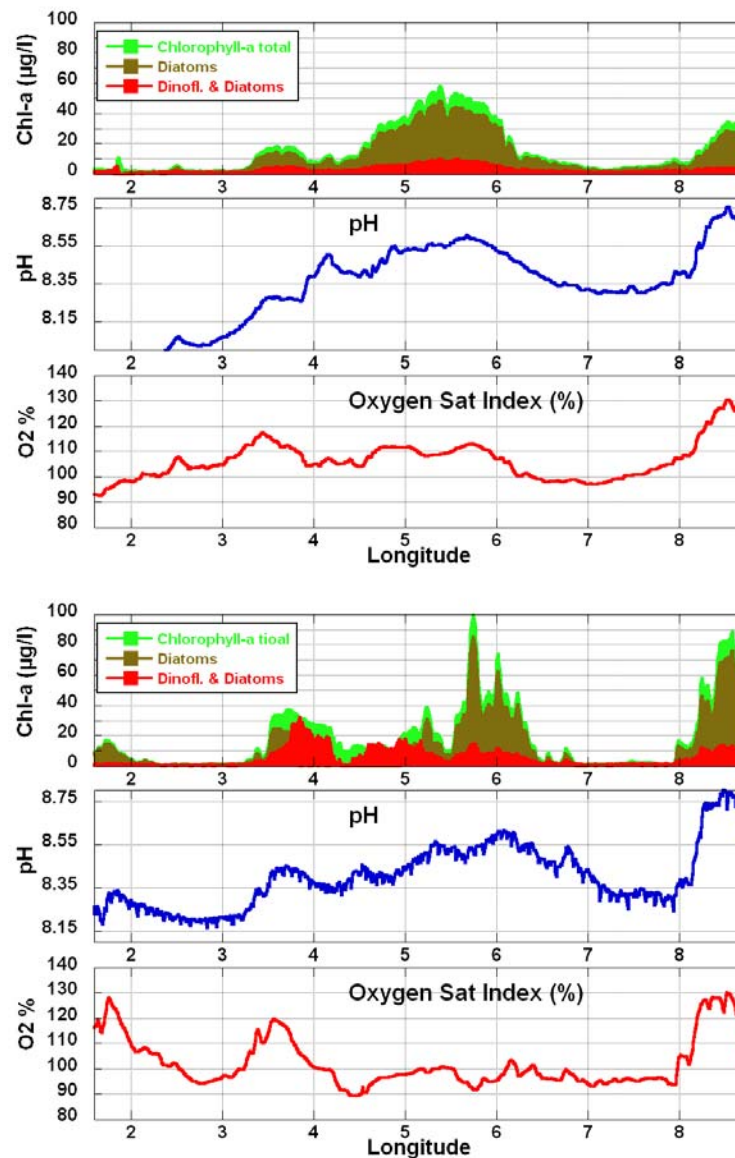


Figure 4-6: Results from Algal Group Measurements on May 15<sup>th</sup> (left) and May 28<sup>th</sup> (right) 2005.

Only partly this can be attributed to the lower salinities and the lower buffering capacity of the waters in front of the Elbe estuary. The patchy but high chlorophyll concentrations at 6° show no response in the oxygen signal and only slightly elevated pH values. A first assumption could be that the algae bloom was already declining (still high chlorophyll content but already low activity). Additional measurements of algal productivity with a Fast Repetition Rate Fluorometer could possibly have solved this question.

#### 4.5 Measurement of Algal Activity/Productivity (FRRF)

The claimed benefits of FRRF are that it can be used to estimate the relative photosynthetic state and so differentiate marine plankton populations and so provide information about the stage of the bloom (i.e., growing or dying off) and how active they are.



So far we have been able to carry out a preliminary analysis of the data available. Plotting  $F_m$  either as a dot plot in space and time (Figure 3-22) or as individual traces against latitude (**Fehler! Verweisquelle konnte nicht gefunden werden.**) suggests that the data returned by the FRRF and a CTG Minipack Fluorometer, as would be expected show very similar patterns of fluorescence activity in the plankton populations. When  $F_v/F_m$  is plotted (**Fehler! Verweisquelle konnte nicht gefunden werden.** and Figure 4-9) this data is consistent with the idea the value of  $F_v/F_m$  being higher where nutrients are less likely to be limiting in the English Channel.

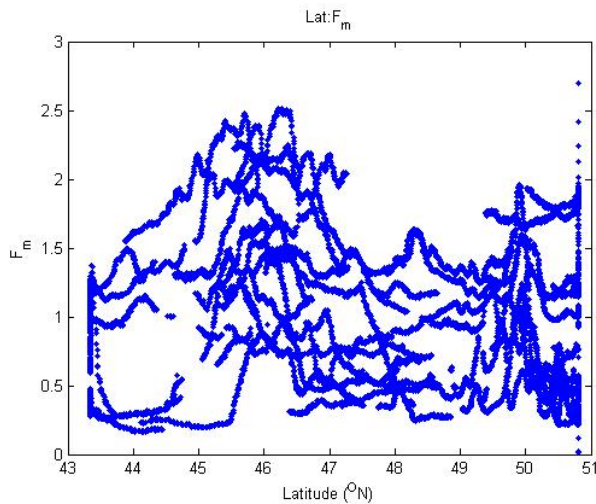


Figure 4-7: Plot of all the night time (PAR less than 200)  $F_m$  values from FRRF.

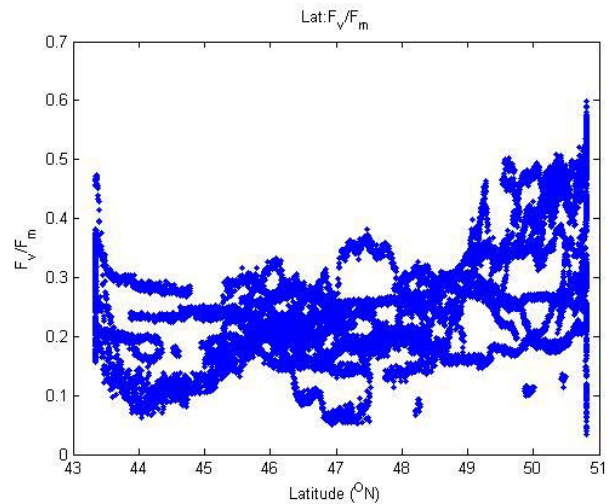


Figure 4-8: Plot of all the night time (PAR less than 200)  $F_v/F_m$  values from FRRF.

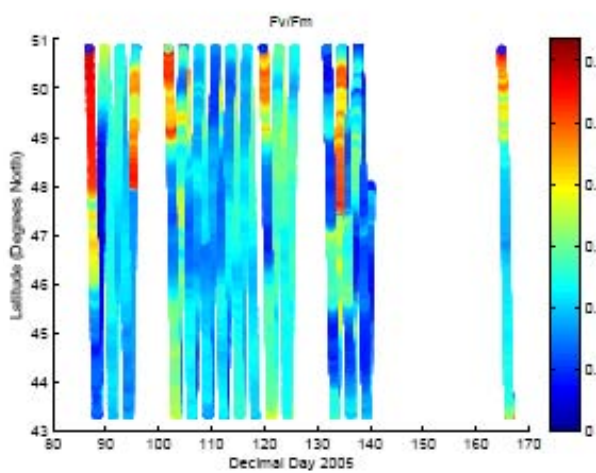


Figure 4-9: Plot of all the  $F_v/F_m$  data collected in 2005.

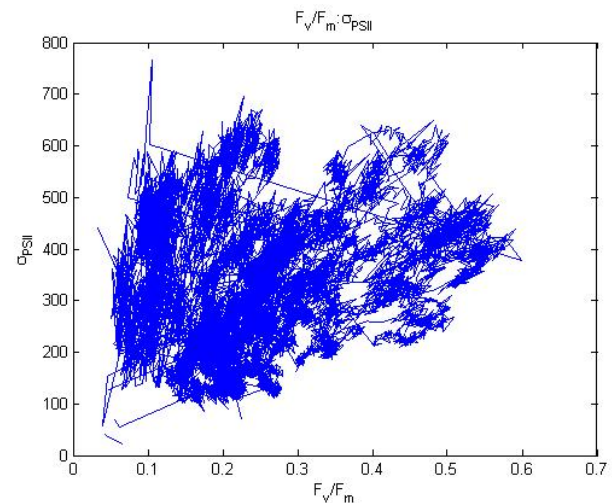


Figure 4-10: Plot of  $F_v/F_m$  against  $\sigma_{PSII}$  from the FRRF data collected in 2005.

The idea that  $\sigma_{PSII}$  should be inversely related to  $F_v/F_m$  is not confirmed by the data at this stage. In Figure 4-10 all the available data are plotted and no relationship between the parameters is apparent. This probably reflects that the more FRRF instruments are being used in marine systems the more complexity is revealed – in particular the range of difference between the photo-physiology of different organisms (e.g. Moore et al., 2005).

## 4.6 Measurement of Nutrients

Continuous measurements of nutrients by a Ferrybox allow an overview of the nutrient development over time and space. As an example in Figure 4-11 nitrate concentration in the Southern North Sea are depicted. They originate from measurements with the TriOS UV Nitrate Analyser on the GKSS ferry Cuxhaven – Harwich during the first spring bloom in March/April.

As can be seen, there are relatively high nitrate concentrations near the English coast (km 0-50) and in the German Bight (km 450 – 600). The very high concentrations around km 600 originate from the plume of the river Elbe, which discharges large amounts of nutrients into the North Sea. In the area between km 100 and km 250 nutrient-poor water bodies originating from water bodies south of England are dominating. Along the Dutch and Belgian coast the concentrations are relatively high presumably due to the influence of fresh water input (this can be seen in the salinity measurements, not shown here). The decrease of nitrate concentrations near km 300 starting around April 8<sup>th</sup> originates from the starting of an algae bloom in this area (compare Figure 4-1 in Section 4.9)

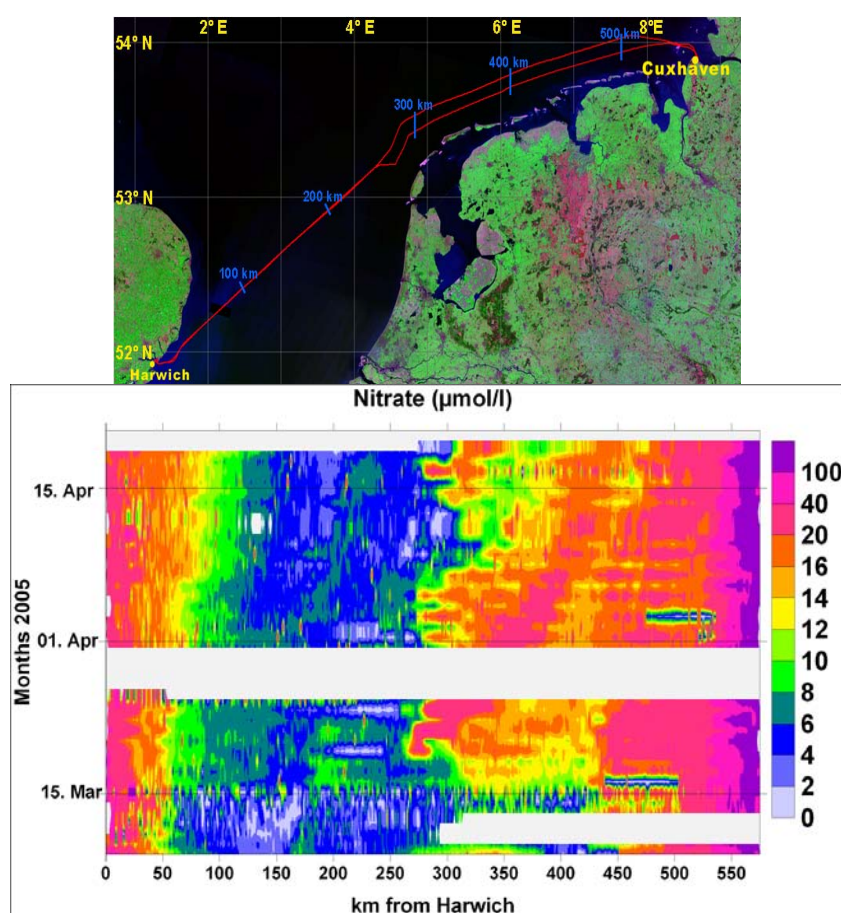


Figure 4-11: Ferry route Cuxhaven – Harwich and results from nitrate measurements March/April 2005.

## 4.7 Light Measurements

The data were used to study the Chl-a/fluorescence ratio and in addition for validation of satellite PAR values.



## 4.8 Application of Water Samplers

The automated water sampling provides a tool for studying the phytoplankton species distribution along the ferry route. The samples for phytoplankton counting may be chosen according to chlorophyll-a or phycocyanin fluorescence profiles, measured with the flow-through systems. The phytoplankton species are counted within a few days and so may be used also for the warning of potentially harmful species. For example, FIMR publishes the list of dominant taxa within a week in the Baltic Sea Portal web page. The condition of phytoplankton seem not suffer from the sort storage time (max 54 hours).

The fluorescence of phytoplankton species depends on community structure and physiological condition of cell, s i.e., is the population in the growth phase or dying phase. Therefore, it is highly important to validate the fluorescence readings in vivo against the laboratory analysis of chlorophyll-a in vitro.

The inorganic nutrients (N-NO<sub>2</sub>+NO<sub>3</sub>, N-NH<sub>4</sub>, P-PO<sub>4</sub>, total-N, total-P) are also analyzed from the water samples. Because the analysis is not immediate, for instance ammonium analysis results should be vied with criticism, but tot-N, tot-P analysis can is more conservative and so more reliable.

**Specific comment from NIVA:** Since the Ferry used by NIVA comes to the harbour every evening the samples are prepared latest the next day. This is then in accordance with the laboratory routines. The samples are stored in the ISCO samples of about 8-10 °C during the 6-hour trip and are the transferred to the laboratory refrigerator. If the samples are taken during night (Oslo-Hirtshals) the samples will be preserved when the ship is back in Oslo the next evening.

Nutrients samples (PO<sub>4</sub>, NO<sub>3</sub>, NH<sub>4</sub>) are preserved with 1 ml 8N sulphuric acid/100 ml sample and analysed according to NIVA methods. Silicate is not preserved but analysed fresh. Longer storage is not recommended.

Turbidity should be analysed as soon as possible and not stored more that 24 hours. NIVA has observed that during high productive periods the turbidity changes. If the particles are more inorganic the changes will not occur as fast as if the samples are dominated by phytoplankton. For control of the turbidity sensor using water samples this should be done immediately on-board the ship.

Samples for TSM are filtered after maximum one day (24 hours) using the recommended method for satellite validation. Washed and pre weighted GFF filters is used. The filters should be cleaned with min 3\*50 ml distilled water as well as the filter rim (3 times). Yellow substance (coloured dissolved organic material, CDOM) is filtered with 0.2 µm Nucleopore filters and analysed spectrophotometrically. Samples for Chl-a are also filtered after maximum one day (24 hours). Longer storing is not recommended. The filter is frozen at -80 °C and analysed according method used for satellite validation (HPLC).

Very important as well is the application of the water sampler for the correction/validation of satellite data.

## 4.9 Applications of New Emerging Technologies

### 4.9.1 Example of Measurements with the Cytosense

Due to the “pre-operational” status of the Cytosense and due to the huge amounts of data, which –at the time being- need individual interpretation, the instrument was not used on a ferry. However, the instrument was tested on a cruise with the research vessel FS. Polarstern from Bremerhaven to Capetown in October/November 2005 (Andreas Ruser, FTZ Büsum, pers. communication). During the cruise measurements with the Cytosense were carried out on the daily “biological” stations with water samples. Here, only the online measurements (water pumped by a peristaltic pump from the moon pool in 7 m depth), which were carried out every hour, are discussed for the cruise section Bremerhaven – Vigo (Spain).

In Figure 4-12 the experimental set-up on board of FS Polarstern is shown. The sample intake for the instrument was via a special Perspex block, which was continuously supplied with seawater by a peristaltic pump (ship).

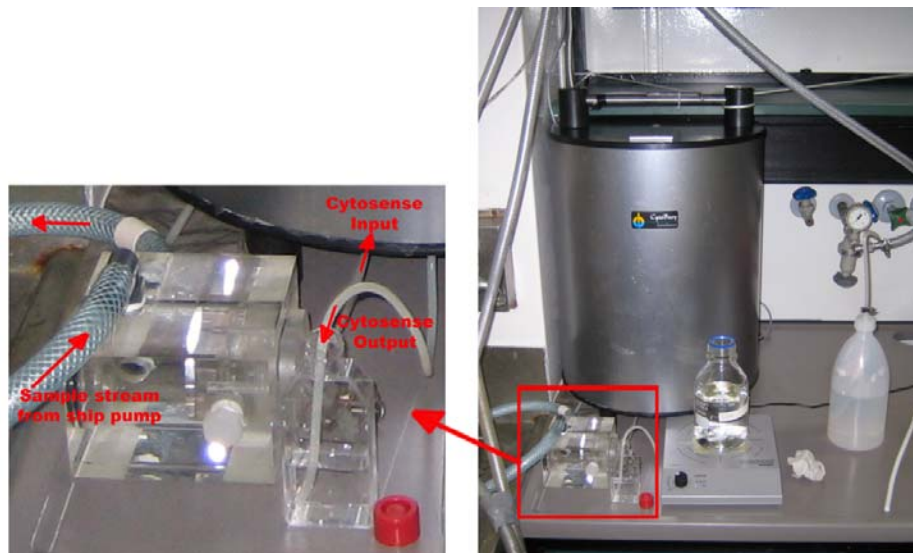


Figure 4-12: Cytosense measurements on board of FS Polarstern.

Due to the complexity of the results and since these measurements were not included in a Ferrybox only a rough overview of some preliminary results can be given here.

In Figure 4-13 some relationships are displayed in four graphs. The most ones important are:

Upper left: Forward scatter vs. no. of cells. This is quasi a size spectrum of the measured algae. As can be seen the distribution is relatively narrow and uniform.

Upper right: Red fluorescence vs. cell size (from forward scatter): This indicates that over different cell sizes a relatively uniform red fluorescence (chlorophyll signal) is obtained (yellow). However, there are as well some algae with smaller chlorophyll content (blue).

Lower left: Quotient red fluorescence/forward scatter (normalised to size) vs. 90° scatter.

Lower right: Quotient of orange fluorescence/red fluorescence vs. quotient yellow fluorescence/red fluorescence. Here, the orange-fluorescing and yellow-fluorescing pigments are normalised to their chlorophyll-content (red fluorescence). As can be seen there are specific clusters of different algal properties. The final selection for further processing was carried out by using this graph (see the yellow, green, blue and red boundaries).

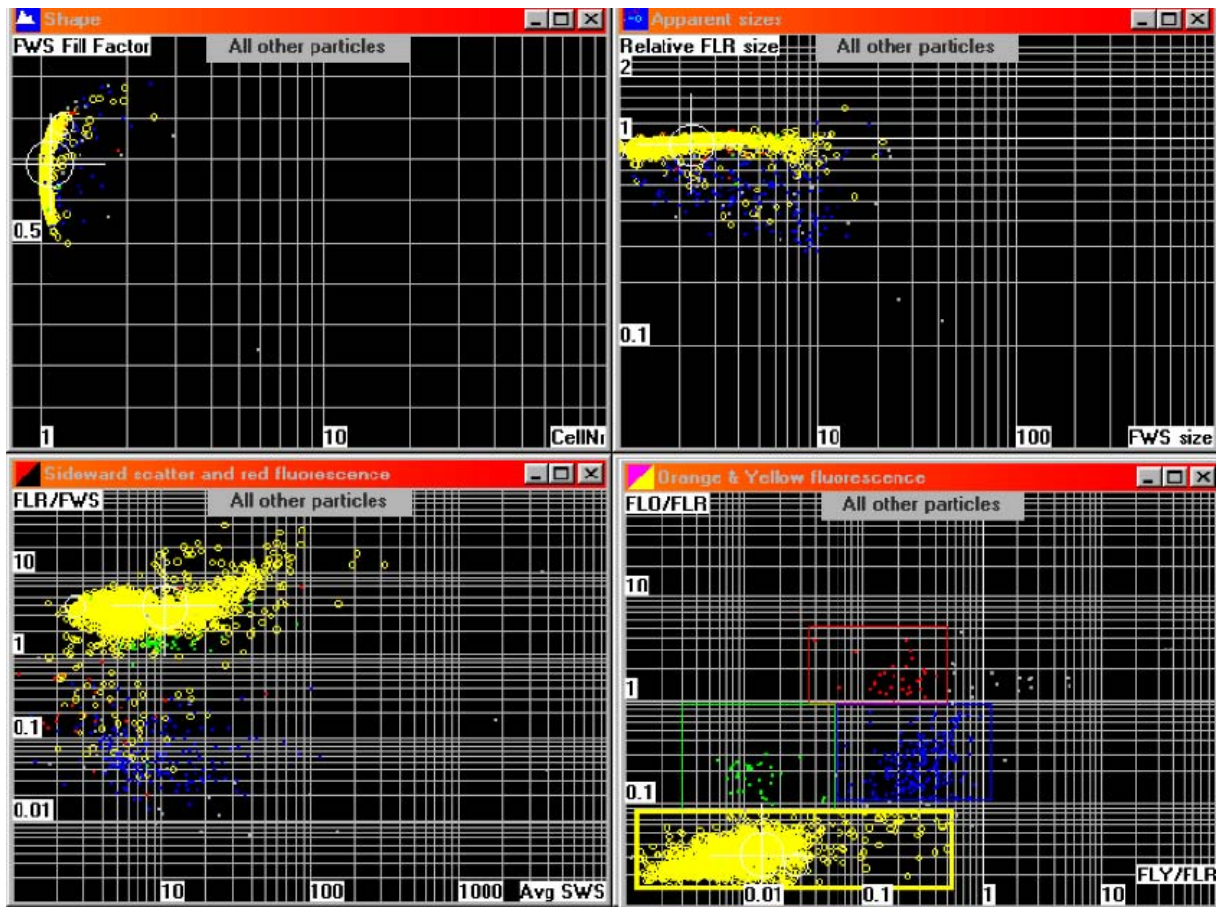


Figure 4-13: First overview with the analysis program "CytoPlus" which is used to select relevant parameter sets.

Explanation: FWS= Forward scatter, SWS= 90° scatter, FLR= red fluorescence, FLO= orange fluorescence, FLY= yellow fluorescence.

The variation of algal properties along the transect Bremerhaven – Vigo can be observed in Figure 4-14. In the left graph the cell numbers of the different sets and in the right graph the red fluorescence of the different cell types is depicted.

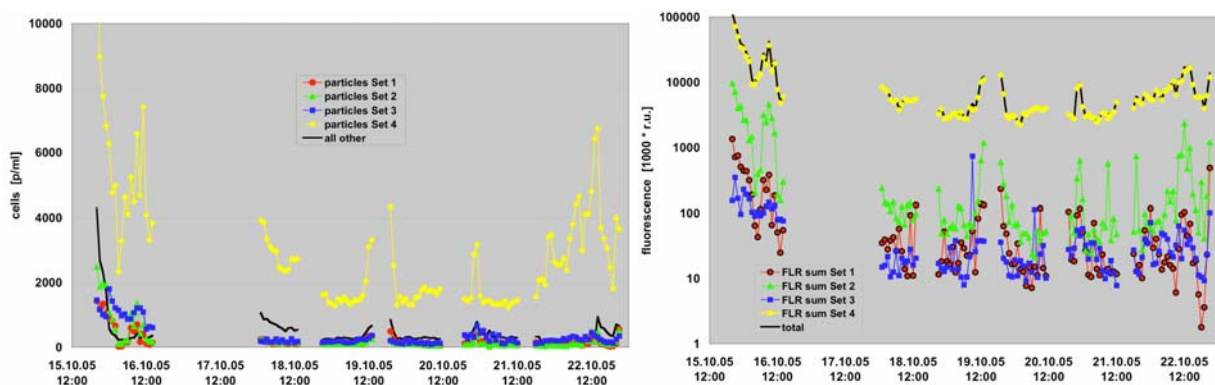


Figure 4-14: Results: Cell numbers (left) and fluorescence values (right) of the different parameter sets selected in Figure 4-13 along the transect Bremerhaven – Vigo.

From the graph it is evident that phytoplankton is dominated by cells which have the properties (fluorescence and scatter) of parameter set 4 (yellow). Unfortunately, an accurate identification by microscopic counts (light microscope) was not possible because the cells were too small. Presumably, it was a mixture of *Prochlorococcus* and *Synechococcus*. Pigment analyses by HPLC will be carried out soon and will bring some clarification.

**Conclusion:** It is relatively easy to measure the size and fluorescence “classes” on a cruise. However, the identification what the different parameter sets mean and which algal species cause these signals needs to be verified by independent measurements such as HPLC and additional microscopic identifications.

#### 4.9.2 Examples of CO<sub>2</sub> Measurements

Within the project CO<sub>2</sub> analysers were not tested in the Ferryboxes. Therefore, the following descriptions are derived from literature.

CO<sub>2</sub> measurements for global carbon budgets are carried out, for example, in the CAVASSOO-project (“Carbon Variability Studies by Ships Of Opportunity”). CAVASSOO will provide reliable estimates of the uptake of CO<sub>2</sub> by the North Atlantic, and how this varies from season to season and year to year. These will in turn assist in constraining estimates of European and North American terrestrial (vegetation) sinks, using atmospheric inverse modelling techniques. To obtain whole-basin estimates four routes were set-up on which automated surface pCO<sub>2</sub> and related measurements are made using ships of opportunity (<http://tracer.env.uea.ac.uk/e072/>).

Besides such global investigations pCO<sub>2</sub> measurements were successfully carried out for the assessment of biological processes, e.g., the determination of the net production of organic matter on the basis of the surface water CO<sub>2</sub>-balance.

For example, Schneider et al. (2005) collected pCO<sub>2</sub> data during June 2003 and September 2004 in different regions of the Baltic Sea. These data were used to identify biological production events such as the spring bloom and the midsummer cyanobacteria bloom. To quantify the net biomass production, the decrease of the total CO<sub>2</sub>/HCO<sub>3</sub> amounts during the production periods was calculated using the pCO<sub>2</sub>, temperature and salinity records and the mean alkalinity. Taking into account the CO<sub>2</sub> air/sea exchange and the formation of dissolved organic carbon, a simple mass balance yielded the net production of particulate organic carbon, which represents the total biomass. The chlorophyll-a concentrations obtained from the fluorescence data showed peaks that in most cases coincided with the production maxima and thus supported the interpretation of the pCO<sub>2</sub> data.

Other investigations by Schneider et al. (2003) were used to estimate N<sub>2</sub> fixation rates: The concept of utilising CO<sub>2</sub> budget estimations for the determination of N<sub>2</sub> fixation rates emerged from observations of the seasonal cycle of pCO<sub>2</sub> in Baltic Sea surface water. During investigations in the eastern Gotland Sea it was found that pCO<sub>2</sub> continued to decrease after the spring plankton bloom in May and reached a minimum in July. This was unexpected because with a temperature increase of about 15 °C the concentrations should increase if no competing processes occur (solubility). The reason for the drop of pCO<sub>2</sub> was seen by different authors (Thomas et al. (1999) and Osterroht and Thomas (2000)) as continuing net biomass production and preferential nitrogen recycling which presumably occurred despite the complete depletion of dissolved inorganic nitrogen (measured DIN values). Their conclusions were based on a coupled CO<sub>2</sub>/nitrogen budget, which included N<sub>2</sub> fixation. This was endorsed by observed C/N ratios. All the results, e.g. for N<sub>2</sub> fixation rates, were based on the calculation of the net POC production by the carbon balance.



## 5 Recommendations for Ferrybox Applications, Known Problems and Limitations

### 5.1 Membrane-Covered Oxygen Sensor

Even when membrane-covered oxygen sensors do not have the stability of the Optodes and are as well more sensitive to biofouling they are cheaper and can very well be used for the measurement of oxygen deficiencies and oxygen surplus due to primary production. Care has to be taken in choosing the right sensor. In general, sensors used for industrial applications are more robust than sensors for laboratory environments. For ferry applications it is not necessary to choose expensive in situ sensors that very often have a pressure-compensation for larger depths. However, an automated cleaning system is recommended for longer maintenance-free applications. Care has to be taken in the check or calibration of the sensors. Normally a calibration and check in water-saturated air is sufficient. However, when a check is carried out in extreme environments on board a ship (e.g., machine room) the temperature equilibrium should be reached and any rapid temperature changes must be avoided. For the following measurements the salt influence has to be corrected.

### 5.2 Optode

The recommendation following from this work is that the Aanderaa Optode is a reliable tool for making measurements of both biological production and respiration. That data is potentially more quantitative than that which can be obtained on the basis of measurements of fluorescence. The sensor itself is robust and not significantly affected by fouling unlike fluorimeters. In 2006 the NERC.NOC Ferrybox will only use Optodes for measuring biological activity the fluorimeters will be removed from the system.

Care has to be taken when chlorination techniques are used to prevent biofouling. Even when tests from IFEMER within the EU project "BRIMOM" showed no influence with small concentrations of chlorine ("local chlorination") this should be checked.

### 5.3 pH

pH measurements are a valuable tool for the estimation of biological respiration/production and of the CO<sub>2</sub> budget in coastal waters. Together with oxygen, light and chlorophyll measurements it can be expected that in the near future more quantitative data on respiration and production rates can be gained.

However, it has to be kept in mind that very precise pH measurements are necessary for these purposes. When pH glass electrodes are applied for this purpose they have to be checked/calibrated frequently. With automated cleaning procedures, which remove any biofilms, a weekly re-calibration is recommended in order to reach an accuracy of 0.05 pH units.

For more precise measurements with long-time stability new spectrometrical methods emerged within the last years: pH-sensitive dyes, which change their colour with pH, are used. Either spectral fluorescence or absorption measurements of these dyes enable pH measurements with an absolute accuracy of 0.01 and a resolution of 0.001 pH units.

## 5.4 Current Profilers (ADCP)

ADCP measurements are as well a valuable tool for the estimation of water and sediment transports through channels/straits etc. as for the interpretation of movements of water constituents.

However, care should be taken when applying this method on fast ferries or ships of opportunity: The applicability depends very much on the relationship between the ferry speed and the current velocities to be measured. For example it may be difficult to measure currents of 5-10 cm/s as they can be found in open waters of the Baltic Sea from a ferry with cruising speed of 25 knots. What is possible depends on the

- Speed of the ferry
- Accuracy with which the ferry speed can be determined (ADCP bottom signal, differential GPS)
- Current speed in the sea area and
- Number of scatterers (e.g., amount of suspended matter).

It is recommended that prior to installing an ADCP a test cruise should be carried out.

The installation of an ADCP on a ferry is not trivial. Either the transducers have to be mounted under the keel of the ship (in a cage to prevent damage) or –if applicable- in a moon-pool. The latter will seldom be found on ferries.

Servicing of the system is not required very often, but is difficult and without a moon-pool divers are needed.

Whereas the calibration of the current measurements are standardised the calibration of the backscatter intensity to suspended matter is not trivial. Due to the composition of the suspended matter (organic content etc.) there are many uncertainties associated with these measurements.

## 5.5 Multi-wavelength Fluorometer for Algal Group Detection

The algal group detection is a valuable tool for detection of changes in the algal composition (“finger print”). Its value depends of the algae divisions, which are abundant. For example, if blue-green algae can be found together with diatoms or green algae the sensor give a good estimation on the occurrence of these (sometimes harmful) algae. If on the other hand mainly diatoms and flagellates are abundant the interpretation of the different instrument channels is ambiguous.

The sensitivity of the sensor is not very high, preventing meaningful measurements in oligotrophic waters.

Another feature of the instrument is the measurement of the photosynthetic activity after illumination. The usefulness of the methods has not yet been tested within the project. The implementation within a water loop on the ferry has to be investigated since under certain circumstances it may be necessary to stop the flow through the instrument during measurement.



## 5.6 FRRF

So far we have only carried out a preliminary analysis of the data. The higher Fv/Fm values observed in the English Channel and their variability over time suggests that a more detailed scientific study in this would be profitable. However to do this FRRF data would have to be used in conjunction with a wide range of other data as was done in the case of the Smyth et al (2004) study. The FRRF would need to be used in conjunction with continuous measurements of nutrients and HPLC studies to determine the plankton taxa present to provide detail on the factors controlling plankton photo-physiology in relation to nutrient supply.

From the point of view of making operational observations that are of value to monitoring agencies then the complexity of interpretation of FRRF data suggests it should not be considered for routine use. A key claim for FRRF has been the potential for estimating rates of primary productivity. This is only realisable where sufficient ancillary information is available (e.g. Suggett et al., 2001, Moore et al., 2003). In contrast the measurement of dissolved oxygen using the Aanderaa Optode presents a much simpler and more cost effective means of achieving the goal of making rough productivity estimates. In addition to the oxygen data itself, this requires (realistic) wind speed data at the location (Bargeron et al. in Preparation).

## 5.7 Chemical Nutrient Analyser

The determination of nutrients is an important task for any biology-related measurements. Due to high local heterogeneity and temporal variability automated measurements from ferries and ships of opportunity are of paramount significance. At the time being, automated chemical analysers that use wet chemistry are the only instruments, which cover the whole range of parameters ( $\text{NH}_4^+$ ,  $\text{NO}_2^-$ ,  $\text{NO}_3^-$ ,  $\text{o-PO}_4^{3-}$ ,  $\text{SiO}_4^{3-}$ ) and the required concentration ranges (<0.1  $\mu\text{mol/L}$  to 100  $\mu\text{mol/L}$ ). The instruments are complex and prone to mechanical failures. They require a very thorough “chemical maintenance”. One limitation is the small concentration range for the photometric measurements of about 1: 20. For ferries covering coastal waters -or even estuaries- and offshore regions either automated dilution procedures or different optical path lengths (cuvettes) have to be used. Depending on the instrument type this may lead to enhanced measuring times (if a second analysis has to be carried out in case of exceeding ranges).

The main limitations of currently existing nutrient analysers are the relatively long time constants of up to 20 minutes. Due to the long gaps between measurements (on a ferry cruising with 25 knots only every 15 km a nutrient measurement exists) concentration variations, e.g., at hydrographic fronts or near a plankton bloom, may be missed.

## 5.8 In situ Nitrate Sensor

The temporal limitations due to sensor characteristics mentioned in the last paragraph may at least be overcome for nitrate by using an in situ Nitrate Sensor. Its main limitation is the poor sensitivity of only about 1  $\mu\text{mol/L}$ . However, it has the main advantage of being much faster (< 1 min) and much easier to handle. Since the sensor is very sensitive to window soiling care must be taken to avoid any biofilm formation by applying automated cleaning/antifouling procedures.

## 5.9 Light Sensor (PAR)

Light sensors are an important tool for the correction or interpretation of chlorophyll-a fluorescence changes caused by different fluorescence yields in daylight and at night.

Special attention must be made to the signal interface and transferring a weak millivolt signal over long cable is not recommended. The data need to be transferring from an analogue to a digital signal and then transferred. Another way is to use a sensor that allows digital values to be transferred over RS232 port (e.g. TriOS irradiance sensors).

For exact PAR measurements a regular manual cleaning of the sensor is required to remove dust and salt residuals from sea spray.

## 5.10 Water Sampler

Cooled water samplers are a very important tool, which should accompany all more sophisticated Ferrybox measurements. They allow regular checks on the function of different sensors such as salinity, turbidity and nutrients. In addition, further lab analyses can be carried out for other parameters. This includes algal species and toxic trace compounds.

For long ferry cruises there should at least 24 one-litre bottles be available. If instead, several smaller bottles are used the longer filling times should be taken into account (the assignment of measurement and corresponding sample gets more difficult).

Care should be taken with the selection of a sampler: Criteria such as the amount of residual water in connections (cross-contamination), filling times, handling of the bottle exchange etc. should be observed.

It should be noted that for Ferrybox systems which operate under pressure, i.e., the water pressure of the water intake (0.1-0.6 bar depending on ferry) only samplers, which can handle this pressure, have to be used (some samplers for on shore use just suck in the water and will overflow if the intake contains excess pressure).



## 6 Conclusions

Within the FerryBox project it could be shown that the Ferrybox is a suitable platform not only for standard oceanographic sensors but as well for new emerging technologies. Most of the existing Ferrybox systems with their flow-through systems and their sophisticated computer control are predestined for the application of new, more complex sensors and analysers. Since some of the Ferrybox systems apply automated antifouling technologies the sensitivity of some of these non-standard methods against fouling and contamination can be overcome.

It could be shown in the project that some new sensor technologies are able to contribute to the solution of important scientific questions. On the other hand, it also became clear that there is the need for the development of further sensors for the measurement of chemical and biological relevant parameters.



## 7 References

- Aminot A., K erouel R. & Birot D. (2001): *Water Research* 35, 1777-1785
- Armstrong, F.A.J.; Boalch, G.T. (1961) *J. Mar. Biol. Assoc. U.K.* 41, 591 - 597.
- Bargeron C P, Hydes D J, Kelly-Gerreyn B A, Qurban M A, *In Preparation*. Estimating new production on the north west European shelf using a ship of opportunity. *Estuarine Coastal Marine Science*.
- Bellerby, R. G. J. Turner, Millward, G. E., and Paul J. Worsfold. 1995. Shipboard flow injection determination of sea water pH with spectrophotometric detection. *Analytica Chimica Acta* 309 (1995) 259-270.
- Beutler M. (1998): Entwicklung eines Verfahrens zur quantitativen Bestimmung von Algengruppen mit Hilfe computergest utzter Auswertung spektralaufgel oster Fluoreszenzanregungsspektren. Dipl. Univ. Kiel, 100 Seiten.
- Beutler M., Wiltshire K.H., Meyer B., Moldaenke C., L uring C., Meyerh ofer M., Hansen U.P., Dau H. (2001): A fluorometric method for the differentiation of algal populations *in vivo* and *in situ*. *Photosynthesis Research*, (submitted).
- Borges, A.V., Frankignoulle, M. 2003. Distribution of surface carbon dioxide and air-sea exchange in the English Channel and adjacent areas. *Journal of Geophysical Research* **108(C5)**, 3140-54.
- Broecker, W.S., Peng, T.S. 1982. *Tracers in the Sea*. Palisades, New York: Lamont-Doherty Geological Observatory, 690pp.
- Byrne R. H., S. McElligott, R. A. Feely, and F. J. Millero. 1999. The role of pH measurements in marine CO<sub>2</sub>-system characterizations. *Deep-Sea Res.* 46A, 11:1985-1997.
- Demas J. N., B. A. De Graff, and P. Coleman. 1999. Oxygen Sensors Based on LuminescenceQuenching. *Analyt. Chem.* 71: 793A-800A.
- Eppley, R.W., Peterson, B.J. 1979. Particulate organic matter flux and planktonic new production in the deep ocean. *Nature*, **282**, 677-680.
- Foster, P. Morris, A.W. (1971) *Water Res.* 5, 19 - 27.
- Frankignoulle, M., Borges, A.V. 2001. European continental shelf as a significant sink for atmospheric carbon dioxide. *Global Biogeochemical Cycles* **15(3)** 569-576.
- Fuhrmann, R; Zirino, A. 1988. High-resolution determination of the pH of seawater with a flow-through system. *DEEP-SEA RES. (A OCEANOGR. RES. PAP.)*. Vol. 35, no. 2, pp. 197-208. 1988.
- Geider R J, Greene R M, Kolber Z, MacIntyre H, Falkowski P G ,1993. Fluorescence assessment of the maximum quantum efficiency of photosynthesis in the western North Atlantic. *Deep Sea Research*, 40, 1205-1224.
- Gillian L. Robert-Baldo, Michael J. Morris, and Robert H. Byrne. 1985. Spectrophotometric Determination of Seawater pH Using Phenol Red. *Anal. Chem.* 1985, 57, 2564-2567
- Glud R. N., J. K. Gundersen, and N. B. Ramsing. 2000. Electrochemical and optical oxygen microsensors for in situ measurements. In *in situ monitoring of aquatic systems: Chemical analysis and speciation*. John Wiley & Sons Ltd (eds J. Buffle & G. Horvai). Chapter 2: 19-73.
- Grasshoff, K., M. Ehrhardt, K. Kremling. 1983. *Methods of Seawater Analysis*, 2nd edition, Verlag Chemie pg. 125-131.
- Holligan, P.M. 1981. Biological implications of Fronts on the Northwest European Continental Shelf. *Philosophical Transactions of the Royal Society of London, Series A* **302(1472)**, 547-562.
- Holligan, P.M. 1989. Primary Productivity in the Shelf Sea of North-West Europe. *Advances in Botanical Research Incorporating Advances in Plant Pathology*, **16**: 194-252.
- Holst G., M. K uhl, and I. Klimant. 1995. A novel measuring system for oxygen microoptodes based on a phase modulation technique. *Proceedings SPIE* 2508, 45, 387-398.
- Hydes, D.J., Gowen, R.J., Holliday, N.P., Shammon, T., Mills, D. 2004. External and internal control of winter concentrations (N, P and Si in north-west European shelf seas. *Estuarine, Coastal and Shelf Science* **59**, 151-161.
- Hydes, D.J., Yool, A., Campbell, J.M., Crisp, N.A., Dodgson, J., Dupee, B., Edwards, M., Hartman, S.E., Kelly-Gerreyn, B.A., Lavin, A.M., Gonz alez-Pola, C.M., Miller, P. 2003. Use of a Ferry-Box System to look at Shelf Sea and Ocean Margin Processes. In *Building the European capacity in operational oceanography*. Proceedings of the Third International Conference on EuroGOOS, 3-6 Dec 2002. Athens Greece, pp297-303.

- Joint, I., Wollast, R., Chou, L., Batten, S., Elskens, M. *et al.* 2001. Pelagic production at the Celtic Sea shelf break. *Deep-Sea Research II* **48**, 3049-3081.
- Joos, F.,G.-K. Plattner, T.F. Stocker, A. Körtzinger, and D. W. R. Wallace (2003). Trends in marine dissolved oxygen: Implications for ocean circulation changes and the carbon budget. *Eos Trans Amer. Geophys. Union*, **84**, 197-204.
- Keeling, R.F., Shertz, S.R. 1992. Seasonal and interannual variations in atmospheric oxygen and implications for the carbon cycle. *Nature* **358**, 723-727.
- Kenneth S. Johnson, Luke J. Coletti (2002). In situ ultraviolet spectrophotometry for high resolution and long-term monitoring of nitrate, bromide and bisulfide in the ocean. *Deep-Sea Research I* **49** (2002) 1291–1305
- K erouel R. & Aminot A. (1997): *Marine Chemistry* **57**, 265-275
- Kirk J T O, 1994. Light and photosynthesis in aquatic ecosystems. 2<sup>nd</sup> Edition Cambridge University Press 509 pp
- Klimant I., C. Huber, G. Liebsch, G. Neurauder, A. Stangelmayer, and O. S. Wolfbeis. 2000. Dual Lifetime Referencing (DLR) - a New Scheme for Converting Fluorescence Intensity into a Frequency-Domain or Time-Domain Information. In *Fluorescence Spectroscopy: New Methods and Applications*, Valeur B. & Brochon C. eds. Springer Berlin (2000).
- Klimant I., M. K uhl, R. N. Glud, and G. Holst. 1996. Optical measurement of oxygen and temperature in microscale: strategies and biological applications. *Sens. Actu. B*, 000-000: 1-9.
- Kolber Z, Falkowski P G, 1993. Use of active fluorescence to estimate phytoplankton photosynthesis in situ. *Limnology and Oceanography*. **38**, 1646-1665.
- Kolber Z, Prasil O, Falkowski P G, 1998. Measurements of variable chlorophyll fluorescence using fast fluorimetry techniques: defining methodology and experimental protocols. *Biochimica et Biophysica Acta*. **1367**, 88-106.
- K rtzinger, A. and J. Schimanski (2004). High Quality Oxygen Measurements from Profiling Floats: A Promising New Technique. *J. Atmos. Oceanic Technol.*, **22**, 302-308
- Minas, H.J., Minas, M. 1992. Net community production in "High nutrient - low chlorophyll" waters of the tropical and Antarctic Oceans: grazing vs iron hypothesis. *Oceanologica Acta* **15(2)**, 145-162.
- Moldaenke C., Vanselow K.H., Hansen, U.P. (1995): The 1-Hz fluorometer: A new approach to fast and sensitive long-term studies of active chlorophyll and environmental influences. *Helgol nder Meeresuntersuchungen* **49**, Seite 785-796.
- Moore C M, Lucas M I, Sanders R, Davison R, 2005. Basin scale variability in phytoplankton bio-optical characteristics in relation to bloom state and community variability in the Northeast Atlantic. *Deep Sea Research I*, **52**, 401-409.
- Moore, C.M., Suggett, D., Holligan, P.M., Sharples, J., Abraham, E.R., Lucas, M.I., Rippeth, T.P., Fisher, N.R., Simpson, J.H. and Hydes, D.J. (2003) Physical controls on phytoplankton physiology and production at a shelf sea front: a fast repetition-rate fluorimeter based field study. *Marine Ecology – Progress Series*, **259**, 29-45.
- Najjar, R.G., Keeling, R.F. 2000. Mean annual cycle of the air-sea oxygen flux: A global view. *Global Biogeochemical Cycles* **14(2)**, 573-584.
- Nakamura, N. , Yutaka, A. 2003. Optical sensor for carbon dioxide combining colorimetric change of a pH indicator and a reference
- Nightingale, P.D., Liss, P.S. 2003. Gases in Seawater, pp49-81. In Holland HD and Turekian KK Eds., *Treatise on Geochemistry Volume 8 Biogeochemistry*. Amsterdam: Elsevier Ltd.
- Ogura, N. Hanya, T. (1967) *Int. J. Oceanology and Limnology*. **1**, 91 - 102.
- Ogura, N.; Hanya, T. (1966) *Nature*, **212**, 758.
- Pingree, R.D., Pugh, P.R., Holligan, P.M., Forster, G.R. 1975. Summer phytoplankton blooms and red tides along tidal fronts in the approaches to the English Channel. *Nature* **258**, 672-677.
- Puillat, I., Lazure, P., J gou, A.M., Lampert, L., Miller, P.I. 2004. Hydrographical variability on the French Continental shelf in the Bay of Biscay, during the 1990s. *Continental Shelf Research* **24**, 1143-1163.
- Qurban, M.A., Hydes,D.J., Lavin, A.M., Gonz lez-Pola, C.M., Kelly-Gerreyn, B.A., Miller, P. 2004. Sustained 'Ferry-Box' Ship of Opportunity observations of physical and biogeochemical conditions across the Bay of Biscay. ICES Annual Science Conference Vigo Spain 2004, paper no. CM2004/N:09 19pp CD ROM publication
- Redfield, A.C. 1934. On the proportion of organic derivatives in seawater and their relation to the composition of plankton, pp176-192. In James Johnstone Memorial Volume, Liverpool.

- Redfield, A.C., Ketchum, B.H., Richards, F.A. 1963. The influences of organisms on the composition of seawater, pp26-77. In Hill, M.N. Ed, The Sea vol. 2, New York: Wiley.
- Richardson K. & Pedersen F.B. (1998) Estimation of new production in the North Sea: consequences for temporal and spatial variability of phytoplankton ICES Journal of Marine Science, 55, 574-580.
- Ruser A. (1992): Entwurf und Erprobung eines schnellen digitalen Korrelators für systemtheoretische Untersuchungen der Chlorophyll-Fluoreszenz bei geringen Frequenzunterschieden zwischen Messlicht und aktinischem Licht. Dipl. Univ. Kiel, 117 Seiten.
- Ruser A. (2001), Untersuchungen zur Erkennung von Algengruppen und deren photosynthetischer Aktivität im marinen Bereich. Dissertation Univ. Kiel. And in: Berichte, Forschungs- und Technologiezentrum Westküste d. Univ. Kiel, Nr. 25, 206 S., Büsum 2001 ISSN 0940 - 9475
- Ruser A., Popp P., Kolbowski K.H. (1999): Comparison chlorophyll-fluorescence chlorophyll-a „Primärproduktionsbestimmung Verf.). Berichte Forschungs- und Technologiezentrum Westküste d. Univ. Kiel, Nr. 19, Seite 27-38.
- Schröder C. R. ;Weidgans, B. M. and Ingo Klimant. 2005. pH Fluorosensors for use in marine systems. The Analyst, 2005, 130(6), 907 – 916.
- Smyth T J, Pemberton, K L, Aiken J, Geider R J, 2004. A methodology to determine primary production and phytoplankton photosynthetic parameters from Fast Repetition Rate Fluorometry. Journal of Plankton Research 26, 1337-1350.
- Steele, J.H.1964. A study of production in the Gulf of Mexico. Journal of Marine Research 22, 211-221.
- Suggett D, Kraay G, Holligan P, Davey M, Aiken J, Geider R, 2001. Assessment of photosynthesis in a spring cyanobacterial bloom by use of a fast repetition rate fluorimeter. Limnol. Oceanogr., 46, 802–810.
- Strickland. J.D.H., and Parsons, T.R. 1968. Strickland, J.D.H., and Parsons, T. R., 1968. A manual for sea water analysis. Bull. Fish. Res. Bd. Canada, 167.
- Tengberg A, J. Hovdenes, J. H. Andersson, O. Brocande, R. Diaz, D. Hebert, T. Americh, C. Huber, A. Körtzinger, A. Khipounoff, F. Rey, C. Rönning, S. Sommer and A. Stangelmayer (submitted) Evaluation of a Life Time based Optode to measure Oxygen in Aquatic Systems Limnology & Oceanography, Methods
- Thomas, O. Gallot, S. (1990) Fres. J. Anal. Chem. 338, 234 - 237.
- Thomas, O., Gallot, S., Mazas, N., 1990. Ultraviolet multiwavelength absorptiometry (UVMA) for the examination of natural waters and waste waters: Part II: determination of nitrate. Fresenius Journal of Analytical Chemistry 338, 238–240.
- Urlick, R.J., 1975. Principles of underwater sound. McGraw-Hill, New York, 384 pp.
- Weidgans, Bernhard M. 2004. New Fluorescent Optical pH Sensors with Minimal Effects of Ionic Strength. Dissertation Univ. Regensburg
- Weiss, R.F. 1970. Oxygen solubility in seawater. Deep-Sea Research 17, 721-735.
- Winkler L. W. 1888. Die Bestimmung des im Wasser gelosten Sauerstoffes. Ber. Dtsch. Chem. Ges. Berlin. 21: 2843-2846.
- Wolfbeis O.S. 1991. Fiber optic chemical sensors and biosensors. Volumes I+II, CRC Press, Boca Raton.
- Wollast, R., Chou, L. 2001. The carbon cycle at the ocean margin in the northern Gulf of Biscay. Deep-Sea Research II 48(14-15), 3265-3293.
- Zhang, H., Byrne, R. H. 1996. Spectrophotometric pH measurements of surface seawater at in-situ conditions: absorbance and protonation behavior of thymol blue. Marine Chemistry 52 ( 1996) 17-25

## References for “New Emerging Technologies, Part CO<sub>2</sub>”

- Cooper, David J., Watson, Andrew J., Ling, Roger D. 1998. Variation of PCO<sub>2</sub> along a North Atlantic shipping route (U.K. to the Caribbean): A year of automated observations. Marine Chemistry 60 1998.147–164
- Copin-Montegut, C., 1985. A method for the continuous determination of the partial pressure of carbon dioxide in the upper ocean. Mar. Chem. 17: 13-21.
- DOE, 1994. A.G. Dickson and C. Goyet (Editors), Handbook of Methods for the Analysis of the Various Parameters of the Carbon Dioxide System in Sea Water, Version 2. ORNL/CDIAC-74.



- Feely, Richard A., Wanninkhof, Rik, Milburn, Hugh B., Cosca, Catherine E., Stapp, Mike and Paulette P. Murphy. 1998. A new automated underway system for making high precision pCO<sub>2</sub> measurements onboard research ships. *Analytica Chimica Acta* 377 (1998) 185-191
- Goyet, C. and Peltzer, E., 1994. Comparison of the August-September 1991 and 1979 surface partial pressure of CO<sub>2</sub> distribution in the Equatorial Pacific Ocean near 150°W. *Mar. Chem.* 45: 257-266.
- Goyet, C., Beauverger, C., Bonnet, C. and Poisson, A., 1991. Distribution of carbon dioxide partial pressure in surface waters of the Southwest Indian Ocean. *Tellus*, 43B: 1- 11.
- Inoue, H., Sugimura, Y. and Fushimi, K.. 1987. pCO<sub>2</sub> and  $\delta^{13}\text{C}$  in the air and surface sea water in the western North Pacific. *Tellus*, 39B: 228-242.
- Keeling, C.D., Rakestraw, N.W. and Waterman., L.S., 1965. Carbon dioxide in surface waters of the Pacific ocean. 1. Measurements of the distribution. *J. Geophys. Res.*, 70: 6087-6097.
- Keeling, C.D., Wharf, T.P., Wahlen, M. and van der Plicht, J., 1995. Interannual extremes in the rate of rise of atmospheric carbon dioxide since 1980. *Nature*, 375: 666-670.
- Kelley Jr., J.J., 1970. Carbon dioxide in the surface waters of the North Atlantic Ocean and the Barents and Kara Seas. *Limnol. Oceanogr.*, 15: 80-97.
- Kimoto, T. and Harashima, A., 1993. High resolution time/space monitoring of the surface seawater CO<sub>2</sub> partial pressure by ship-of-opportunity. Paper presented at the 4th Int. CO<sub>2</sub> Conf., Carqueiranne, September 14- 19.
- Koertzinger, A., Thomas, H., Schneider, B., Gronau, N., Mintrop, L., Duinker, J.C., 1996. At-sea intercomparison of two newly designed underway pCO<sub>2</sub> systems — encouraging results. *Mar. Chem.* 52, 133– 145.
- Ohtaki, E., Yamashita, E. and Fujiwara, F., 1993. Carbon dioxide in surface sea waters of the Seto Inland Sea. *Jpn. J. Oceanogr.*, 49: 295-303.
- Osterroht, C., Thomas, H., 2000. New production enhanced by nutrient supply from non-Redfield remineralization of freshly produced organic matter. *J. Mar. Syst.* 25, 33– 46.
- Poisson, A., Metzl, N., Brunet, C., Schauer, B., Bres, B., Ruiz-Pino, D. and Louanchi, F., 1993. Variability of sources and sinks of CO<sub>2</sub> in the Western Indian and Southern Oceans during the year 1991. *J. Geophys. Res.*, 98(C12), 22,759-22,722, 22,778.
- Robertson, J.E., Watson, A.J., Langdon, C., Ling, R.D. and Wood, J.W., 1993. Diurnal variations in surface pCO<sub>2</sub> and O<sub>2</sub> at 60°N, 20°W in the North Atlantic. *Deep-Sea Res.* 40: 409-422.
- Schneider, B., , S. Kaitala, S., P. Maunula 2005. Identification and quantification of plankton bloom events in the Baltic Sea by continuous pCO<sub>2</sub> and chlorophyll a measurements on a cargo ship. *Journal of Marine Systems* (2005) in press
- Schneider, B., Kremling, K. and Duinker, J.C., 1992. CO<sub>2</sub> partial pressure in Northeast Atlantic and adjacent shelf waters: Processes and seasonal variability. *J. Mar. Syst.*, 3: 453-463.
- Schneider, B., Kuss, J., 2004. Past and present productivity of the Baltic Sea as inferred from pCO<sub>2</sub> data. *Cont. Shelf Res.* 24, 1611– 1622.
- Schneider, B., Nausch, G., Kubsch, H., Petersohn, I., 2002. Accumulation of total CO<sub>2</sub> during stagnation in the Baltic Sea deep water and its relationship to nutrient and oxygen concentrations. *Mar. Chem.* 77, 277–291.
- Schneider, B., Nausch, G., Nagel, K., Wasmund, N., 2003. The surface water CO<sub>2</sub> budget for the Baltic Proper: a new way to determine nitrogen fixation. *J. Mar. Syst.* 42, 53– 64.
- Takahashi, T., 1961. Carbon dioxide in the atmosphere and in Atlantic Ocean water. *J. Geophys. Res.*, 66: 477-494.
- Thomas, H., Ittekkot, V., Osterroht, C., Schneider, B., 1999. Preferential recycling of nutrients—the ocean's way to increase new production and to pass nutrient limitation? *Limnol. Oceanogr.* 44 (8), 1999–2004.
- Thomas, H., Schneider, B., 1999. The seasonal cycle of carbon dioxide in Baltic Sea surface waters. *J. Mar. Syst.* 22, 53–67.
- Wanninkhof, R.H., and K. Thoning. 1993. Measurement of fugacity of CO<sub>2</sub> in surface water using continuous and discrete sampling methods. *Marine Chemistry*, 44(2-4):189-204, (1993)
- Weiss, R.F., 1981. Determinations of CO<sub>2</sub> and methane by dual catalyst flame ionization chromatography and nitrous oxide by electron capture chromatography. *J. Chromatogr. Sci.*, 19: 611-616.